

การศึกษาผลของคุณสมบัติของระบบรองรับแบบแหนน
ต่อความสบายในการขับขี่ของรถบรรทุกเล็ก



นางศิริพร แซ่เหล่ม

ศูนย์วิทยพัทยากร
จุฬาลงกรณ์มหาวิทยาลัย

วิทยานิพนธ์นี้ เป็นส่วนหนึ่งของการศึกษาตามหลักสูตรปริญญาวิศวกรรมศาสตรมหาบัญชิต


สาขาวิชาวิศวกรรมเครื่องกล ภาควิชาวิศวกรรมเครื่องกล

คณะวิศวกรรมศาสตร์ จุฬาลงกรณ์มหาวิทยาลัย

ปีการศึกษา 2553

ลิขสิทธิ์ ของจุฬาลงกรณ์มหาวิทยาลัย

AN INVESTIGATION INTO THE EFFECTS OF LEAF SPRING SUSPENSION
PARAMETERS ON RIDE COMFORT OF LIGHT TRUCKS



Mrs. Sirithon Saelem

ศูนย์วิทยทรัพยากร
A Thesis Submitted in Partial Fulfillment of the Requirements
for the Degree of Master of Engineering Program in Mechanical Engineering
Department of Mechanical Engineering

Faculty of Engineering

Chulalongkorn University

Academic Year 2010

Copyright of Chulalongkorn University

Thesis Title AN INVESTIGATION INTO THE EFFECTS OF LEAF SPRING
SUSPENSION PARAMETERS ON RIDE COMFORT OF LIGHT
TRUCKS


By Mrs. Sirithon Saelem

Field of Study Mechanical Engineering

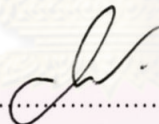
Thesis Advisor Assistant Professor Sunhapos Chantranuwathana, Ph.D.

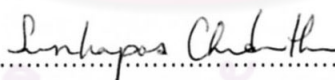
Thesis Co-Advisor Nuksit Noomwongs, D.Eng.

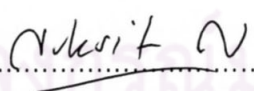
Accepted by the Faculty of Engineering, Chulalongkorn University in Partial
Fulfillment of the Requirements for the Master's Degree



..... Dean of the Faculty of Engineering
(Associate Professor Boonsom Lerdhirunwong, Dr.Ing.)

THESIS COMMITTEE


..... Chairman
(Assistant Professor Witaya Wannasuphoprasit, Ph.D.)


..... Thesis Advisor
(Assistant Professor Sunhapos Chantranuwathana, Ph.D.)


..... Thesis Co-Advisor
(Nuksit Noomwongs, D.Eng.)


..... External Examiner
(Associate Professor Prakob Surawattanawan, Ph.D.)

ศิริธร แซ่เหล่ม : การศึกษาผลของคุณสมบัติของระบบรองรับแบบหนบต่อความสบายในการขับขี่ของรถบรรทุกเล็ก. (AN INVESTIGATION INTO THE EFFECTS OF LEAF SPRING SUSPENSION PARAMETERS ON RIDE COMFORT OF LIGHT TRUCKS) อ. ที่ปรึกษาวิทยานิพนธ์หลัก : ผศ.ดร.สันหพศ จันทรานุกวัฒน์, อ. ที่ปรึกษาวิทยานิพนธ์ร่วม : อ.ดร.นักสิทธิ์ นุ่มวงษ์, 105 หน้า.

ในงานวิจัยนี้ แบบจำลองของสปริงหนบได้ถูกสร้างขึ้นเพื่อใช้ศึกษาผลของคุณสมบัติของระบบรองรับแบบหนบต่อความสบายในการขับขี่ของรถบรรทุกเล็ก ซึ่งมีวัตถุประสงค์หลักคือการสร้างแบบจำลองของสปริงหนบที่ประกอบด้วยพารามิเตอร์ที่สามารถนำไปใช้ในการออกแบบเพื่อผลิตสปริงหนบและเพื่อใช้สำหรับการทำนายระดับค่าความสบายในการขับขี่ แบบจำลองที่ถูกสร้างขึ้นนี้จะถูกตรวจสอบความถูกต้องโดยเปรียบเทียบผลที่ได้จากการจำลองปัญหากับผลที่ได้จากการทดลองจริงด้วยชุดแทนทดสอบหนบที่สามารถวัดระยะการเคลื่อนที่ภายใต้สภาวะการรับแรงแบบคงที่

แบบจำลองของสปริงหนบที่ได้รับการตรวจสอบความถูกต้องแล้ว จะถูกนำไปใช้เพื่อศึกษาผลของพารามิเตอร์ของสปริงหนบต่อค่าความสบายในการขับขี่ของรถบรรทุกเล็กด้วยแบบจำลองระบบรองรับของยานพาหนะแบบหนึ่งในสี่ และในการจำลองแบบปัญหานั้นพารามิเตอร์บางตัวที่ใช้ในการออกแบบสปริงหนบได้แก่คุณสมบัติของโตงเตงหนบ (shackle) ถูกนำมาพิจารณาและหาความสัมพันธ์ต่อค่าความสบายในการขับขี่ด้วยวิธีคำนวณตามมาตรฐาน ISO 2631-1 ที่ค่าพารามิเตอร์ต่างๆของสปริงหนบและชนิดของแบบจำลองของถนนที่ถูกสร้างขึ้นภายใต้สภาวะความเร็วคงที่ ผลจากการทดลองพบว่า ค่าความสบายในการขับขี่จะดีกว่าเมื่อถนนเรียบ ซึ่งค่าจะค่อยๆเปลี่ยนแปลงเมื่อเปลี่ยนชนิดของถนนจากเรียบ(very good) ไปสู่ ถนนขรุขระ(poor) แต่จะเพิ่มขึ้นอย่างฉับพลันเมื่อเปลี่ยนชนิดของถนนจากถนนขรุขระไปสู่ถนนขรุขระมาก(very poor) นอกจากนี้ยังพบว่าค่าความสบายในการขับขี่จากการทดลองด้วยแบบจำลองของระบบรองรับที่มีสปริงหนบแบบไม่เชิงเส้นและแบบเชิงเส้นนั้นมีความแตกต่างกัน จึงสรุปได้ว่าแบบจำลองของสปริงหนบที่สร้างขึ้นนี้มีผลอย่างมีนัยสำคัญต่อค่าความสบายในการขับขี่

ภาควิชา.....วิศวกรรมเครื่องกล.....ลายมือชื่อนิสิต..... *ser ohr*

สาขาวิชา.....วิศวกรรมเครื่องกล.....ลายมือชื่อ อ.ที่ปรึกษาวิทยานิพนธ์หลัก..... *สันหพศ จันทรานุกวัฒน์*

ปีการศึกษา 2553 ลายมือชื่อ อ.ที่ปรึกษาวิทยานิพนธ์ร่วม *นักสิทธิ์ นุ่มวงษ์*

4970598421 : MAJOR MECHANICAL ENGINEERING

KEYWORDS : LEAF SPRING MODEL / DESIGN PARAMETERS / RIDE COMFORT

SIRITHON SAELEM : AN INVESTIGATION INTO THE EFFECTS OF LEAF SPRING SUSPENSION PARAMETERS ON RIDE COMFORT OF LIGHT TRUCKS. THESIS ADVISOR : ASSISTANT PROFESSOR SUNHAPOS CHANTRANUWATHANA, Ph.D., THESIS CO-ADVISOR : NUKSIT NOOMWONGS, D.Eng., 105 pp.

A simulation-based leaf spring model was created to study the effect of leaf spring suspension parameters on vehicle ride comfort. The main objective is to build a simulation model for ride comfort prediction from leaf spring parameters which can be used in design process. In this research, an experimental leaf spring model was verified by using a leaf spring test rig that can measure vertical static deflection of leaf spring under static loading condition.

The verified model was then used to study the effect of leaf spring parameters on ride comfort of a light truck, using a simple 2-degree-of-freedom quarter-car model. In simulation, some design parameters of leaf spring, including the effect from shackle was applied, and the relationship between ride comfort performance (ISO2631-1) and variations in leaf spring design parameters were obtained upon different types of synthetic road irregularity profiles at constant velocity. The overall results show that ride comfort is better on smooth road with gradual changes from "very good" to "poor" road and sudden increase for "very poor" road. The values obtained from the proposed leaf spring model are different from those of the linear leaf spring model's. Hence, it can be concluded that the proposed leaf spring model has significant effects on vehicle ride comfort.

Department :Mechanical Engineering..... Student's Signature Sakon Sakon
 Field of Study :Mechanical Engineering..... Advisor's Signature Sunhapos Chantranuwathana
 Academic Year : 2010..... Co-Advisor's Signature Nuksit Noomwongs

ACKNOWLEDGEMENTS

First of all, Most of values and success must be dedicated to my supervisor, Asst. Prof Dr. Sunhapos Chantranuwathana who has supported me throughout my thesis with his patience and knowledge. For many years of study, he has devoted his time to provide advice and also brought me a lot of perspective vision in solving problems.

I am also grateful for my co-advisor, Dr. Nuksit Noomwongs for his advice and valuable recommendations, especially for the inspirations on the alternative methods of leaf spring modeling.

Great admiration for a senior project team who has changed ideas and theory into a very useful leaf spring test rig, a very important element in research completion. During the time of works, I have been aided by friends and the university staffs. They are very kind and helpful. I am grateful for the Department of Mechanical Engineering who has provided the support and equipment I have needed to produce and complete my thesis.

Final words, I would like to give a special thank to my family for all kind of support, encouragement and love, especially for my husband who has offered me on financial support and encouraged me to complete this work. My deeply regards to my beloved grandmother who has passed away in the very hard moment when this thesis was being carried on.

ศูนย์วิทยทรัพยากร
จุฬาลงกรณ์มหาวิทยาลัย

CONTENTS

TITLE	PAGE
ABSTRACT (THAI).....	IV
ABSTRACT (ENGLISH).....	V
ACKNOWLEDGEMENTS.....	VI
CONTENTS.....	VII
LIST OF TABLES.....	XI
LIST OF FIGURES.....	XII
LIST OF ABBREVIATIONS.....	XVI
CHAPTER I INTRODUCTION.....	1
1.1. Research Background.....	1
1.2. Research Objective.....	2
1.3. Scope of the Research.....	2
1.4. Obtained Results.....	2
1.5. Research Operating Structure.....	3
1.6. Outline of the Thesis.....	3
CHAPTER II LITERATURE REVIEW.....	5
2.1. Ride Comfort.....	5
2.1.1. Definitions.....	6
2.1.2. Ride Characteristic of Vehicles.....	7
2.1.3. Application of Ride Comfort in Automotive Field.....	8
2.1.4. Ride Comfort Measurement.....	10
2.1.4.1. Objective Measurement.....	12
2.1.4.2. Subjective Measurement.....	12
2.1.5. Ride Comfort Standards.....	14
2.1.5.1. ISO 2631–1 General Requirements.....	16
2.1.5.2. Basic Ride Comfort Evaluation Methods.....	16

2.1.5.2.1. Power Spectral Density (PSD) Analysis.....	16
2.1.5.2.2. RMS Accelerations.....	18
2.1.5.2.3. Frequency–Based Weighting Technique of Acceleration Spectra.....	18
2.2. Leaf Spring.....	20
2.2.1. Characteristic of Leaf Spring.....	25
2.2.2. Interleaf Friction and Stick-slip Phenomena.....	26
2.2.3. Shackle Effects.....	27
CHAPTER III RESEARCH METHODOLOGY.....	29
3.1. Description of Research Procedure.....	29
3.2. Research Tools.....	30
3.2.1. Field Experiment Tools.....	31
3.2.2. Simulation Tools.....	31
3.3. Methodology.....	31
3.3.1. Data Collecting.....	31
3.3.1.1. Measured quantities.....	32
3.3.1.2. Sensor Positioning.....	32
3.3.2. Data Analysis.....	33
3.3.2.1. Time Domain Analysis.....	33
3.3.2.2. Frequency Domain Analysis.....	33
3.4. Summary of Research Approach.....	34
CHAPTER IV PRELIMINARY TEST.....	36
4.1. Objective.....	36
4.2. Test Instruments.....	36
4.3. Tested Vehicle.....	37
4.4. Sensors positioning.....	38
4.5. Testing Locations.....	39
4.6. Driving Conditions.....	39

4.7. Procedure.....	39
4.8. Data Analysis.....	42
4.8.1. Time Domain Analysis.....	42
4.8.2. Frequency Domain Analysis.....	42
4.9. Results.....	42
4.9.1. Results of Time domain Analysis.....	43
4.9.2. Results of Frequency domain Analysis.....	44
4.9.3. Results of Frequency Weighting Analysis.....	49
4.10. Conclusions and Further Recommendations.....	53
CHAPTER V LEAF SPRING MODELING AND VERIFICATION.....	54
5.1. Leaf Spring Modeling.....	54
5.1.1. Existing Leaf Spring Models.....	55
5.1.1.1. Classical Beam Theory.....	55
5.1.1.2. Finite-Element Method.....	56
5.1.1.3. Multibody Kinematic.....	56
5.1.1.4. The Three Link Equivalent Model.....	56
5.1.2. Friction Model and Hysteresis Effects.....	57
5.1.3. Description of the Leaf Spring Model.....	57
5.1.4. The Full Leaf Spring Model Construction.....	59
5.2. Verification of the Leaf Spring Model.....	62
5.2.1. Design and Construction of the Leaf Spring Test Rig.....	62
5.2.1.1. Test Rig Frame.....	62
5.2.1.2. Load Measuring Unit.....	63
5.2.1.3. Deflection Measuring Unit.....	64
5.2.2. Verification Testing.....	64
5.2.3. Parameters Identification.....	68
CHAPTER VI SIMULATION OF SUSPENSION MODEL AND PARAMETRIC STUDY INTO THE EFFECTS ON RIDE COMFORT.....	71
6.1. Quarter-Car Model.....	71

6.1.1. Model Characteristics.....	72
6.1.2. Mathematical Equations of the Model.....	73
6.2. Road Input Profile.....	73
6.3. Completed Vehicle Suspension Model.....	75
6.4. Parametric Study by Simulation.....	75
6.5. Ride Comfort Results from Simulating Model Subjected to Random White- Noise Input.....	78
6.6. Discussion of Results and Conclusion.....	89
CHAPTER VII DISCUSSION OF THE RESULTS AND CONCLUSION.....	91
7.1. Summary of the Research.....	91
7.2. Conclusion.....	92
7.3. Further Recommendations.....	92
REFERENCES.....	94
APPENDICES.....	96
APPENDIX A.....	97
PRINCIPAL FREQUENCY WEIGHTINGS IN ONE-THIRD OCTAVES.....	98
APPENDIX B.....	100
DEFINITION OF VEHICLE'S COORDINATE SYSTEM.....	101
APPENDIX C.....	102
MATLAB M-FILE CODE.....	103
BIOGRAPHY.....	105

LIST OF TABLES

TABLE	PAGE
Table 2–1 ISO 2631 approximate comfort/discomfort scale based on magnitude of overall vibration.....	15
Table 4–1 Technical information of the tested vehicle.....	37
Table 4–2 The weighted RMS accelerations results.....	51
Table 5-1 Experimental result of leaf spring deflection subjected to vertical applied load.....	66
Table 6-1 Parameters of the simulated quarter-car model.....	75
Table 6-2 The weighted RMS accelerations, representing the level of ride comfort/ discomfort subjected to different classes of roads (non-linear suspension)	79
Table A-1 Principal frequency weightings in one-third octaves.....	98



 ศูนย์วิจัยทรัพยากร
 จุฬาลงกรณ์มหาวิทยาลัย

LIST OF FIGURES

FIGURE	PAGE
Fig.2-1 The vibration isolation property of vehicle suspension.....	8
Figs.2-2(a) – (b) Recommended vibration tolerance limits of a seated person based on different studies.....	9
Fig.2-2(c) The discomfort boundary contour based on vertical floor accelerations	10
Fig.2-3 Ride comfort model.....	11
Fig.2-4(a) SAE recommended practice for subjective rating scale for evaluation of noise and ride comfort characteristics related to motor vehicle tires	13
Fig.2-4(b) Subjective rating scale with separated opinion questions on property of vehicle component.....	13
Fig.2-4(c) Schedule of the “couple by couple” method to rank 12 different vehicles.....	13
Fig.2-5 Standard criteria limits as a function of frequency and exposure time for vibration in vertical direction.....	15
Fig.2-6 Frequency weighting curves for the principle weightings.....	20
Fig.2-7 Leaf spring components and construction.....	21
Figs.2-8(a) – (d) Different design of leaf spring eyes.....	22
Fig.2-9 Center bolt.....	22
Fig.2-10 Rebound clips.....	23
Figs.2-11(a) – (d) Types of leaf spring ends.....	24
Fig.2-12(a) – (f) Leaf spring configurations.....	24
Fig.2-13(a) – (b) Single and variable rate leaf spring.....	25
Fig.2-14 Load–deflection diagram of tested leaf spring.....	26
Figs.2-15(a) – (b) the Leaf spring configuration at installation.....	27
Fig.3-1 Schematic diagram of working procedure.....	29
Fig.3-2 Basicentric axes of a seated person, adapted from ISO 2631-1.....	32
Fig.4-1 The tested vehicle used in the investigation.....	37
Fig.4-2(a) position of sensors installed within a cabin.....	38

Fig.4-2(b) Positions of sensors installed outside a cabin.....	38
Fig.4-2(c) Attachment of a video camera.....	39
Fig.4-3 Different driving situation of test tracks.....	41
Fig.4-4(a) Acceleration results of driving situation case 1 captured by two different sensors installed within a cabin.....	45
Fig.4-4(b) Acceleration results of driving situation case 6 captured by two different sensors installed within a cabin.....	46
Fig.4-5 Rotational acceleration results of driving situation case 1 and case 2 captured by X-BOW (six-axis) sensor.....	47
Fig.4-6 Vertical acceleration results of driving situation case 1 captured by two different sensors installed outside a cabin.....	48
Fig.4-7 PSD results of acceleration spectra for driving situation case1 and case 6 captured by two different sensors installed within a cabin.....	49
Fig.4-8 graphic results of weighted RMS accelerations.....	52
Fig.5-1 Symmetrical multi-leaf spring with design parameters.....	55
Fig.5-2 Five link mechanism of a leaf spring model.....	58
Fig.5-3 Equivalent linkage of the upturned eye cantilever spring.....	58
Fig.5-4 Full leaf spring model, regarding hysteresis effects.....	60
Fig.5-5 Hysteresis component of a leaf spring model.....	61
Fig.5-6 Final design of the test rig frame.....	62
Fig.5-7 Configuration of the leaf spring test rig.....	63
Fig.5-8 The guide base for load cell and force-actuator attachment.....	63
Fig.5-9 The LVDT measuring unit.....	64
Fig.5-10 Five link mechanism of a leaf spring model.....	65
Fig.5-11 The animated results of simulated model.....	65
Fig.5-12 The load-deflection curve result obtained from test rig experiment.....	67
Fig.5-13 The load–deflection curve of torque and angular displacement	67
Fig.5-14 Load-deflection curve result of linear leaf spring model.....	68
Fig.5-15 Load-deflection curve of force (kg) and displacement (cm).....	69

Fig.5-16 Comparison between load-deflection curve results from experiment and simulation.....	69
Fig.6-1 Conceptual design of the quarter-car model for suspension system.....	72
Fig.6-2 Road surface roughness classification by ISO.....	74
Fig.6-3 The result of simulated road inputs compared with the classification standard.....	74
Fig.6-4 A simple road model used to simulate road inputs.....	75
Fig.6-5 Completed vehicle suspension model.....	77
Fig.6-6 The relationship between torque and angular displacement at the rotational joints.....	78
Fig.6-7 The relationship between torque and angular displacement obtained from linear-leaf spring suspension model.....	78
Fig.6-8(a) The plots of RMS vertical acceleration of vehicle suspension at 60° of shackle angle.....	80
Fig.6-8(b) The plots of RMS vertical acceleration of vehicle body (cross line) and tire (circle line) at 60° of shackle angle.....	80
Fig.6-9(a) The plots of RMS vertical acceleration of vehicle suspension at 90° of shackle angle.....	81
Fig.6-9(b) The plots of RMS vertical acceleration of vehicle body (cross line) and tire (circle line) at 90° of shackle angle.....	81
Fig.6-10 Ride comfort results of nonlinear and linear model at shackle angle 60°....	82
Fig.6-11 Ride comfort results of nonlinear and linear model at shackle angle 70°....	83
Fig.6-12 Ride comfort results of nonlinear and linear model at shackle angle 80°...	83
Fig.6-13 Ride comfort results of nonlinear and linear model at shackle angle 90°...	84
Fig.6-14 Ride comfort results of nonlinear and linear model at shackle angle 110°..	84
Fig.6-15 Ride comfort results of nonlinear and linear model at shackle angle 120°..	85
Fig.6-16(a) Ride comfort results of nonlinear leaf spring model at different shackle angles.....	86
Fig.6-16(b) Ride comfort results of nonlinear leaf spring model for “very good” to “average” road.....	87

Fig.6-17 Ride comfort results of nonlinear leaf spring model at different classes of roads..... 87

Fig.6-18 Ride comfort level of nonlinear leaf spring model at different classes of roads..... 88

Fig.6-19 Symmetrical leaf spring with shackle..... 90

Fig.B-1 Definition of vehicle coordinate system..... 101



ศูนย์วิทยทรัพยากร
จุฬาลงกรณ์มหาวิทยาลัย

LIST OF ABBREVIATIONS

Terms, Abbreviations and Acronyms	Meaning
CG	Centre of gravity. The center of gravity is the average location of the weight of an object. The point at which a body's mass may be said to be concentrated for purposes of determining forces on that body.
f	Frequency (Hertz)
g	Acceleration due to gravity at earth's surface (9.81 m/s^2)
L	The distance between leaf spring eyes, representing full span length of leaf spring subjected to zero loading.
m_b /Sprung Mass	The sprung mass is the portion of the vehicle's total mass that is supported above the suspension. The sprung weight typically includes the body, frame, the internal components, passengers, and cargo, but does not include the mass of the components suspended below the suspension components such as wheels, axles and brakes.
m_w /Unsprung Mass	The unsprung mass is the mass of the various parts of a vehicle that are not carried on the springs, such as wheels, axles, and brakes.
PSD	Power Spectral Density
Ride	Ride or ride quality is quantified by acceleration measured at vehicle body while traveling on road.
RMS	Root mean square value
SAE	the Society of Automotive Engineers
Shackle	Shackle is a swinging link that connect a leaf spring with the vehicle frame to provide more degree of freedom when the leaf spring is moving under applied load.

Terms,Abbreviations and Acronyms	Meaning
α	Shackle angle (rad)
x_s / Suspension stroke	The approximated suspension stroke or suspension displacement applied in this research is the absolute displacement of the sprung mass compared to the unsprung mass which represents vehicle ride's height upon different type of road irregularities.
x_g /Spring Deflection	The distance that a spring travels under a compressive force, measured at CG point of the leaf spring
Y/Camber Height (cm)	The leaf spring's arc length measured at axle's seat



ศูนย์วิทยทรัพยากร
จุฬาลงกรณ์มหาวิทยาลัย

CHAPTER I

INTRODUCTION

1.1. Research Background

Leaf spring is one of the classical components of suspension systems that still exist in present use, especially in heavy loaded vehicles such as trucks. In Thailand, the design process of leaf spring is not directly related to the consideration of ride comfort. Most manufacturers mass produced the product, by using detail drawings created by their customers. Nowadays, general light trucks available in commercial are used as multi-purposed transports as they are sometimes treated as normal passenger cars whose ride comfort of passengers are also concerned. In this research, the relation between ride comfort/discomfort level and some parameters of suspension parts; i.e., leaf spring is examined and investigated experimentally in order to propose methods or guidelines of leaf spring design for manufacturers related to ride comfort in light commercial vehicles.

General manufacturing of leaf spring, a conservative vehicle suspension part that has been used widely until present, usually begins with the design process which performed using specifications relating to their usage. Few main leaf spring parameters, using in design are mentioned in the "Spring Design Manual" the handbook that was published and approved by SAE International [1]. The manual provides useful background as well as design guidelines for designing leaf spring to meet the essential requirements. However, the conventional method usually employs some prototype testing which might takes time before the final design is satisfied. Nowadays, the modern computational methods are used widely and have been adapted as tools to facilitate the tasks. Due to the fact that leaf spring is a complicated-to-analyze element in a vehicle suspension as it combines some nonlinearities, arising from its mechanism and from other relevant components in the installation. It also has significant effect on vehicle performance and ride quality. For such the reasons, the very precise model is necessary to be carefully made as it can reflect very close-to-nature characteristic which

is meaningful in the analysis and interpretation when investigation is performed within the computational environment.

1.2. Research Objective

The purpose of this research is to develop a method for ride comfort prediction of a light commercial vehicle, related to the design parameters of leaf spring. The experimental verified leaf spring model was used to investigate such a relationship so that the study can be developed and contributed to a new method of leaf spring design, in such a manner that the precise value of ride comfort level is evaluated by the leaf spring parameters in a predictive way. The main objectives can be stated clearly as follows,

1. To build a leaf spring model that includes hysteresis leaf spring parameters which can be used in the design process
2. To investigate and verify the leaf spring model by the leaf spring test rig
3. To investigate significance of nonlinear leaf spring model on ride comfort of a light truck

1.3. Scope of the Research

1. In this study, all investigations were performed based on the assumptions or conditions applied to the light commercial vehicles (i.e., passenger cars and small pick-up trucks)
2. The suspension components, involving in this study are one semi-elliptic leaf spring, one damper, and one shackle.
3. Ride comfort evaluation is based on ISO 2631 standard

1.4. Obtained Results

1. Relationship between ride characteristic of vehicle and design parameters of suspension system is achieved.

2. New verified criteria of automotive suspension components design, based on predicted value of ride comfort is proposed.

3. Approved simple method of automotive ride comfort investigation in the field experiment.

1.5. Research Operating Structure

The structure of research operation is divided into three phases as follows,

Phase 1

1. Study of past research and theory relating to ride comfort evaluation and applications

2. Revision of ride characteristic of vehicles and suspension systems

3. Study of data analysis and data processing for ride comfort investigation

Phase 2

1. Set up data collection system and related equipment i.e., accelerometers, data logger

2. Perform the preliminary testing

3. Practice Ride evaluation method with collected data, based on ISO Standard

Phase 3

1. Study of leaf spring characteristic.

2. Build up quarter car model and sub-system, representing suspension properties of leaf spring.

3. Investigate the effect of suspension parameters on ride comfort from simulating model.

1.6. Outline of the Thesis

This thesis contains seven chapters. Chapter 1 is a comprehensive introduction of the thesis. Chapter 2 focuses on literature review to describe past studies on related topics. In this chapter, the principal concepts such as ride comfort and fundamental theories are also introduced. Chapter 3 will summarize the methodology of the whole thesis including the research construction and relevant analyzing tools. Chapter 4

consists of the content of the preliminary study on field testing. Some results will also be presented in this chapter. Chapter 5 reviews the leaf spring modeling description and its verification process. Chapter 6 is a major part of the thesis. It provides details on parametric study of suspension model's parameter and the effects on ride comfort. Chapter 7 reviews the summary, final conclusion and further recommendation of this research.



ศูนย์วิทยทรัพยากร
จุฬาลงกรณ์มหาวิทยาลัย

CHAPTER II

LITERATURE REVIEW

In this chapter, the literature review is presented to describe past studies on related topics. The principal concepts such as ride comfort and fundamental theories which the suspension system and the leaf spring model are based on are also introduced.

Concepts and Relevant Theory

The concepts of ride comfort, the basic tool for ride evaluation and the “three link equivalent” model are presented below. The nonlinear effects and hysteresis phenomena are also discussed in the following topics.

2.1. Ride Comfort

Ride comfort is sensation of human relevant to vibration, noises and motions of a traveling vehicle, experienced by the driver and the passengers. In this research, ride comfort is used as the technical evaluation of dynamic quantities which are the motions of the vehicle. This evaluation method is based on human reactions to these dynamic quantities. There have been many studies concerning about the evaluation methods; e.g., various kinds of weighting curves, evaluation formulas and statistical approach. From the past, ride comfort has been taken into account as one of the important factors in cruising environment. It is mainly related to the amount of vibration exposure perceived by driver and passengers during the journey.

Vibration as an input from natural sources, initially produced from road irregularities can transmit to human body through the interfacing points such as floor and seat, subjected to body postures. This contributes the feeling of discomfort and also the effect on health and motion sickness. There have been many researches and studies involving the methods of ride comfort evaluation and their applications. Ride comfort can be assessed and evaluated in many ways. A general approach is to correlate dynamic parameters (i.e., accelerations and velocity), measured from traveling

vehicles (objective testing) and the level of comfort/discomfort, based on passengers' judgment (subjective testing).

2.1.1. Definitions

The Society of Automotive Engineers stated the ride comfort description as “ride is a subjective perception, normally associated with the level of comfort experienced when traveling in a vehicle”. However, the definition for the term cannot be specifically made and the methods of measurement are also subjective. Typically, ride comfort can be evaluated by subjective comments based on passengers' perceptions which are different for each individual. In practical, human can sense so many factors in the environment. In addition, the limitation of physical human senses that vary from time to time can lead to the lack of accuracy as the drivers or the passengers sometimes cannot notice the difference of different rides. It is also difficult to control the test conditions and keep the driving manner exactly the same from run to run when field testing is performed.

The ISO 5805 standard [2] gives the definition of the relevant terms as follows,

- Ride: “measurable motion environments (including vibration shocks, translational and rotational accelerations) as experienced by people in or on a vehicle”
- Ride quality: “degree to which the whole subjective experience (including the motion environment and associated factors) of a journey or ensemble of journeys by vehicle is perceived and rated as favorable or unfavorable by passengers or operators”
- Comfort: “subjective state of well-being or absence of mechanical disturbance in relation to the induced environment (concerning mechanical vibration or repetitive shocks)”

2.1.2. Ride Characteristic of Vehicles

Random vibrations in form of broadband spectrum usually occur when the vehicles are traveling on the road at high speed. The spectrum may be divided into two different categories, lying in two frequencies ranges. The natural vibrations in vehicles generally contain both ride and noise, so it is not easy to consider them separately. The "ride" vibrations are defined in the range of 0-25 Hz while "noise" is in the range of 25-20,000 Hz. Vehicle is a dynamic system that gives response in the form of vibrations to the excitation inputs and these vibrations can be perceived by the operator as well as the passengers exposed to them. As a kind of dynamic response (subjected to the characteristics of vehicle structures and the excitation inputs), vibration is a very important indicators or criteria to determine comfort or quality of the vehicle which is based on judgment or perception of individuals. Vehicle ride quality is concerned with feelings and senses of driver and passengers experienced while traveling on a vehicle. Within the ride, the amount of vibration is related to the movement and dynamic of vehicle's body as well as its components.

Vehicle systems give response to their excitation inputs. Some of them respond in a linear manner to the increasing excitation. However, with the nonlinear property of some components such as suspension components i.e., leaf springs, this sometimes leads to the appearance of the nonlinear behaviors. Past research has shown that heavy vehicle ride is most sensitive to excitations of the low frequency modes in the range of 1-8 Hz. In general, the cars are designed to reduce the road inputs transmission at the most sensitive frequency (about 4-8 Hz) which are known as the resonant frequency range with human abdomen. By this requirement, the car body generally produces a resonant frequency at about 1-2 Hz and the wheel hop resonance usually occurs at about 10-15 Hz. From Fig.2-1, vehicle systems can be considered as mechanical filters. The road roughness in the form of acceleration spectrum passes through the suspension system which behaves as a filter and results in the acceleration spectrum of a car's body. This transmission gain is the frequency response of the vehicle.

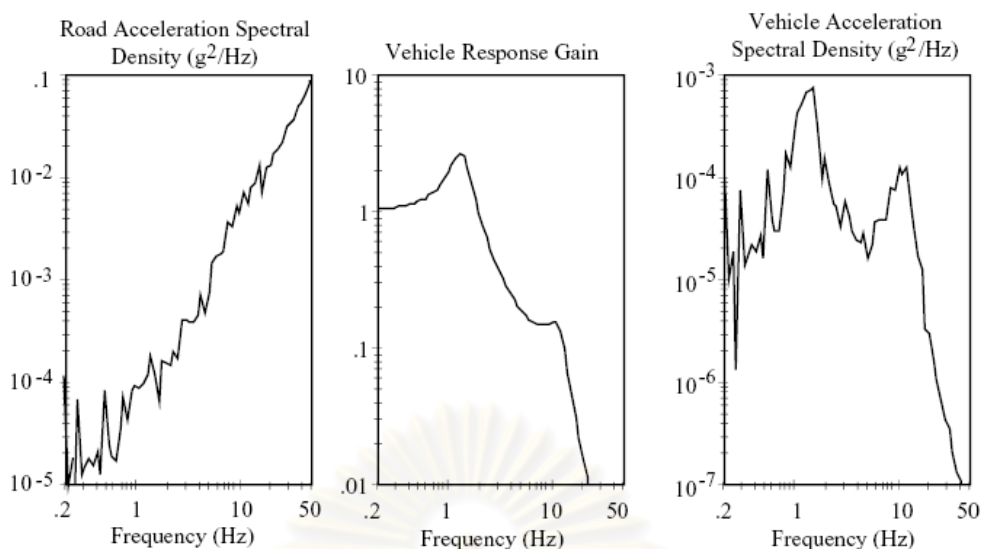
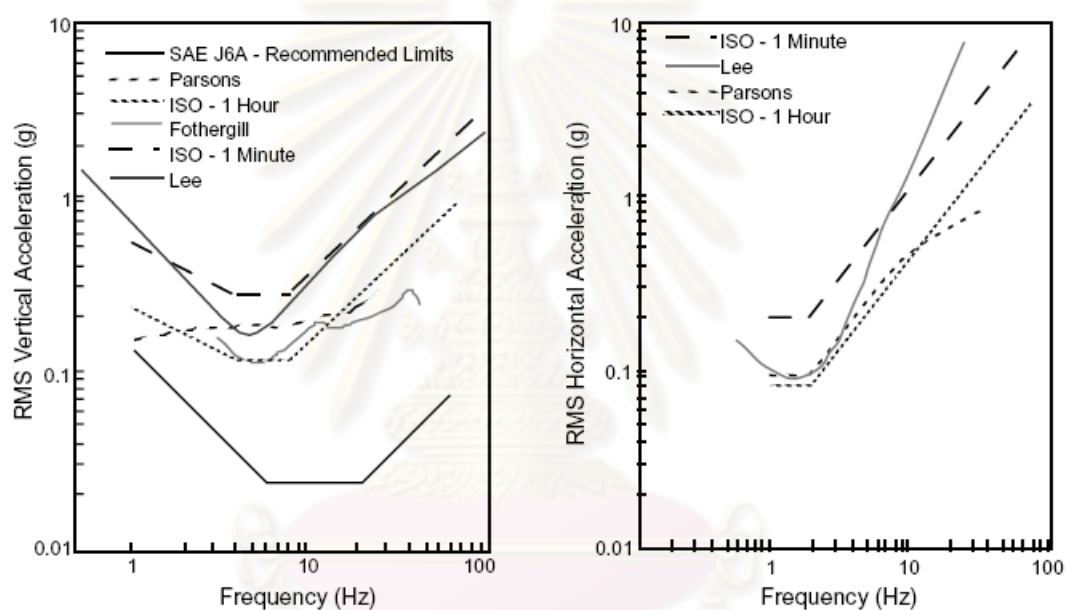


Fig.2-1 The vibration isolation property of vehicle suspension [3]

2.1.3. Application of Ride Comfort in Automotive Field

Nowadays, ride comfort evaluation becomes a very useful tool for application in many purposes. At some stage, with acceptable Gain assumptions, it is used as a guideline for automotive parts design. In the field of automotive, the ride comfort measurement systems were designed and carried out upon various kind of vehicles, ranged from motor scooter [4], wheel chair [5], passenger cars, public transport; i.e., trains and city buses to off-road vehicles and heavy trucks. Numbers of researchers carried out their works towards the goal to reduce the amount of vibration occurring during the ride. The human-interfaced components such as vehicles seats where the whole-body vibration transmits to the drivers' body through the contact points/area were closely examined. For example, Johan Lindén [6] has conducted "the test method for Ride Comfort Evaluation of Truck Seats" to improve quality and design. In his study, different seat prototypes, both suspended and non-suspended types were used to give different seat dynamic characteristics. The methods for ride comfort evaluation, based on his literature survey were revised and finally found two suitable approaches applicable with obtained data, based on acceleration and pressure distribution measurement. The evaluated objective results correlated well with subjective opinions. Seat vibrations have been conducted into a number of researches. Fig.2-2(a), (b) illustrates the human tolerance

limits to vertical and horizontal acceleration, respectively based on different method of evaluation and studies. However, vibrations are generated and transmitted from part to part all over the vehicle during the ride. Whole-body vibration takes place when human body is supported or in contact with any vibrating surface such as seat back. Vibrations appearing at the other parts such as floor and steering wheel are also found to have significant effect on ride perception of passengers. The discomfort boundary contour, based on experimental study and investigation of the floor vibration is shown in Fig.2-2(c).



Figs.2-2(a) - (b) Recommended vibration tolerance limits of a seated person based on different studies [7]

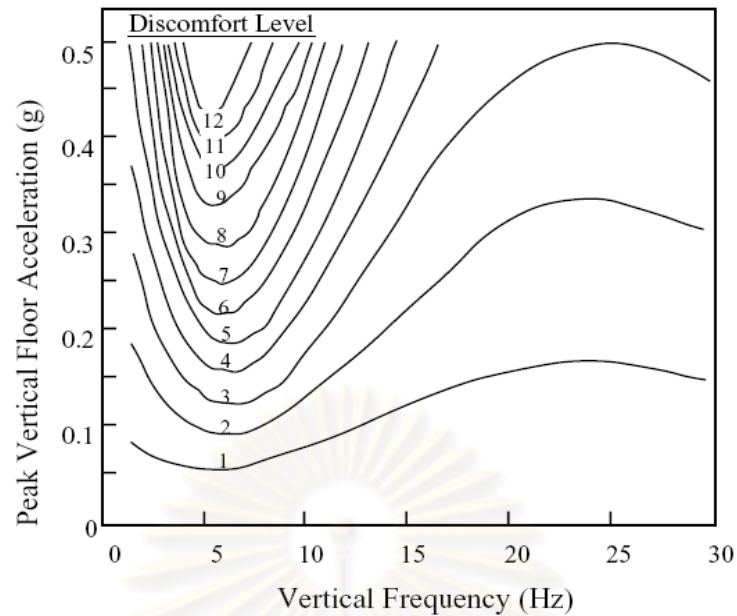


Fig.2-2(c) The discomfort boundary contour based on vertical floor accelerations [7]

2.1.4. Ride Comfort Measurement

Typically, ride comfort of a vehicle is quantified by the amount of acceleration measured at the seat or other body interface points during the operation of the vehicle. Among the existing approach to measure ride comfort of vehicles, on purposes of the improvement in driving quality or even the minimization of human health risks caused by vibration hazard, the objective information is generally obtained either by the field test in real driving situation or the proper use of ride comfort evaluation standard such as ISO 2631. In real situation, the vehicles must experience random input from road irregularities which is very unpredictable and complex. The drivers are also subjected to the other elements such as light, sound, and any other factors far from concern such as age, gender, physical abilities of the operators, etc. For such a reason mentioned above, the good use of computational simulation has been introduced and used to eliminate all difficulties and allows users to closely examine the specific factors of their interests. In simulation environment, the virtual models that represents the dynamic characteristics of particular system (vehicles suspensions, tire, seats etc.) are exposed to the road profile input (pulse, step, ramp, pure sinusoidal at single frequency, white noise) that can be created from simulation program such as Simulink. However,

different methods have both advantage and disadvantage points. Real experiment might lack of repeatability of data, due to the effects from uncontrollable factors while the precise models that can represent most of system characteristics might encounter some limitations and needed to be taken into account. Therefore, Trade-off and comparison of the results obtained from both methods should be worth wide in term of verification.

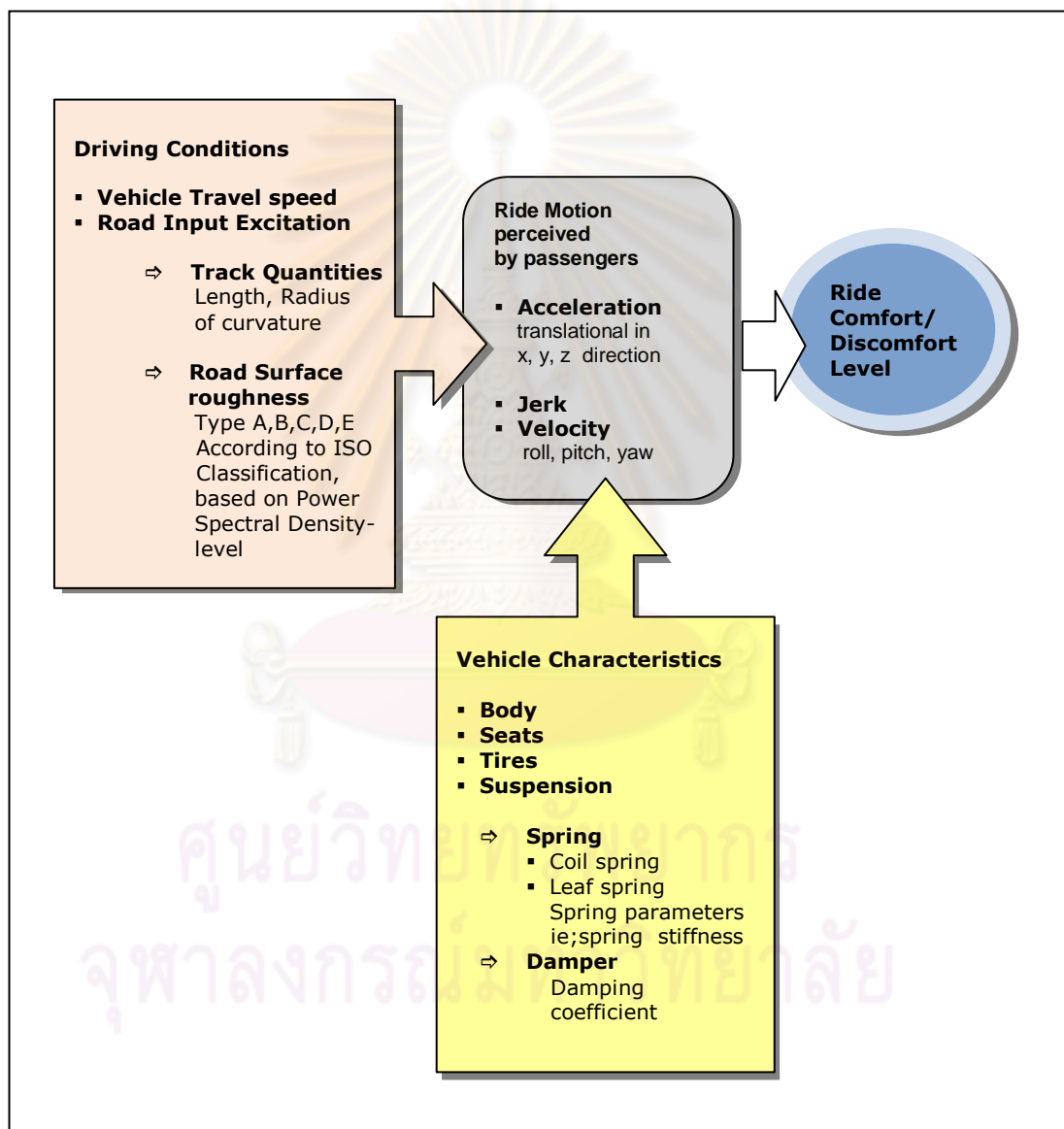


Fig.2-3 Ride comfort model

2.1.4.1. Objective Measurement

Traditional method to run an objective test in the field experiment, the vehicle is driven on long-distance test tracks or real existing road sections. As mentioned before, the drivers are subjected to many factors including the unpredictable sources of discomfort within real driving situation. These uncontrollable factors sometimes cannot be identified and hence result in large variation of data, due to the lack of data repeatability. For the research being carried in this thesis, the field experiment is not the main task of primary concern and the main objective investigations are based on simulation through Simulink models. After the relation between characteristic of vehicle and design parameters of leaf spring is found, the result can be developed to a new verified criteria of automotive suspension components design and the simplification of the test procedure in field experiment.

2.1.4.2. Subjective Measurement

Subjective measurement is a method to observe the information in the form of opinion and judgment. This method has been used in evaluation process of ride comfort traditionally. In the past, this technique was used to compare ride quality among different vehicles. The well-designed testing scheme and suitable amount of test subjects (jury) should be planned. In the procedure, the trained jury, in a traveling vehicle was asked to rate the ride comfort level, subjected to various conditions of road surfaces. The example of rating panel is shown in Fig.2-4(a) - (c). With determination of correlation between subjective ratings and measured quantities obtained in the field experiment, the ride quality and comfort/discomfort level of different vehicles can be compared.

1	2	3	4	5	6	7	8	9	10	
UNACCEPTABLE				BORDER LINE	ACCEPTABLE					
CONDITION NOTED BY										
ALL OBSERVERS		MOST OBSERVERS		SOME OBSERVERS		CRITICAL OBSERVERS		TRAINED OBSERVERS		NOT OBSERVED
INTOLER-ABLE	SE-VERE	VERY POOR	POOR	MARGINAL	BARELY ACCEPT.	FAIR	GOOD	VERY GOOD	EXCELLENT	
1	2	3	4	5	6	7	8	9	10	

Fig.2-4(a) SAE recommended practice for subjective rating scale for evaluation of noise and ride comfort characteristics related to motor vehicle tires [8]

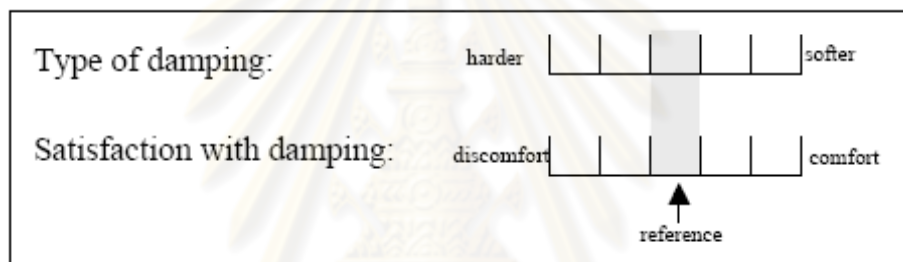


Fig.2-4(b) Subjective rating scale with separated opinion questions on property of vehicle component

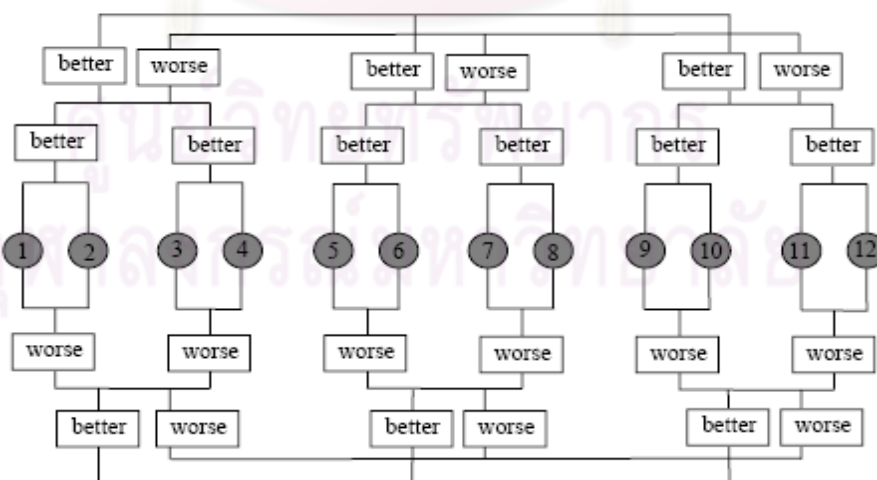


Fig.2-4(c) Schedule of the “couple by couple” method to rank 12 different vehicles

2.1.5. Ride Comfort Standards

Various standards to evaluate ride comfort level, based on field study and statistic approach were proposed. Current standards that provide the measuring methods and evaluation for ride comfort from Whole body vibration are ISO 2631 and BS 6841. ISO 2631 was first published in 1974 with the purpose of giving “numerical values for limits of exposure for vibrations transmitted from solid surfaces to the human body in the frequency range 1 to 80 Hz” [9] and had been revised and republished in a few editions before the present version (1997). BS 6841 was published in 1987 against the failure of ISO 2631 in Britain. ISO 2631 standard proposed the whole vibration exposure limits for human and the method to calculate the comfort contours while BS 6841 provides procedure in evaluation method and measurement, based on frequency weighting technique and the vibration dose value, (VDV). However, the application of ISO standard has been revised by number of researchers. The validation of the evaluation methods based on different experimental schemes were established. From the revision of Griffin [10], “On the Comparison of Standard Methods for Predicting the Hazards of Whole-body Vibration”, he made a comment that the standard were not clear in several points in evaluation method such as the determination of body postures and axes to be assessed or which kind of vibrations, the worst axis or overall vibrations in all directions the evaluation in multi-axis should be based on. Therefore, the use of evaluation method is based on the user’s determination.

The well known and widely used are ISO 2631-1, 1997 “Mechanical Vibration and Shock-the evaluation of human exposure to Whole-Body vibration”[11] and BS6841,1987 “Measurement and Evaluation of Human Exposure to Whole-Body Mechanical Vibration and Repeated Shock”[12]. These standards provide methods to process the measured quantities (normally captured in signal forms) and transform them into a single number which represents the level of ride comfort/discomfort in order to be compared with standard criteria in which the acceptable values or limits are indicated as a boundary. In the standard there were also different limits depending on the role of the passenger. The fatigue decreased proficiency boundary applies to workers, the exposure limit ensures that people are not physically harmed and the reduced comfort

boundary pertains to passengers and tasks such as reading. The examples are fatigue-decreased proficiency limits, based on vibration exposure time (Fig.2-5) and an approximate comfort/discomfort scale, based on magnitude of overall vibration (Table 2-1). In this research, the quarter car model with sub-system, representing the characteristics of nonlinear suspension of a light commercial vehicle was used to investigate the effect of parameters settings for leaf spring on ride comfort. The evaluation method provided by ISO 2631 was applied with these objective results.

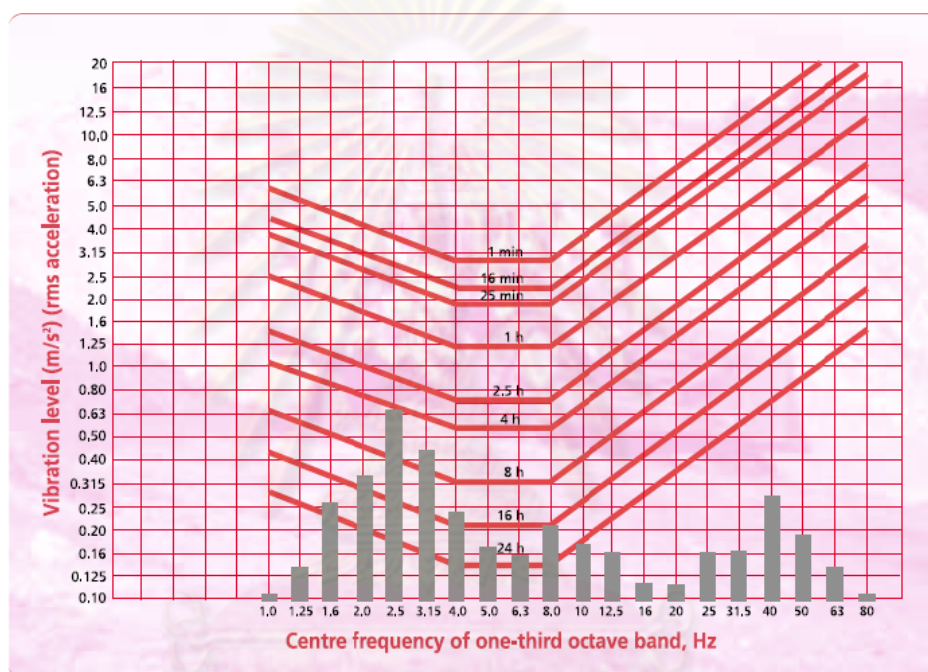


Fig.2-5 Standard criteria limits as a function of frequency and exposure time for vibration in vertical direction [9]

Less than 0.315 m/s^2 :	not uncomfortable
0.315 m/s^2 to 0.63 m/s^2 :	a little uncomfortable
0.5 m/s^2 to 1 m/s^2 :	fairy uncomfortable
0.8 m/s^2 to 1.6 m/s^2 :	uncomfortable
1.25 m/s^2 to 2.5 m/s^2 :	very uncomfortable
Greater than 2 m/s^2 :	extremely uncomfortable

Table 2-1 ISO 2631 approximate comfort/discomfort scale based on magnitude of overall vibration [11]

2.1.5.1. ISO 2631-1 General Requirements

In this research, general experimental setup and evaluation methods are based on this part of ISO 2631. Methods for the measurement of periodic, random and transient whole-body vibration is well defined as well as the principal factors that combine to determine the degree to which a vibration exposure will be acceptable. According to the guideline appearing in this section, the frequency range considered is 0.5 Hz to 80 Hz for health, comfort and perception and 0.1 Hz to 0.5 Hz for motion sickness. This part of ISO 2631 is applicable to motion transmitted to the human body as a whole-body vibration through the supporting surfaces or interface points such as the feet of a standing person, the buttocks, back and feet of a seated person or the supporting area of a recumbent person. The other parts in ISO 2631 series are ISO 2631-2 Whole Body Vibration in Buildings, ISO 2631-3 Motion Sickness, ISO 2631-4 Whole Body Vibration in Transport, and ISO 2631-5 Response to Multiple Shocks.

2.1.5.2. Basic Ride Comfort Evaluation Methods

Basic method to evaluate comfort is based on Power spectral density analysis, root mean square value (RMS), and frequency weightings. The introduction of each term is given as follows.

2.1.5.2.1. Power Spectral Density (PSD) Analysis

Power spectral density is a basic analyzing method to describe the events lying in frequency contents. It shows the amount of power contained in each spectral component of a signal. PSD is the frequency response of a random signal such as white noise. In general, random signals such as road irregularities have power distribution in all frequency components so that the white noise signal tends to give a flat PSD spectrum. The general units are acceleration (G^2/Hz) versus frequency (Hz) and the acceleration can also be represented by metric units such as $(m/sec^2)^2 / Hz$.

PSD of a random signal in time domain $x(t)$ can be expressed in the following forms,

1. The average of the Fourier transform magnitude squared in long time interval.

$$S_x(f) = \lim_{T \rightarrow \infty} E \left\{ \frac{1}{2T} \left| \int_{-T}^T x(t) e^{-j2\pi f t} dt \right|^2 \right\} \quad 2-1$$

2. The Fourier transform of the auto-correlation function

$$S_x(f) = \int_{-T}^T R_x(\tau) e^{-j2\pi f t} dt \quad 2-2$$

Where

$$R_x(\tau) = E\{x(t)x^*(t + \tau)\} \quad 2-3$$

and the power of a random signal over a given frequency band can be calculated as the following,

Total power of a random signal $x(t)$,

$$P = \int_{-\infty}^{\infty} S_x(f) df \quad 2-4$$

Power of signal $x(t)$ in frequency range f_1 - f_2 ,

$$P_{12} = \int_{f_1}^{f_2} S_x(f) df \quad 2-5$$

Conceptually, a PSD of a signal is the partial derivative of the mean square of the signal with respect to frequency, such that

$$\int_0^{\infty} G_{xx}(f) df = \sigma_x^2 + u_x^2 \quad 2-6$$

Where G_{xx} is the PSD of a variable x , f is circular frequency, σ_x^2 is the variance of x , and u_x is the mean value of x . When considering vehicle responses, the mean values of the variables of interest are either zero by definition, or they are set to zero as a part of routine data processing. With u , identically zero, the mean square value is equal to the variance, and the root-mean-square (RMS) value is equal to the standard deviation.

2.1.5.2.2. RMS Accelerations

Root-mean-square acceleration in each direction shall be used to determine the frequency weighted value, according to the evaluation method described by ISO 2631-1. The weighted RMS acceleration in three principal directions can be combined together to give the total value as well as the addition of the rotational vibrations. The root mean square value is determined as follows,

$$RMS = \sqrt{\frac{1}{N} \sum_{n=1}^N a_n^2} \quad 2-7$$

Where a_n is the sampled acceleration data

2.1.5.2.3. Frequency-Based Weighting Technique of Acceleration Spectra

Most ride comfort criteria standards, including ISO 2631 proposed the human sensitivity to vibration in term of frequency function. Different kinds of frequency weighting functions were defined to apply with the measured vibration spectra. The general ride weighted index can be defined as the frequency weighted root mean square value. The acceleration was frequency-weighted using the frequency weightings defined in ISO 2631-1 [11].

$$a_w = \sqrt{\int_0^{f_m} w(f)P(f)df} \quad 2-8$$

Where a_w is denoted as the weighted acceleration signal.

$w(f)$ is the weighting function.

$P(f)$ is the auto spectral density of the ride acceleration signal.

f_m is the highest frequency of interest.

According to ISO 2631-1 standard, the acceleration signal may be analyzed and reported as constant bandwidth or proportional bandwidth (e.g. one-third octave band) spectra of unweighted acceleration. The frequency-weighted RMS acceleration shall be determined by weighting and appropriate addition of narrow band of one-third octave band data. The weighted factors tabulated in table A-1(given in appendix A) shall be

used and the overall weighted acceleration can be calculated from the following equation,

$$a_w = [\sum_i (w_i a_i)^2]^{\frac{1}{2}} \quad 2-9$$

Where a_w is the frequency weighted acceleration.

w_i is the weighted function in each direction, i.e., vertical(z) and lateral(x, y) according to the definition of Basicentric axes of the human body shown in Fig.2-6. For seated persons, w_d is applied to vibration at supporting surface in lateral (x, y) direction while w_k is applied to vibration in vertical(z) direction a_i is the RMS acceleration for the i^{th} one-third octave band.

Vibrations in more than one direction can be combined as total value of weighted RMS acceleration. The amount under determination in orthogonal coordinates shall be obtained from the equation below,

$$a_v = (k_x^2 a_{wx}^2 + k_y^2 a_{wy}^2 + k_z^2 a_{wz}^2)^{\frac{1}{2}} \quad 2-10$$

Where a_v is the total value of weighted RMS acceleration.

a_{wx}, a_{wy}, a_{wz} are the weighted RMS accelerations in the orthogonal axes x, y, z, respectively.

k_x, k_y, k_z are multiplying factors. For seated persons, $k_x = k_y = k_z = 1$

ศูนย์วิทยทรัพยากร
จุฬาลงกรณ์มหาวิทยาลัย

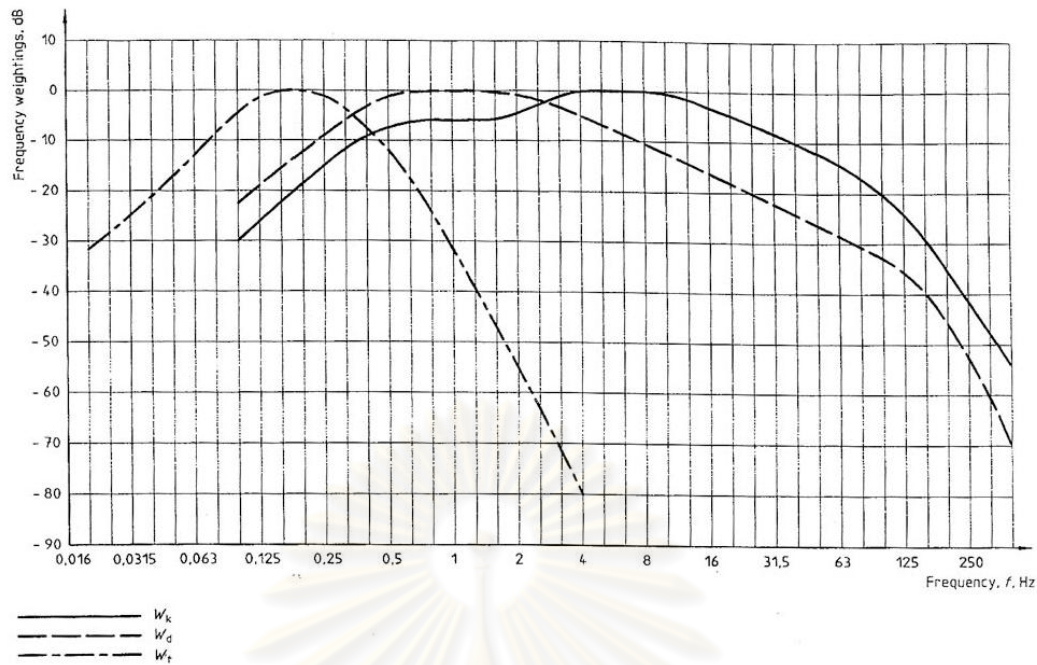


Fig.2-6 Frequency weighting curves for the principle weightings [9]

2.2. Leaf Spring

Spring is a component of the machine that treats as an absorbing element to support vibrations and shocks. This property allows flexibility for spring when the external force is applied and restore back to its initial state when the force is released. Leaf spring is a special kind of spring used in vehicle to carry loads and support chassis frame at which the high fatigue load is found. Springs are included in the suspension system of a car in order to reduce and control body roll and to keep the wheels in contact with the ground. Springs are placed between the wheels and the vehicle body so that the body is partially isolated from the axle. There are two basic types of springs which are constant rate (linear) type and progressive rate (nonlinear) type. The constant rate spring is predictable in its rating. In other words, it requires a constant amount of weight to compress it a constant number of inches. With the progressive rate or nonlinear spring, the more it is compressed, the stiffer it gets. Leaf springs are generally nonlinear or progressive rate in nature. But they can be operated in a linear (constant rate) range under the condition to compress to a certain amount and then are only used

in a certain range of deflection, for example, 2½ or 3 inches of travel. This range of travel and compression can be rated and the spring's reaction can then be predictable. But if that spring is overloaded, its rating will go up drastically and change the predictability of handling. Theoretically, leaf spring has better stress distribution than any other types of spring.

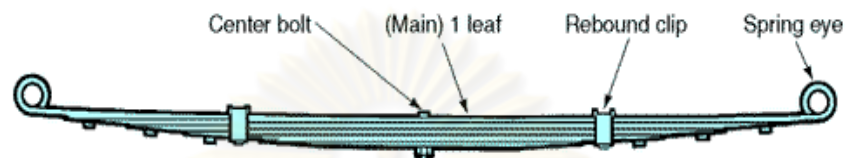
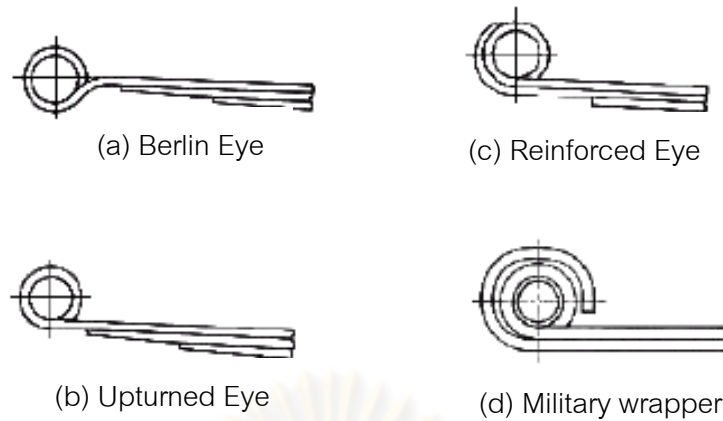


Fig.2-7 Leaf spring components and construction

Leaf spring is composed of four main components as shown in Fig.2-7 which are briefly described as follows,

1. Spring leaves: Spring leaves are flat sheets which are made from cold drawn steel. They are simply held together as a stack by a center bolt and fastened by two rebound clips. The spring leaves are made from tempered steel with one of the following width: 35, 40, 45, 50, 55, 60, 65, 70, 75, 80, 90, 100, 110, 120, and 140 mm, and one of the following thickness: 3, 3.5, 4, 4.5, 5, 5.5, 6, 6.5, 7, 8, 9, 10, 11, 12, 14, 16, and 20 mm. In a set of spring leaves, they are different in length and the longest one is called the main leaf. The measurement of distance between leaves should be made at the point located at 10 mm. away from the leaf edge. The leaf end may be produced in different shapes, as shown in Figs.2-11(a) - (d).

2. Spring eyes: Spring eyes are the loops formed at both ends of the main leaf. They are used to mount the leaf spring with the vehicle frame. There are different design of spring eyes, according to the guidance available in the Spring Design Manual [1]. Some examples of them are given in Figs.2-8(a) - (d). Some springs have the ends of the second leaf rolled around the eyes of the main leaf, as reinforcement. This leaf is called the wrap leaf (Figs.2-8(c),(d)).



Figs.2-8(a) - (d) Different design of leaf spring eyes [1]

3. Center bolt: Center bolt is a screw pin that passes through a hole in the center of each leaf. It is also used to locate the axle on the spring.



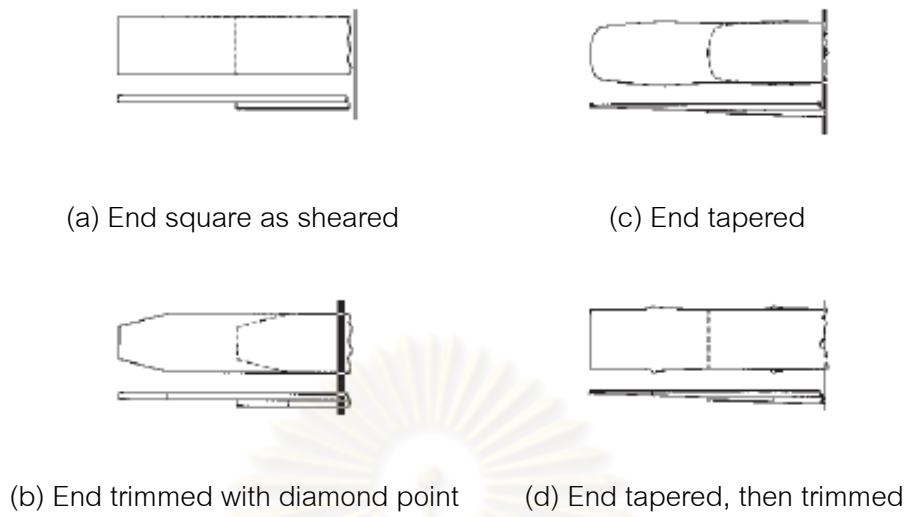
Fig.2-9 Center bolt

4. Rebound clips: Two rebound clips are U-shape parts that are formed at intervals around the leaves. They prevent excessive flexing of the main leaf during rebound, and also keep the leaves in alignment.



Fig.2-10 Rebound clips

There have been various design of leaf springs from the past as shown in Figs.2-12(a) - (f). The fully elliptic spring was used in coaches in the past days but now it is used in commercial vehicles while the three-quarter elliptic spring provides soft support but more rigidity. The most commonly used and the one that was investigated for this research is the half or semi-elliptic leaf spring (Fig.2-12(c)). It is the component of rear suspensions for car and both front and rear suspensions for heavy vehicle. The quarter-elliptic spring is used on small sports cars where a compact short spring is preferred. Transverse semi-elliptic springs are commonly used to form bottom, top, or both transverse link-arms for both front and rear independent suspensions. The cantilever-mounted semi-elliptic spring has been used in some cars such as the Jaguar for the rear suspension. The central pivot of this spring extends the effective spring length. The spring lies parallel and very close to the chassis, so that a compact and effective suspension is achieved. Leaf springs are also available as single rate or variable rate. Fig.2-13(a) shows a single rate spring while Fig.2-13(b) shows a variable rate spring both in unloaded and loaded configurations.



Figs.2-11(a) - (d) Types of leaf spring ends [1]

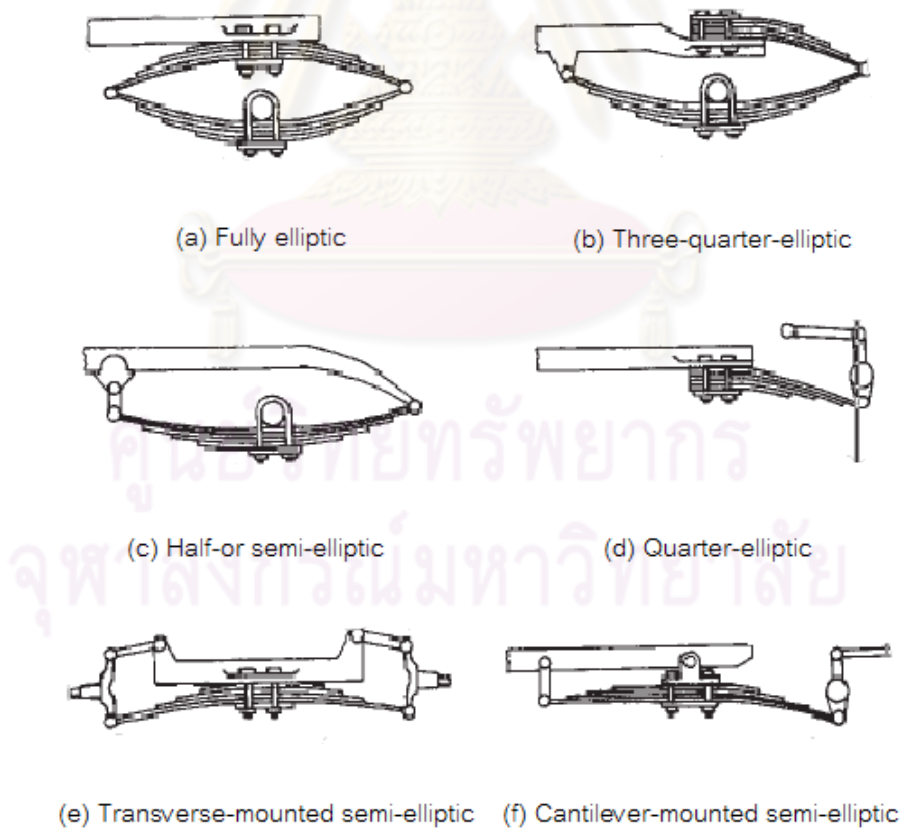


Fig.2-12(a) - (f) Leaf spring configurations [13]

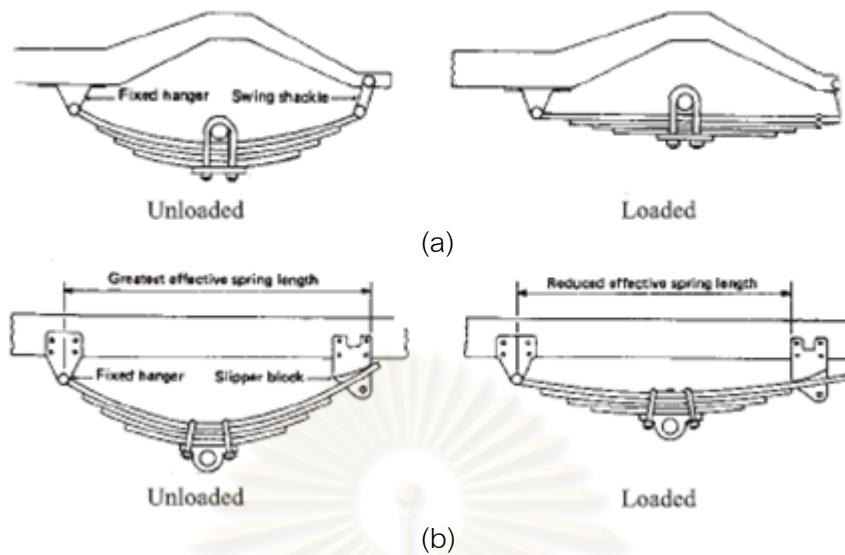


Fig.2-13(a) - (b) Single and variable rate leaf spring [13]

2.2.1. Characteristic of Leaf Spring

Leaf spring is an element which can be used as a structural component in vehicle suspension, providing strength to carry loads. In term of spring functions, it absorbs and stores energy, based on its maximum allowable stress which more or less is related to material properties and the design parameters. One advantage of leaf spring is that it has simple structure which does not require high technology for manufacturing and not-too-complicated installation. However, Leaf spring possesses some properties which make it become very complicated to analyze. For example, it contains both active and inactive parts such as spring eyes. This can result in less amount of energy to be stored within when the areas of inactive parts are considered. Moreover, the combination between other components required in the installation such as bushings and shackle and the Interleaf friction of the leaf spring itself leads to nonlinear relationship between applied load and leaf spring deflection about which shall be mentioned in the next section.

2.2.2. Interleaf Friction and Stick-slip Phenomena

The interleaf friction is the dry friction generated within the area between adjacent leaves of multi-leaf spring when moving in contact with each other. It produces friction force which dissipates energy and provides damping effect to vehicle suspension. This kind of nonlinear relationship can be described in a form of “hysteresis loop”. From the characteristic curve shown in Fig.2-14, as the leaf spring undergoes the increasing compressive load from its initial position, the deflection remains constant until the external applied force is large enough to overcome the friction force at contact surfaces and tends to be more responsive to the applied load by increasing towards the compression path. In the opposite way, the deflection drops sharply at the beginning and follows the release path while the applied load is decreasing. The direction of loads experienced by leaf spring changes during each cycle and is directly subjected to the shackle angle due to an installation effect which is explained in more details in section 2.2.3.

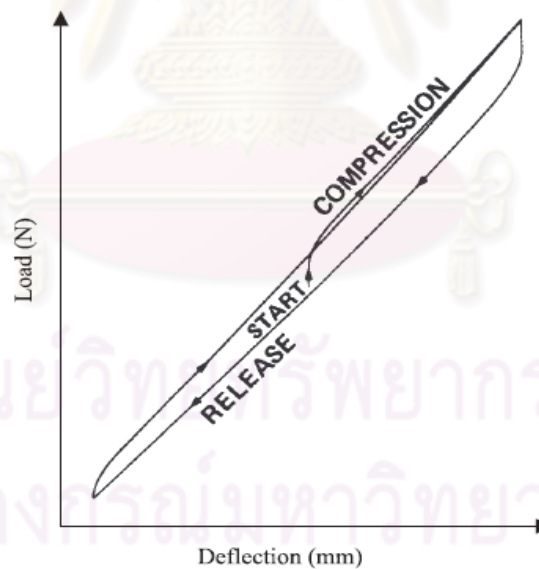


Fig.2-14 Load-deflection diagram of tested leaf spring [1]

The Stick-slip Phenomenon is usually caused by the dry friction between two surfaces when moving in contact, sticking with each other and sliding over each other,

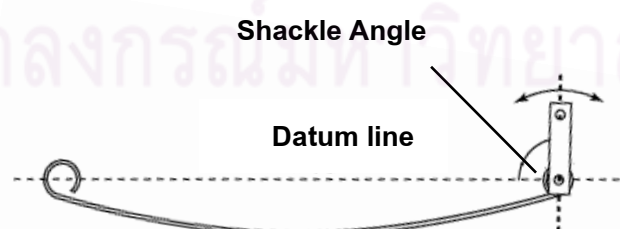
alternatively. In case of multi-leaf spring, stack of leaves contains numbers of flat bars which are held together with clamps and a centre bolt. When leaf spring is subjected to applied load, the relative movement between adjacent surfaces of leaves contributes to the friction force. Typically, the “stick” motion occurs when static friction coefficient between two surfaces is larger than the kinetic friction coefficient. The two adjacent leaves can start to “slip” or “slide” over each other at the point where the applied load is larger than static friction force. As a consequence, the objects are moving with corresponding kinetic friction which may result in the rapid increase in velocities of the movement.

2.2.3. Shackle Effects

As mentioned earlier in the previous section, the shackle angle selected for initial installation is one important factor which cannot be neglected. For a leaf spring installed as one end fixed and the other end shackled (Figs.2-15(a) - (b)), the function of shackle is to allow the leaf spring to move in an extra degree of freedom.



(a)



(b)

Figs.2-15(a) - (b) the Leaf spring configuration at installation

As a leaf spring deflects, its shape and curve starts to change and the shackle swings, making angle with the datum line. The shackle force exerted on leaf spring can either be compression or tension, depending on direction in which the shackle swings. If the shackle swings towards the fixed end of the leaf spring, it results in compressive load while it tends to produce tensile load as the shackle swings in the opposite direction. The maximum distance between two spring eyes is reached when the shackle alignment is perpendicular to the datum line, representing the flat spring with its full span of the entire length. The direction of the shackle swing also changes as well as direction of loading every time the shackle swings pass through this position. The other effect from the shackle angle is that when it is not perpendicular to the datum line, the shackle load possesses its component in longitudinal axis which can be either compression or tension, depending on the direction of the swinging motion as stated before. Under shackle tension, spring rate is increased while it is decreased when subjected to shackle compression.



ศูนย์วิทยทรัพยากร
จุฬาลงกรณ์มหาวิทยาลัย

CHAPTER III

RESEARCH METHODOLOGY

3.1. Description of Research Procedure

The assessment of ride comfort measurement and evaluation can be obtained by objective and subjective methods. The schematic diagram describing the overview of the whole working process and procedure is shown in Fig.3-1.

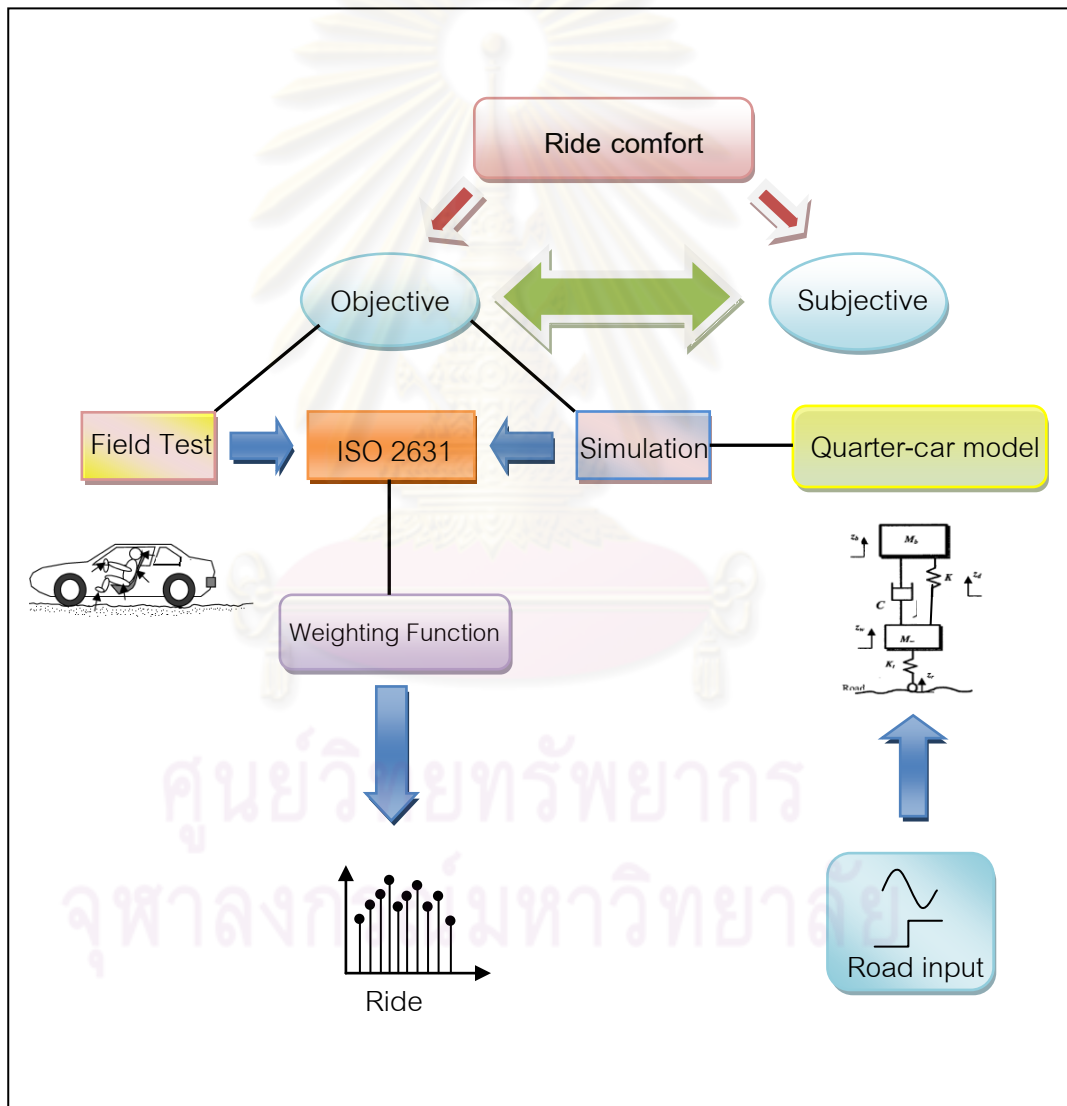


Fig.3-1 Schematic diagram of working procedure

From Fig.3-1, the objective experiments can be made by two measuring schemes, either simulation or field experiment. However, the relationship between ride comfort and suspension parameters was investigated by the first method for this research. The preliminary study was made once by field testing in order to study and practice ride comfort measurement. In the analyzing process, the application of ISO 2631-1 was also implemented as a tool for ride comfort evaluation. The results and detail, including discussion are given and reported in Chapter 4.

Another objective measuring scheme which is not a primary concern of this research is the real field experiment. In the test, the trained experts and the test subjects will rate ride comfort level for each test run. Different roads with various surface roughness and series of leaf springs with corresponding dampers will be used. However, this method was not conducted for this study. The early phase of the research was concerned with the investigation through computational simulation. With the help of MATLAB/SimMechanics program, a quarter car model was built with the main focus on its suspension properties and the investigation into the effect of suspension parameters on ride comfort level were observed similarly to what happened to the field experiment.

The description of a test scheme is given in Fig.3-1. In real situation, accelerations during the ride and other relevant data will be collected by the accelerometers mounted at human interfacing points, i.e., floor and seat. The raw data will be analyzed by using the evaluation method suggested by ISO 2631-1 such as RMS accelerations and weighting function. The ride index can be established from mean ride comfort level, rated by test subjects and parameters of leaf spring. In similar way, the process of simulation starts from road input which was generated by a simple road model. The acceleration response of vehicle can be obtained from the quarter-car model, corresponding to the applied road input and then ride comfort value for each ride was achieved by mean of frequency weighting of ISO 2631-1 standard.

3.2. Research Tools

The study required research tools for both simulation and field experiment so that they can be categorized into two categories as follows,

3.2.1. Field Experiment Tools

For real field test of the preliminary study, the accelerometers were used to collect raw data which are accelerations in different directions, both translational and rotational. One-axis accelerometers are used to measure acceleration in vertical direction. A three-axis typed accelerometer is used to measure accelerations in three orthogonal axes and a six-axis accelerometer is used to measure accelerations in three orthogonal axes with three rotational velocities (pitch, roll and yaw). These quantities were used to analyze the characteristic of the test vehicle and to evaluate ride comfort by mean of ISO standard. Apart from this, ride vision may also be captured by a video camera.

3.2.2. Simulation Tools

The main investigation of this research is based on simulation. The vehicle and suspension model were constructed and implemented on a computer program. MATLAB Simulink is very useful tool for vehicle modeling. For the simulation of leaf spring model, the results were also shown in animation mode so that the leaf spring configuration and behavior could be observed under consideration.

3.3. Methodology

The research methodology includes research approaches, data collecting, and definition of measured quantities are summarized in the following topics,

3.3.1. Data Collecting

In field testing, the accelerometers were attached to the proper positions of a test vehicle. Preparation was taken into account of the following consideration,

3.3.1.1. Measured quantities

When the vehicle is traveling along the road surfaces, vibrations are generated in all directions. The following quantities, related to the amount of vibrations are measured in the investigation. The illustration of measured quantities and directions of measure is shown in Fig.3-2.

1. longitudinal accelerations, A_x
2. lateral accelerations, A_y
3. vertical accelerations, A_z
4. roll velocity, R_x
5. yaw velocity, R_y
6. pitch velocity, R_z

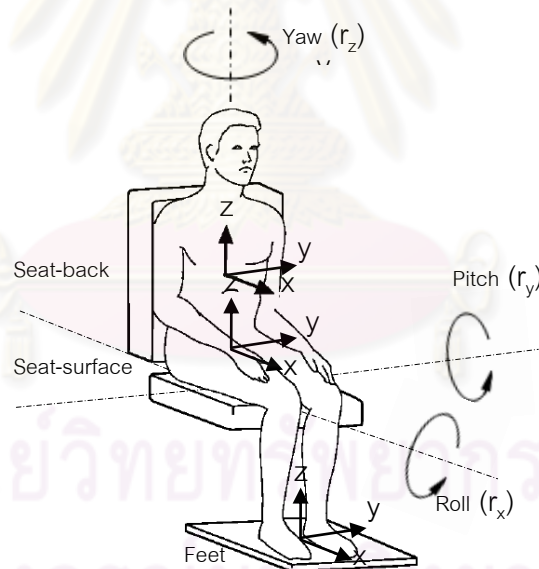


Fig.3-2 Basicentric axes of a seated person, adapted from ISO 2631-1 [11]

3.3.1.2. Sensor Positioning

According to the suggestion of ISO 2631 about transducer mounting, transducers should be attached at the contact area where vibration transmits to human

body. It also suggested that vibrations are measured orthogonally at that point as illustrated in Fig.3-2. In the measurements performed within this research, the selected locations are the points on seat-back area and floorboard and the attachment positions and method in mounting were also subjected to the architectural structure inside the test vehicle.

3.3.2. Data Analysis

The analysis performed within this research were based on two categories, the time domain analysis and the frequency analysis. The following description of the two methods are briefly explained,

3.3.2.1. Time Domain Analysis

The time domain analysis includes data processing of raw acceleration data recorded by data logger and numerical solving of simulating models by computer program. For computer simulation, the response of a dynamic system is predictable, using differential and algebraic equations that describe dynamic equilibrium state of the system. The equations of motion were solved to predict how the system variables change with time as response to inputs. Simulated results were interpreted in the same manner as experimentally measured responses.

3.3.2.2. Frequency Domain Analysis

Direct interpretation of vibrations from the acceleration time histories in time domain is sometimes rather difficult and lacks of essential information. Normally, vibrations are random in nature, so that the signal was generated from number of frequencies. Transformation of time domain data into frequency domain can give more information into the analysis as the frequency content can also be reviewed. The method of Fourier transform is widely used for this transformation process. For ride comfort evaluation, Power spectral density (PSD) method is used to describe the value

in term of RMS acceleration over a frequency range, according to the definition given in Eq. 2-8 and 2-10.

3.4. Summary of Research Approach

The study and investigation into the effect of suspension parameters on ride comfort of light commercial vehicles in this research is mainly based on computer simulation. However, the preliminary field test was performed by few test runs on road sections with different scenarios. During the rides, the acceleration signals were collected by a set of accelerometers and data logger. The data was analytically determined and processed within both time domain and frequency domain. The application of ride evaluating method suggested by ISO 2631-1 was then applied to the test data by the following steps,

1. RMS acceleration in each direction defined in section 3.3.1.1 and Fig.3-2 were calculated by PSD method according to Eq.2-8 and 2-10.

2. The total values of weighted acceleration obtained from calculation were compared with the values suggested by ISO 2631-1, approximate comfort/discomfort scale based on magnitude of overall vibration in Table 2-1.

3. The vibrations obtained from simulating model were determined only in vertical direction so that the values of a_{wx} and a_{wy} in Eq.2-10 were set to zero.

After the preliminary test was completed, the next phase of the research was focused on the investigation through the simulating models. The leaf spring model was constructed, regarding the effect of nonlinearities and friction. For this purpose, the three link equivalent model proposed by the Society of Automotive Engineering was developed and the effect of friction was also included with the additional part of the modified Dahl's model. The details on how the leaf spring was designed and constructed is given in Chapter 5. The leaf spring model includes the geometrical parameters and Dahl's model parameters which were adjusted by comparing the results obtained from real system measurement and the simulated results. A leaf spring test rig that can measure vertical static deflection of leaf spring under static loading condition

was designed and used for this purpose. Finally, the proposed model was verified with the adjusted parameters to satisfy the concordance of both results.

The next phase of the research was the parametric study of the suspension model and its effects on ride comfort. In the study, the quarter-car model was combined with the previous verified leaf spring model to represent whole suspension system of a vehicle that contains nonlinearities. Simple road model was also established to generate synthetic road input to the vehicle model, based on road classification of ISO 8608 [14]. The interest parameter taken into the study was the shackle angle at installation. From the study, ride comfort indices were established to represent the relationship between different values of shackle angle and ride number both for non-linear and linear suspension models (For linear model, the component of Dahl's model was excluded).

The content of each part of the study will be reviewed in the next three chapters. Chapter 4 provides details and results obtained from the preliminary study. Chapter 5 presents the leaf spring modeling description and its verification process. Chapter 6 contains details on parametric study of suspension model's parameters and their effects on ride comfort.



ศูนย์วิทยทรัพยากร
จุฬาลงกรณ์มหาวิทยาลัย

CHAPTER IV

PRELIMINARY TEST

The preliminary test was carried out in real driving environments. Few simple test runs were performed at Somboon Group's factory. Somboon Group is a manufacturer of vehicle parts, including leaf springs. Six rides were performed on roads within the factory and some section of Bangna-Trad road. Data was collected by the accelerometers mounted at various positions of a test vehicle and the visual ride events were also recorded by a video camera attached at the rear glass behind passenger seat. The measured data were processed both in time domain and frequency domain. The application of ride comfort evaluation suggested by ISO 2631 was applied and finally found that the calculated results agree with the data collected from each transducer.

4.1. Objective

1. To study and practice the ride comfort measurement, preparation and settings of the test instruments.
2. To collect the acceleration data and relevant information and bring to an analysis. The results from the application of ride comfort evaluation standard, ISO 2631 was examined and discussed.
3. To gain knowledge from real experiments and test environments in order to improve and adjust the test structure for further investigation.

4.2. Test Instruments

1. One six-axis accelerometer (Crossbow Technology MNAV Series)
2. Accelerometers (KYOWA Electronic Instruments Co., Ltd.), one of three-axis typed (20 G) and four single axis typed (10 G)
3. A data logger (KYOWA Electronics Instruments Co., Ltd.)
4. A video camera and a set of the vacuum suction holder arm

4.3. Tested Vehicle

The test vehicle for the investigation was TOYOTA CAMRY 2002 whose details are given in table 4-1



Fig.4-1 The tested vehicle used in the investigation

Model	CAMRY 2.4Q
Gear system	Automatic
Engine cc	2,400
Engine type	4 cylinders DOHC 16 valves
Steering	rack and pinion PAS
Doors	4
Width (mm)	1,810
Length (mm)	4,825
Height (mm)	1,500
Weight (Kg)	1,460

Table 4-1 Technical information of the tested vehicle

4.4. Sensors positioning

1. The six-axis (Cross bow) accelerometer was attached to the floor and the three-axis typed (Kyowa) was secured on the top of it. The position was at the back of the driver's seat (Fig.4-2(a)).

2. Four remaining accelerators which are single axis typed were mounted at four locations outside cabin to measure acceleration in vertical direction. The positions are at the top of shock-absorber (Fig.4-2(b) left top/FRT), the right front of the car (Fig.4-2(b) right top/FRB), the right corner on the floor inside the rear trunk(Fig.4-2(b) left bottom/RRT), and the rear right location near the wheel (Fig.4-2(b) right bottom/RRB).



Fig.4-2(a) Position of sensors installed within a cabin



Fig.4-2(b) Positions of sensors installed outside a cabin

3. A set of video camera and holder arm was attached to the rear glass within the cabin to record visual ride events that were experienced by a driver and passengers.



Fig.4-2(c) Attachment of a video camera

4.5. Testing Locations

The locations of testing are the road sections within Somboon Group's factory and Bangna-Trad Road, Km 5th to Km 7th. The graphical illustration of the test tracks are given in topic 4.7.

4.6. Driving Conditions

The driving situations are varied from straight track, curve, to road bumps, potholes, lids of water draining pipes, road gaps, etc.

4.7. Procedure

The investigations were performed by one driver and three passengers traveling in a car with a set of transducers. Six rides with multiple measurements were made. The floor accelerations in three orthogonal axes were collected by Kyowa (three-axis) and X-BOW (six-axis) accelerometers, the later one also measured the other rotational

velocities, i.e., roll, pitch, and yaw. Four single-axis accelerometers were measuring the vertical accelerations at the different positions of a traveling vehicle. During the rides, the driving environment was captured by a video camera from the rear glass position. The data collected by crossbow sensor was saved in a notebook and the other ones need to send signals into a data logger. The data collection for all sensors was started to record at the same time. The six-axis accelerometer was measuring with the sampling frequency of 50 Hz while the three-axis accelerometer was measuring with the sampling frequency of 200 Hz. Six test rides were performed on six road section with different scenario. The description and graphical illustrations are given below,

Case 1: Direct track driving over a road bump at speed 20 Km/hr within the factory's area

Case 2: One round completed driving around the factory at speed 30 Km/hr

Case 3: One round completed driving around the factory over lids of water draining pipes

Case 4: Direct track driving on Bangna-Trad road section between Km 15th to a petrol station at speed 80 Km/hr

Case 5 : Driving on Bangna-Trad road section between the petrol station at speed 50 Km/hr, turning back at U-turn and increasing speed to 100 Km/hr

Case 6: Driving over rough surface road track outside the factory's area at speed 20 Km/hr

ศูนย์วิทยพัทยากร
จุฬาลงกรณ์มหาวิทยาลัย

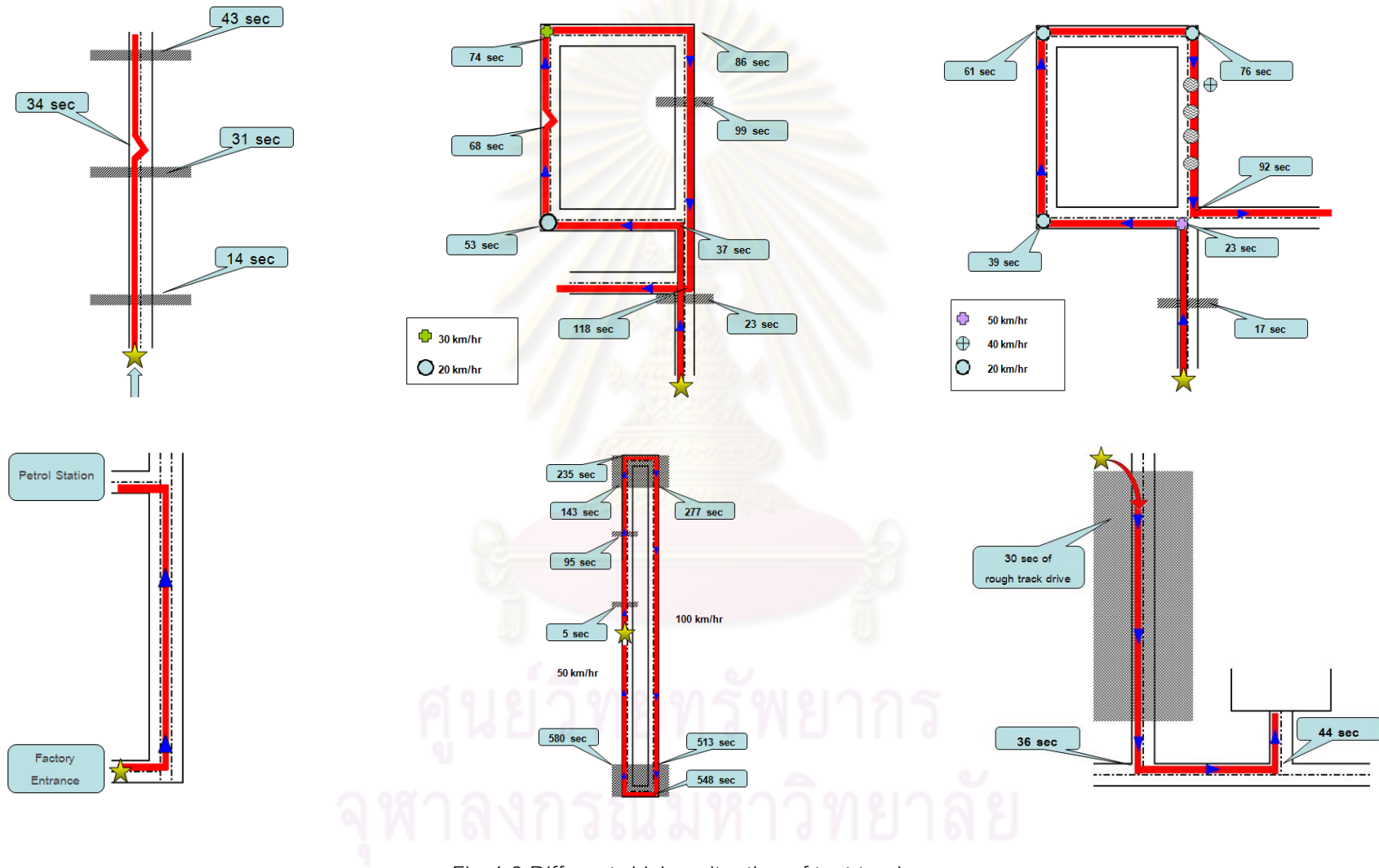


Fig.4-3 Different driving situation of test tracks

4.8. Data Analysis

The analysis of the data includes time domain and frequency domain analysis, which were performed on MATLAB program.

4.8.1. Time Domain Analysis

In this category, the raw data imported were displayed by a plot over time. This method allows the interpreter to notice the amplitude and direction of the acceleration over time. The method of interval root mean square was also employed by taking the group of data of the interested interval. It provides better information with ease of comparison. However, this approximation method can lead to error if the resolution of the data interval is not small enough. For the analysis of the reported results of this study, the raw data was divided into 100 intervals for the interval root mean square method.

4.8.2. Frequency Domain Analysis

Data analysis in frequency domain was performed by mean of PSD method which is based on Fast Fourier Transform (FFT) operation. This analysis allows the interpreter to see the components contained in a measured signal at different frequencies. For this study, the Periodogram technique was employed to estimate the average PSD of signals by Discrete Fourier Transform (DFT), using number of DFT at 1,024 and 256 points.

4.9. Results

For all sensors, acceleration data in time domain agree well with the ride event and the floor acceleration measured from different sensors were the same in all cases. In term of ride comfort evaluation, the frequency weighting technique and method to calculate the average ride comfort were applied to measured data. The results of the weighted RMS acceleration in each directions obtained from a six-axis accelerometer, both translational (A_{wx} , A_{wy} , A_{wz}), rotational (R_{wx} , R_{wy} , R_{wz}), and the total combination of

multi axial (A_v) are shown in table 4-2. The approximated level of ride comfort/ discomfort are represented by the letters a, b, c, d, and e which represents the level of comfort as “not uncomfortable”, “a little uncomfortable”, “fairly uncomfortable”, “uncomfortable”, and “very uncomfortable”, respectively. The results show that the amount of overall vibrations calculated from ISO evaluation method agree with the ride events and conditions of road surface in different cases.

4.9.1. Results of Time domain Analysis

From the comparison of the average root mean square values of the acceleration signals obtained from the X-BOW (six-axis) and Kyowa (three-axis) sensors, in case of direct track driving over a road bump at speed 20 Km/hr within the factory's area (case1) and case6 which was driving over rough surface road track outside the factory's area at speed 20 Km/hr, it is found that the RMS accelerations of case1 in fore-and-aft, lateral, and vertical directions from both sensors tend to agree with each other. The graphs shown in Fig.4-4(a) are the plots of raw data against time and the plots of 100-interval RMS acceleration over time of case1 while Fig.4-4(b) are those of case 6. The results from both sensors show good agreement in the same manner, i.e., they possess the highest peaks at the same point of time. For example in case1, the highest peaks for all three directions appeared at the 14th, 31st, and 43th second which were at the time of driving over a road bump. In case 6, it is found that the maximum swing appeared at the time interval from the first second to the 30th second which was at the time of driving over rough surface road. At the 36th and 44th, the car was turning left, so that the graph posses the high amplitude in positive-lateral direction as shown in Fig.4-4(b).

When considering rotational accelerations; i.e., roll, pitch and yaw, obtained from X-BOW(six-axis) sensors for case1 and case2 as shown in Fig.4-5, it is found that the graphs of roll for both cases possess the highest swing, the lower are in pitch and the lowest are in yaw directions. In case 2, the graphs swing with larger amplitude than those of case 1. From the graph of yaw in case 2, the amplitude tends to increase towards positive direction at the time when the car was turning left (the 37th second). At

the 53th, 74th, 86th, and 118th, the graph exhibits in similar manner but in opposite direction as the car was turning right.

The comparison was also made between the acceleration signals obtained from the other four single-axis accelerometers which were attached at four different positions outside a cabin and the signals obtained from X-BOW and Kyowa sensors which were attached at the positions within a cabin. All measured signals result in the same consequences, i.e., they possess the highest peak at the same point of time when the car was moving over a road bump as shown in Fig.4-6. The acceleration signal obtained from the sensor attached at the rear right back (RRB) of the test vehicle seems to exhibit the highest amplitude, among the results measured from the sensors at the other positions

4.9.2. Results of Frequency domain Analysis

In the frequency analysis, PSD results of the acceleration signals obtained from X-BOW and Kyowa sensors tend to agree with each other for both case 1 (smooth track) and case 6 (rough track) although the sampling frequencies of the two sensors are different. PSD results of the acceleration signals obtained from single-axis typed accelerometers for case 1 which is a smooth track exhibit the highest peak at the frequency around 10 Hz which is the natural frequency of wheel or unsprung mass, especially when road inputs are similar to white noise. It can be obviously seen from the signals measured at the FRB and RRB positions (see Fig.4-7).

ศูนย์วิจัยทรัพยากร
จุฬาลงกรณ์มหาวิทยาลัย

X-BOW (six-axis)

Kyowa (three-axis)

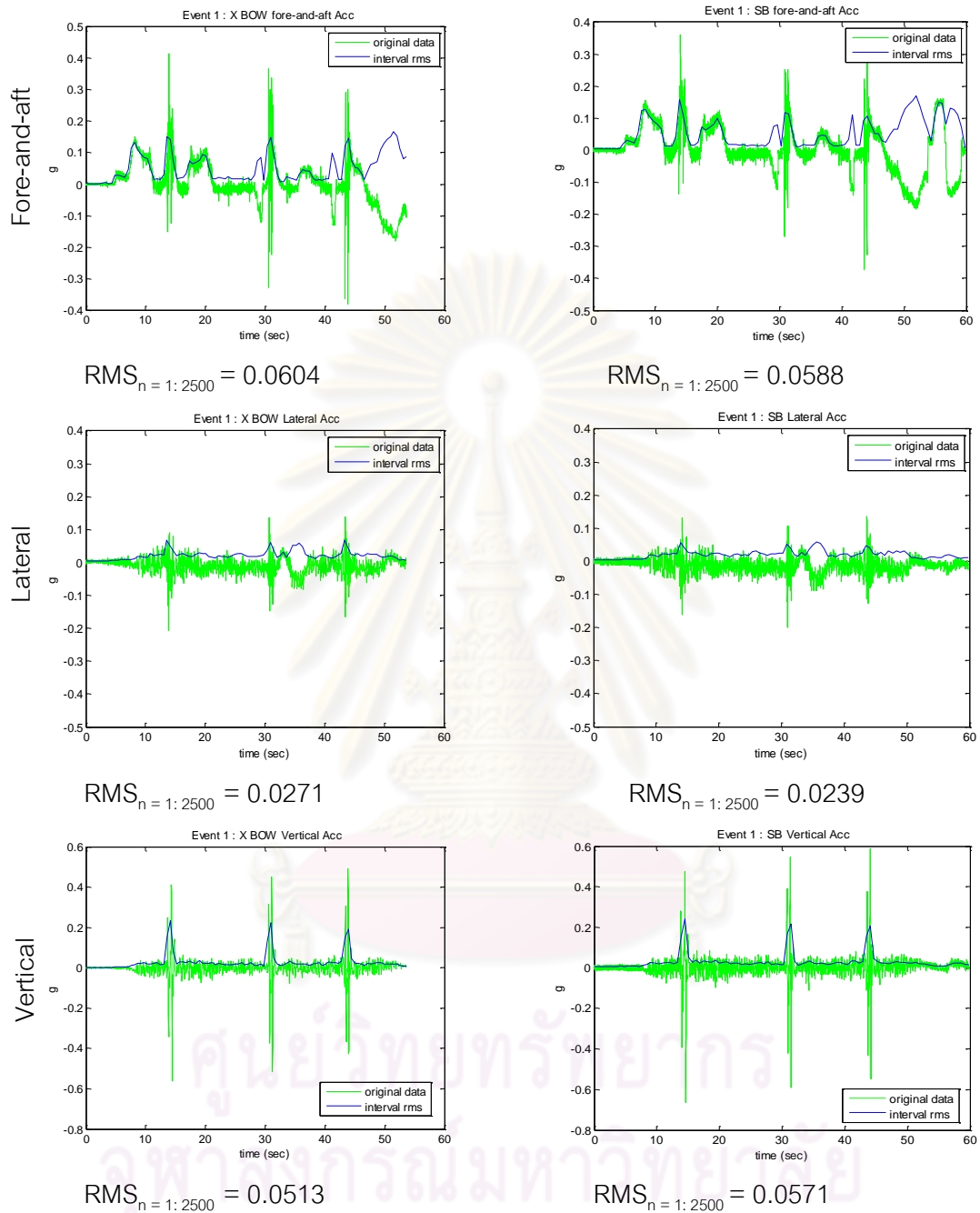
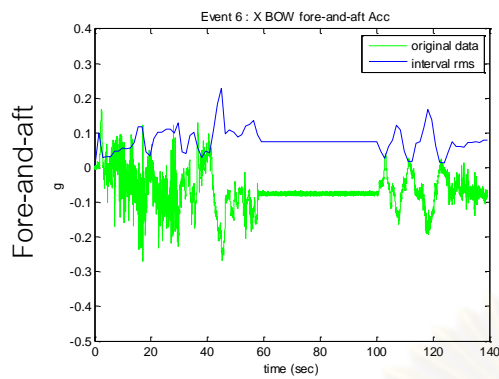


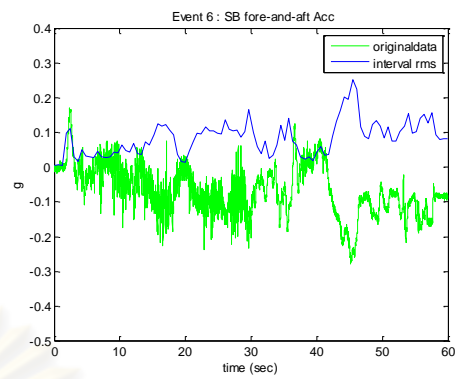
Fig.4-4(a) Acceleration results of driving situation case1 captured by two different sensors installed within a cabin

X-BOW (six-axis)

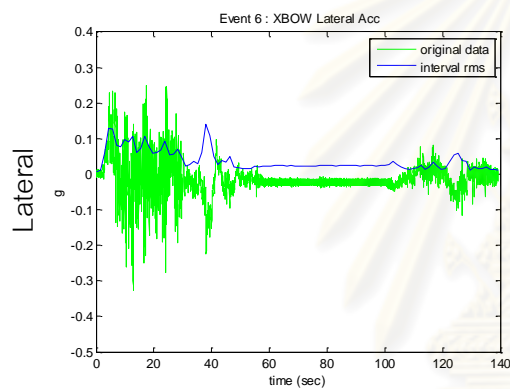
Kyowa (three-axis)



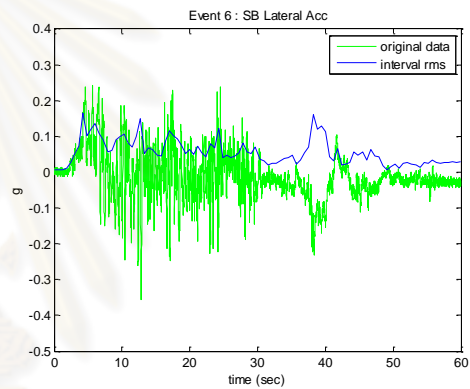
$$\text{RMS}_{n=1:3000} = 0.0948$$



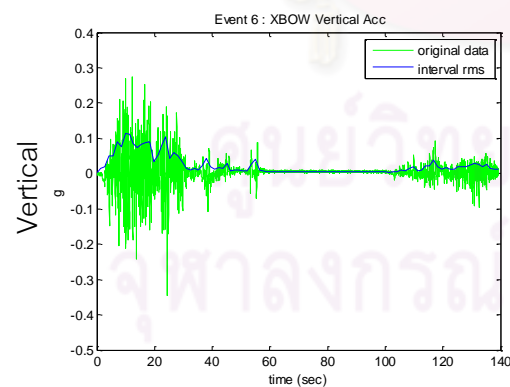
$$\text{RMS}_{n=1:3000} = 0.0953$$



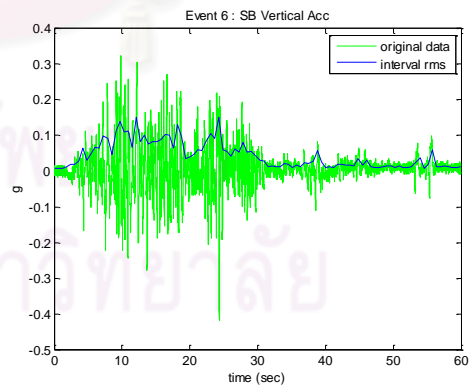
$$\text{RMS}_{n=1:3000} = 0.0670$$



$$\text{RMS}_{n=1:3000} = 0.0675$$



$$\text{RMS}_{n=1:3000} = 0.0526$$



$$\text{RMS}_{n=1:3000} = 0.0581$$

Fig.4-4(b) Acceleration results of driving situation case6 captured by two different sensors installed within a cabin

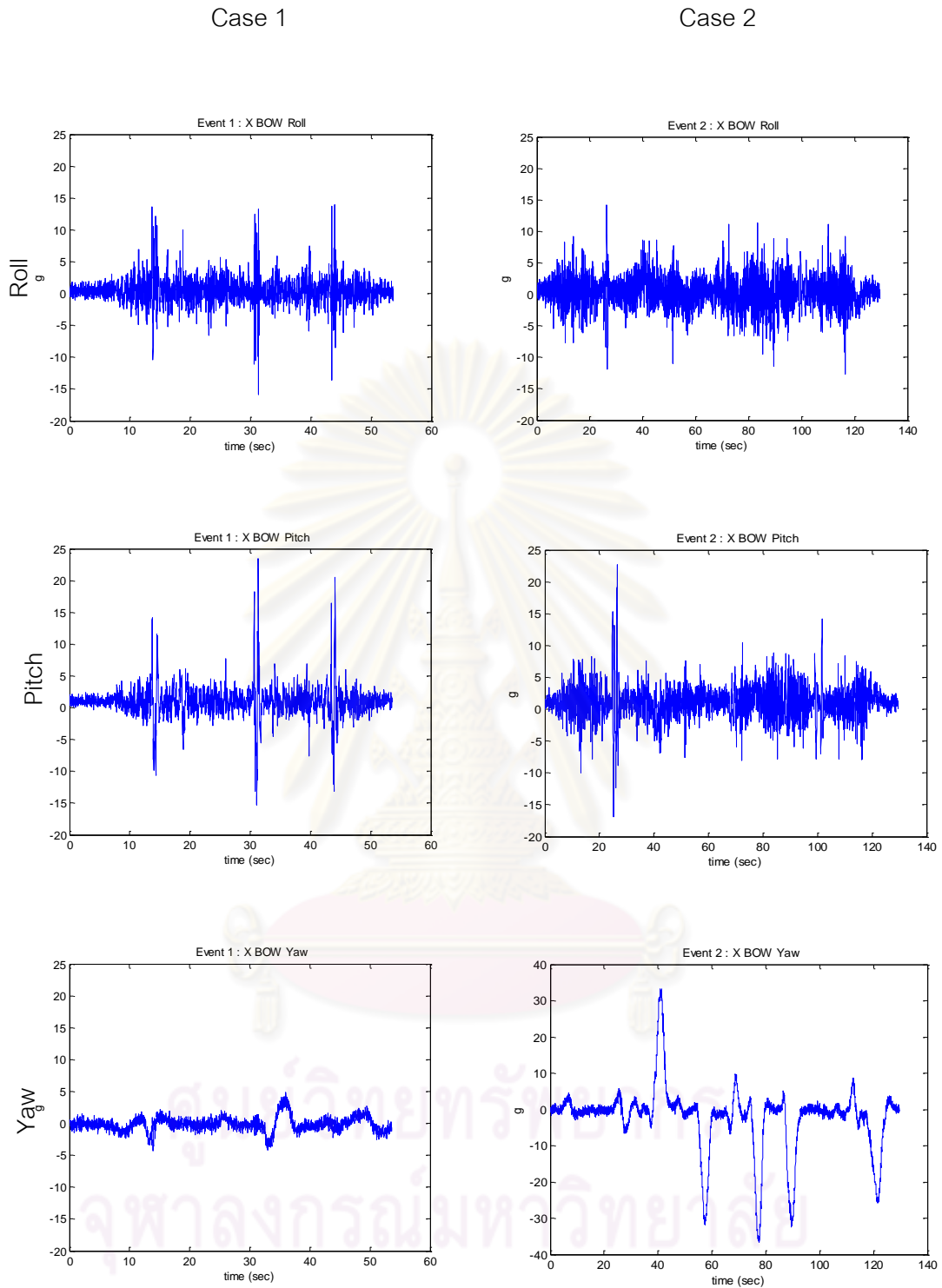


Fig.4-5 Rotational acceleration results of driving situation case 1 and case 2 captured by X-BOW (six-axis) sensor

X-BOW (single-axis)

Kyowa (single-axis)

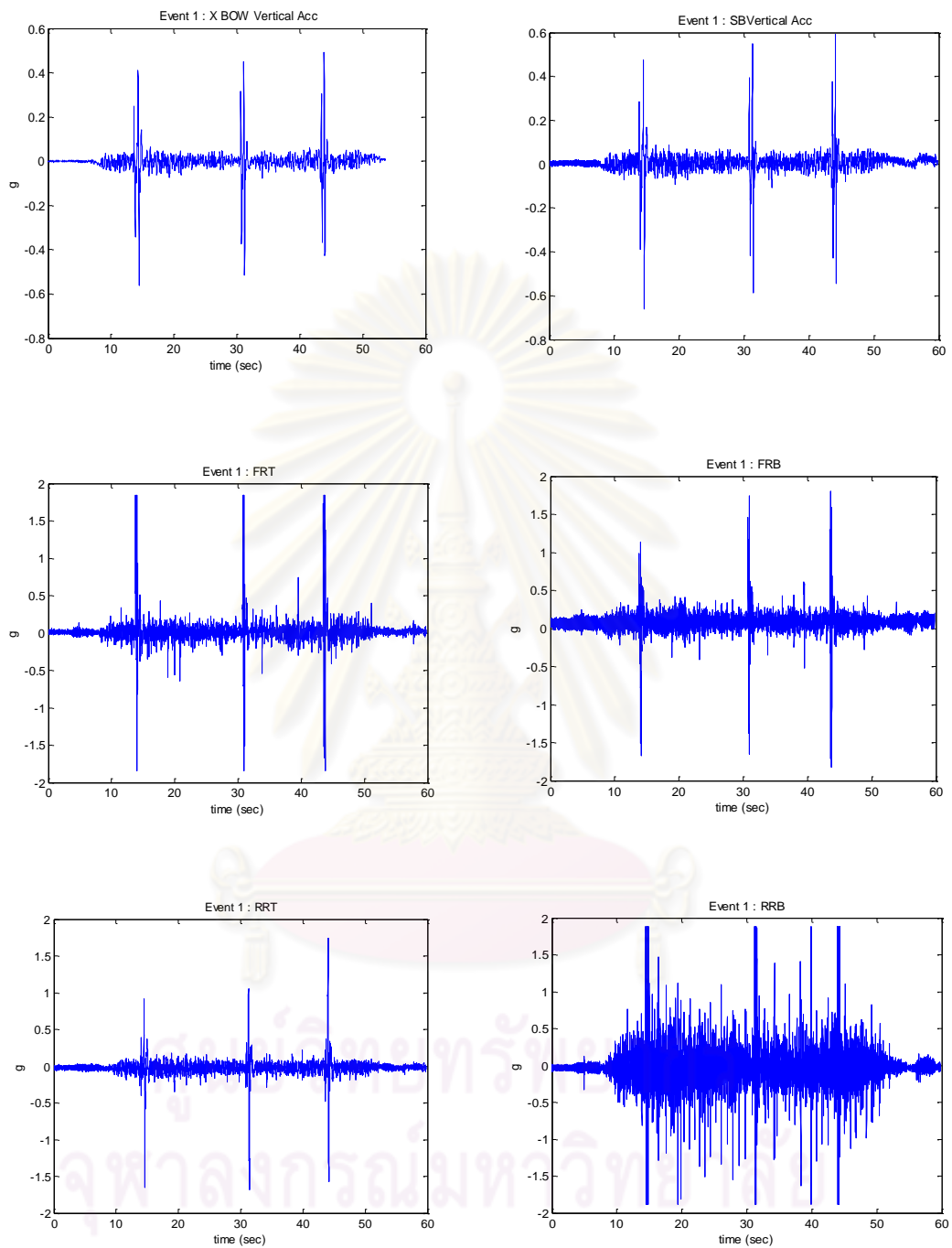


Fig.4-6 Vertical acceleration results of driving situation case 1 captured by two different sensors installed outside a cabin

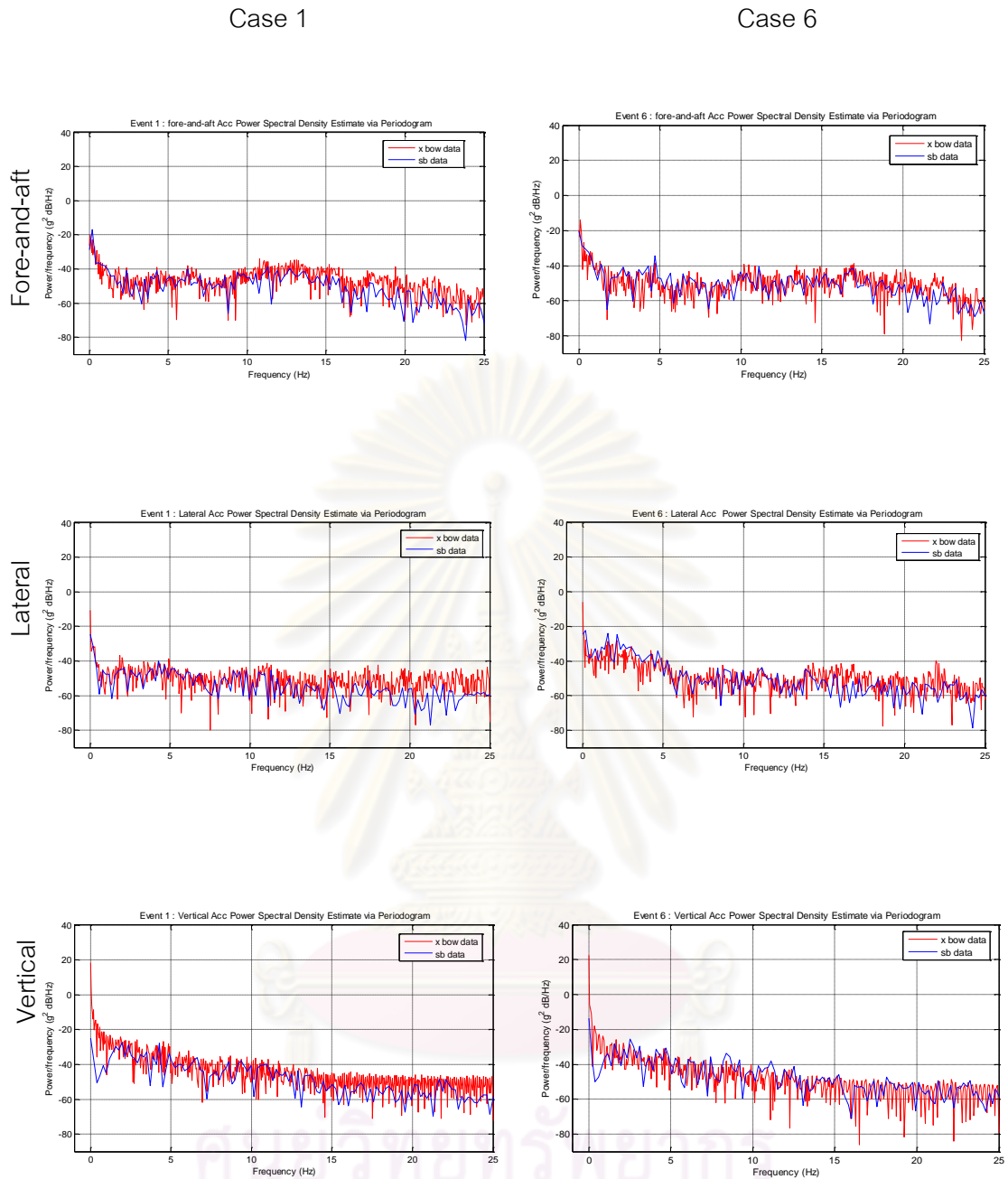


Fig.4-7 PSD results of acceleration spectra for driving situation case1 and case6 captured by two different sensors installed within a cabin

4.9.3. Results of Frequency Weighting Analysis

In the frequency weighting analysis, data of interests from six ride for both translational and rotational cases were randomly selected. All criteria can be divided in to new seven sub-cases as the following,

1. Driving over the smooth track within the factory.
2. Driving over the track with some obstacles, including
 - 2.1. Road bumps
 - 2.2. Lids of water drain pipes
3. Driving over rough surface track
4. Driving over real road sections outside the factory with various speed of
 - 4.1. speed 50 Km/hr
 - 4.2. speed 80 Km/hr
 - 4.3. speed 100 Km/hr

The calculated weighted RMS accelerations for all cases above are reported in Table 4-2 and Fig.4-8. When the total vibration values (a_v) are considered, the highest one is found to be in case 2.1 which was calculated from data obtained from the case of driving over a road bump. It is also found in this case that the weighted RMS of vertical acceleration (a_{wz}) is highest among other cases. In the third case, the total value was calculated from data obtained from the case of driving over rough road surface. The weighted RMS values of the lateral (a_{wx}), vertical (a_{wz}), and roll acceleration (R_{wy}) are higher than those of the other cases, but the total vibration value is close to that of the case 2.1 with the same level of comfort (very uncomfortable), according to ISO 2631-1 standard. In case 1, whose data obtained from the case of driving over a smooth track within the factory, the total weighted value is close to that of the case 4.1 which is a smooth drive over real road section outside the factory at speed 50 km/hr with the same comfort level (a little uncomfortable).

case	Weighted r.m.s. translational acceleration (m ² /sec)			Weighted r.m.s. rotational acceleration (m ² /sec)			Vibration total value (m ² /sec)		
	a _{wx} (lateral)	a _{wy} (fore-and-aft)	a _{wz} (vertical)	R _{wx}	R _{wy}	R _{wz}	a _{vl} (linear)	a _{vr} (rotational)	a _v (total)
1.	0.1411	0.3217	0.2394	0.0929	0.1765	0.0243	0.4251	0.1174	0.4410 (b)
2.1	0.3027	0.7291	1.5813	0.3584	0.1818	0.0471	1.7674	0.1837	1.7770 (e)
2.2	0.3779	0.1954	0.6580	0.1760	0.4678	0.0563	0.7836	0.3032	0.8402 (d)
3.	0.9457	0.3569	0.8107	0.5103	1.5184	0.0747	1.2957	0.9782	1.6235 (e)
4.1	0.2488	0.3198	0.1913	0.0793	0.0739	0.0431	0.4480	0.0570	0.4517 (b)
4.2	0.1970	0.1792	0.6009	0.1361	0.3429	0.0263	0.6572	0.2229	0.6940 (c)
4.3	0.1691	0.3132	0.3836	0.1259	0.2453	0.0248	0.5233	0.1626	0.5480 (c)

Table 4-2 The weighted RMS accelerations results

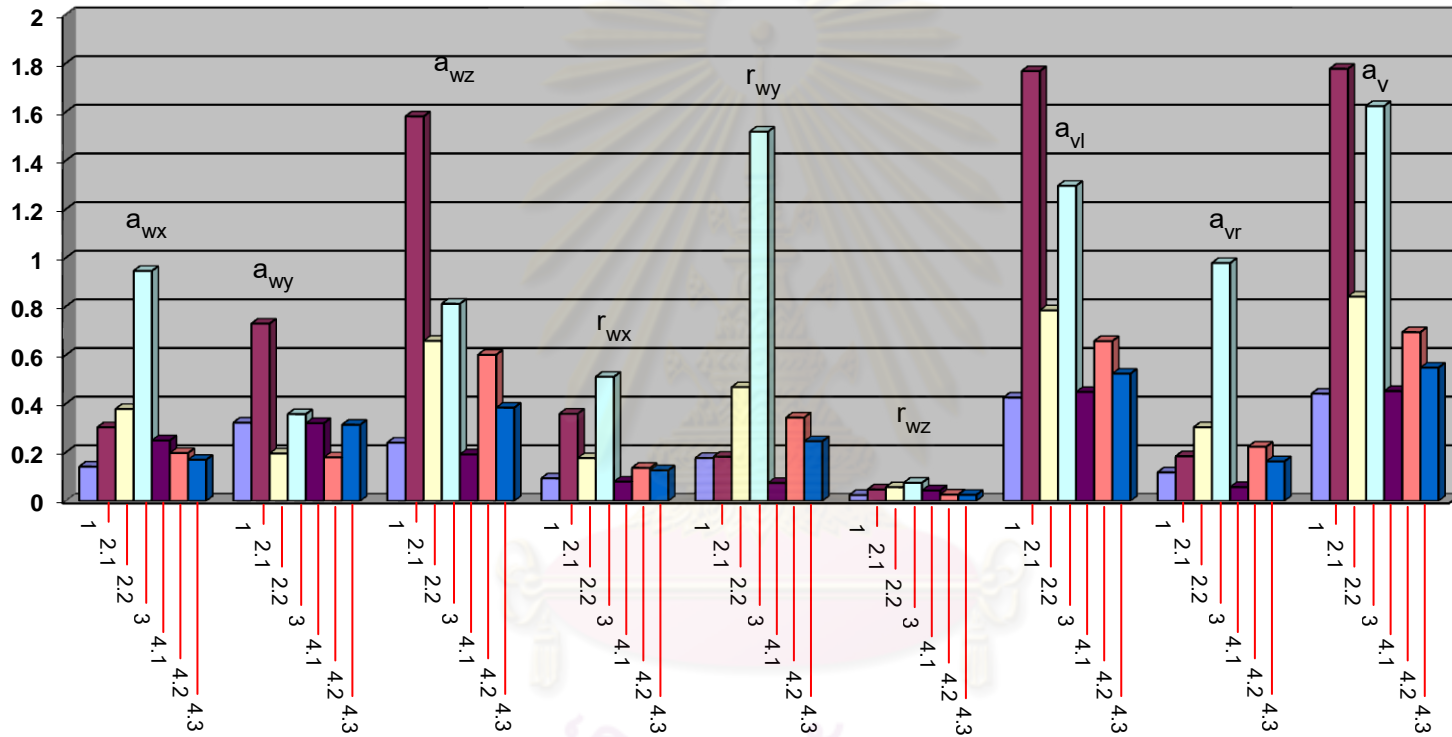


Fig.4-8 graphic results of weighted RMS accelerations

4.10. Conclusions and Further Recommendations

The results show good agreements between acceleration data and ride events/road conditions. However, there were few mistakes occurring during the investigation such as mispositioning of the accelerometers attached to the floorboard, due to difficulty in mounting process. The comparable data from different sensors should be collected at the same sampling frequencies and should be at least 160 Hz to give PSD spectra in the frequency range of 1-80 Hz which is the important range for ride comfort analysis, recommended by ISO standard. From the analysis in frequency domain, the PSD results could not be interpreted clearly as may be because of the road tracks surfaces were not different enough. The results obtained from the frequency weighting analysis shows good agreement with the acceleration signals and real driving events so that the application of ISO in term of comfort evaluation is found to be effective and reasonable. However, the reported results are based on one evaluation method only. The application of the other alternative methods such as VDV (Vibration Dose Value) should be applied and compared the results among each other.



ศูนย์วิทยทรัพยากร
จุฬาลงกรณ์มหาวิทยาลัย

CHAPTER V

LEAF SPRING MODELING AND VERIFICATION

The leaf spring model was created to represent its characteristics and properties. A good precise model must be able to exhibit overall phenomena obtained from real experiment. This research aims to investigate the relationship between spring parameters towards vehicle ride comfort when design parameters are selected. The objective is to build a leaf spring model that is general and reliable enough to predict ride value. The parameters of the model related to physical properties of the leaf spring model can be used for design purpose.

In the investigation, the characteristics were observed mainly on simulation. For this study, a leaf spring model was proposed, regarding the effect of nonlinearities both from contact friction and from the other assembled component at installation. The modified Dahl's model and the three link equivalent model were combined to represent a nonlinear leaf spring system. The model was then verified by a leaf spring test rig that was designed and constructed to perform deflection measurement under static loading condition. The parameters of the leaf spring model were adjusted by successive comparison of the results to the real measured data.

5.1. Leaf Spring Modeling

There are various types and shapes of leaf springs available in market although the term of leaf spring usually referred to a circular shape of flat metal. The basic common design and the one that used for studying and modeling in this research is a symmetrical semi-elliptic with equal eyes at both ends as shown in Fig.5-1. This type of leaf spring is generally used with the Hotchkiss suspensions which are commonly used with general commercial trucks.

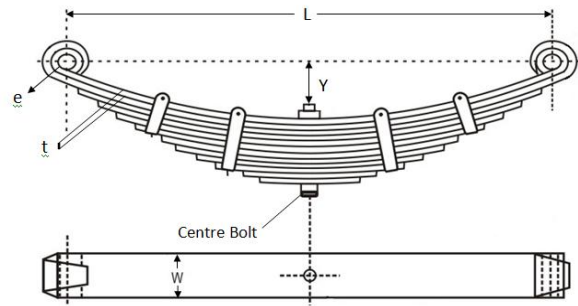


Fig.5-1 Symmetrical multi-leaf spring with design parameters

5.1.1. Existing Leaf Spring Models

There are a lot of theories and methods, both in computational and graphical ways to capture the essence of leaf spring property. The modern computer program such as ADAMS and finite element can be applied to analyze and solve nonlinear problem of leaf spring model, including optimization. One classical simplified method is the linear beam deflection theory which is subjected to small deflections and the other ones mentioned in the leaf spring manual are the center link extension method, the two-point deflection method which are not discussed in details for this paper. Both modern computer programs and classical geometrical techniques have both advantages and disadvantages, so that the users should account for any limitations and assumptions when each method is applied.

5.1.1.1. Classical Beam Theory

This is a commonly used approach to model the leaf spring as a beam and to use the simple beam theory to predict the stiffness of the spring. The basic assumption is to consider the leaf spring as a cantilever beam with variable cross-sectional area.

The Society of Automotive Engineers adopted the beam theory to calculate the equivalent stiffness of the leaf spring. Design formulae and correction factors to account for different leaf spring designs and geometries are available. A comprehensive presentation of different configurations of the leaf spring and the equations used to

calculate the stress induced in the leaf spring can be found in the Spring Design Manual [1].

5.1.1.2. Finite-Element Method

The finite-element method provides a practical approach to analyze frictional contact problems. In this approach, the Lagrange multiplier method or penalty method can be used to treat the geometrical contact. The elastoplastic constitutive laws are adopted in order to overcome the non-differentiability of the friction law.

5.1.1.3. Multibody Kinematic

The method is used to model stiff leaf springs that experience small elastic deformation is based on the finite-element floating frame of reference formulation. Using the assumption that there is no relative rigid body displacement between the leaves of the spring, the leaf spring can be modeled as one flexible body in the floating frame of reference formulation. The leaves are discretized using the finite-element method. The gross motion of the leaves is described by the displacement of the spring (body) coordinate system. The deformation of the leaves with respect to the body coordinate system is described using the finite-element nodal coordinates. The leaves of the spring at some sections can experience intermittent contacts and friction due to the relative displacements.

5.1.1.4. The Three Link Equivalent Model

This method was proposed in 1944 by Maurice Olley and other member of SAE Spring Committee [15]. The model represents the leaf spring as three bar linkages, connected to one another with torsion springs so that each member can move in angle and in plane, relative to each other. This method has been used to model and to study the characteristic of leaf spring in suspension system such as the work of Ekici [16].

In simulation, the shackle linkage is also attached to the original model to allow more degree of freedom for leaf spring displacement when subjected to the external applied force.

5.1.2. Friction Model and Hysteresis Effects

The hysteresis effect is the very important characteristic of leaf springs which arises from interleaf friction and stick-slip phenomena. In the proposed model, the modified first-order differential equation Dahl model is used to describe hysteresis relationship between applied force and spring deflections. This modified version (also known as “the Restoring force model”) was proposed by Al Majid [17]. The details and its formulation can be found in Ref.[15]. For this presented work, the generalized mathematical equations of the modified model which was used to describe the stick-slip phenomena in mechanical system (for example, see Ref.[18]) are presented below,

$$\frac{dF}{dt} = \beta \frac{du}{dt} (h - F \operatorname{sgn} \frac{du}{dt})^\mu \quad 5-1$$

$$h = \frac{1}{2} [(h_u + h_l) \operatorname{sgn} \frac{du}{dt} + (h_u - h_l)] \quad 5-2$$

Where

$$h_u(u) = au + b \quad 5-3$$

$$h_l(u) = du + e \quad 5-4$$

In Eq.(5-1), time derivative of force is related to velocity of displacement u and the other remaining term which depends on the boundary of hysteresis curve and direction of velocity. The terms h_u and h_l represents the upper and lower boundaries of the curve, respectively. Parameters μ , β , a , b , d , and e are related to the shape and characteristic of the enveloped curve so that these parameters can be adjusted to give desirable shape of hysteresis loop, compared with the experimental results.

5.1.3. Description of the Leaf Spring Model

A model was constructed with the three link equivalent model. For the case of leaf spring studied here, a shackle linkage is also attached to allow leaf spring motion when subjected to external load.

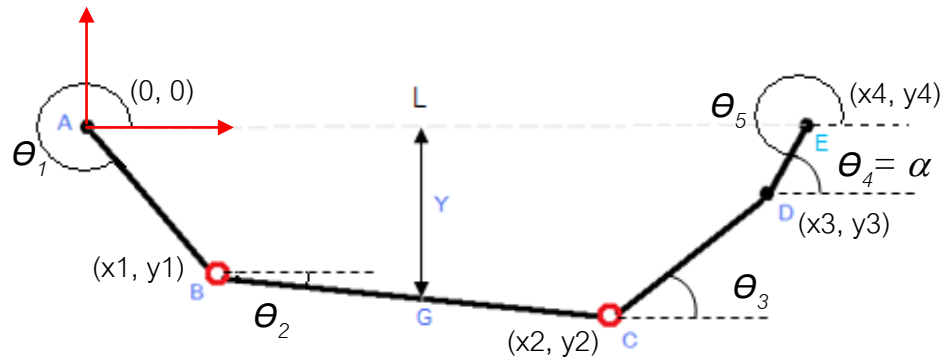


Fig.5-2 Five link mechanism of a leaf spring model

In simulation, the initial model parameters must be prescribed before running the program. The geometric parameters in the five link mechanism, AE, AB, BC, CD, DE, Y, and shackle angle (α) can be measured and calculated from the tested leaf spring at initial static equilibrium state with zero load. The relative motion between linkages was derived from leaf spring geometry as presented below,

$$AB = 0.75L \quad 5-5$$

according to the deflection theory which are recommended by the Spring Design Manual [1] and CD is set to be equal in length with AB.

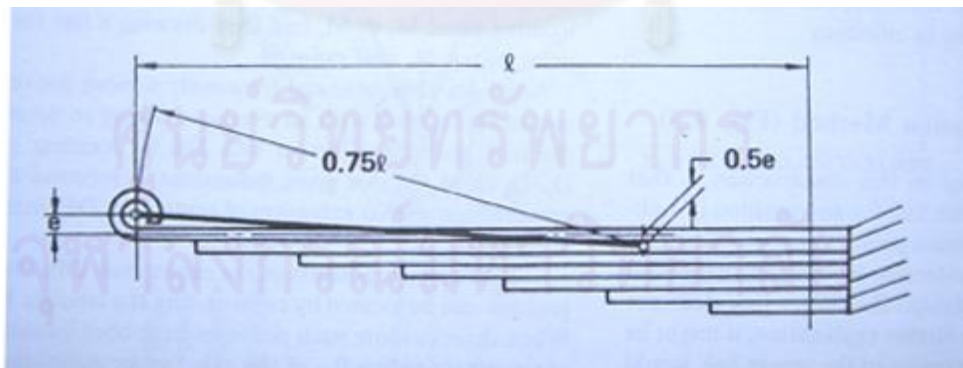


Fig.5-3 Equivalent linkage of the upturned eye cantilever spring [1]

The length of AE, DE, and Y, were measured from a real leaf spring at installation which are 119, 10 and 15 cm, respectively.

From Fig.5-2, the motion of each link is related to the other adjacent member. If a point on one link is considered, it moves in X-Y plane both in vertical and horizontal direction. The two adjacent links are moving in angle with each other to produce angular displacement θ . The coordinates (x_0, y_0) , (x_1, y_1) , (x_2, y_2) , (x_3, y_3) , and (x_4, y_4) represent the position of the joints, referred to the reference frame. The initial parameters θ_1 , θ_5 and θ_4 are set to be 340, 180, and 70 degree, respectively.

$$y_1 = AB \sin \theta_1 \quad 5-6(a)$$

$$x_1 = AB \cos \theta_1 \quad 5-6(b)$$

$$y_2 = 2y - y_1 \quad 5-6(c)$$

$$x_3 = AE - DE \cos \theta_4 \quad 5-6(d)$$

$$y_3 = -DE \sin \theta_4 \quad 5-6(e)$$

$$\theta_3 = \sin^{-1}[(y_3 - y_2)/CD] \quad 5-6(f)$$

$$x_2 = x_3 - CD \cos \theta_3 \quad 5-6(g)$$

$$\theta_2 = \tan^{-1}[(y_2 - y_1) / (x_2 - x_1)] \quad 5-6(h)$$

$$BC = (x_2 - x_1) / \cos \theta_2 \quad 5-6(i)$$

5.1.4. The Full Leaf Spring Model Construction

Full leaf spring system was accomplished by a combination of a five link mechanism model and Dahl's hysteresis model. As illustrated in Fig.5-2. Hysteresis effect was added to the joints between linkages (points B,C). The completed model is shown in Fig.5-4 and the sub system of Dahl's model at two joints is shown in Fig.5-5

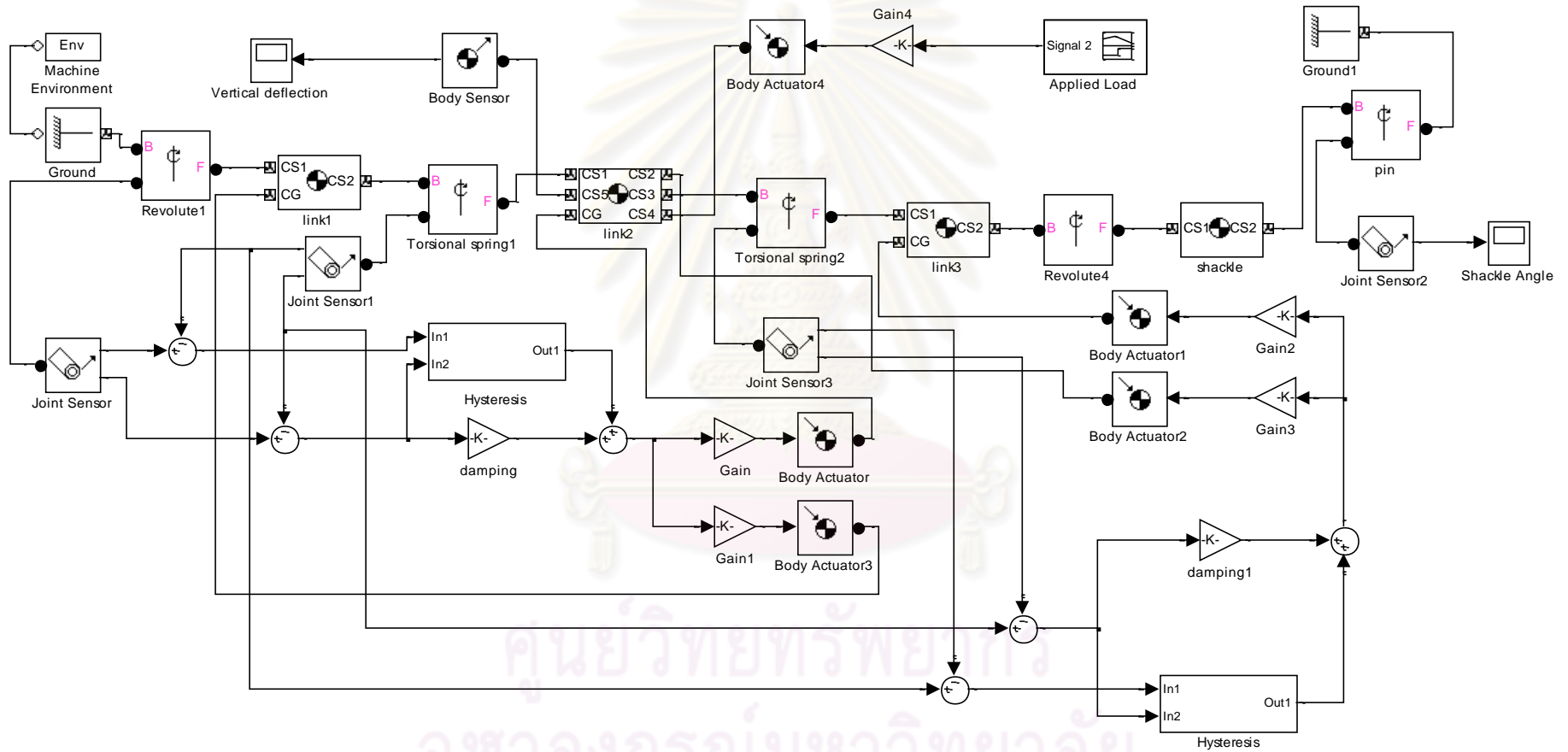


Fig.5-4 Full leaf spring model, regarding hysteresis effects

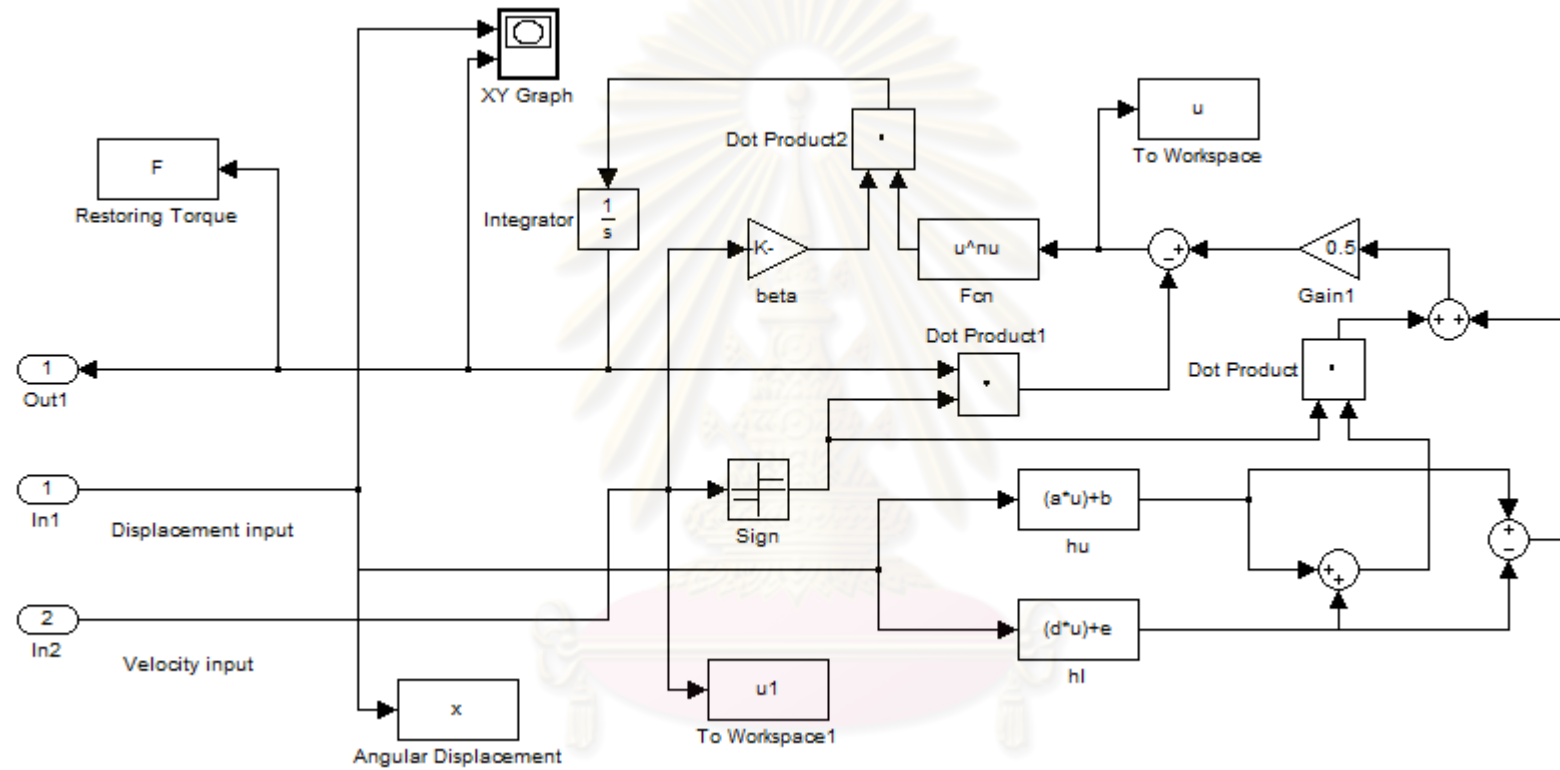


Fig.5-5 Hysteresis component of a leaf spring model

5.2. Verification of the Leaf Spring Model

In order to verify the leaf spring model, some experiments were carried out to compare the results with those of the simulation's. In this work, a leaf spring test rig was designed and constructed by a group of senior students at Chulalongkorn University.

5.2.1. Design and Construction of the Leaf Spring Test Rig

The leaf spring test rig is composed of three main components which are the frame, the load generation and measurement unit, and the deflection measurement unit. Details for each component and their functions is given individually as follows,

5.2.1.1. Test Rig Frame

The test rig frame was designed to withstand the maximum applied load at least 1,000 Kg force as shown in Fig.5-6.

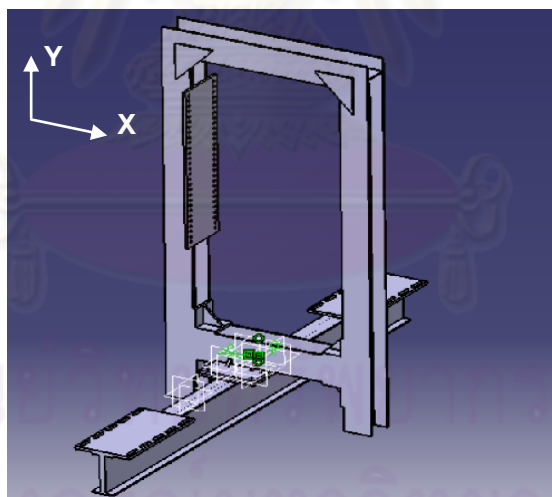


Fig.5-6 Final design of the test rig frame

This main structure can fit with various sizes of leaf springs and provides suitable space for additional attachments. In the test, leaf spring was installed downturned with one end fixed and the other end shackled so that the applied load from an actuator is in -Y direction.

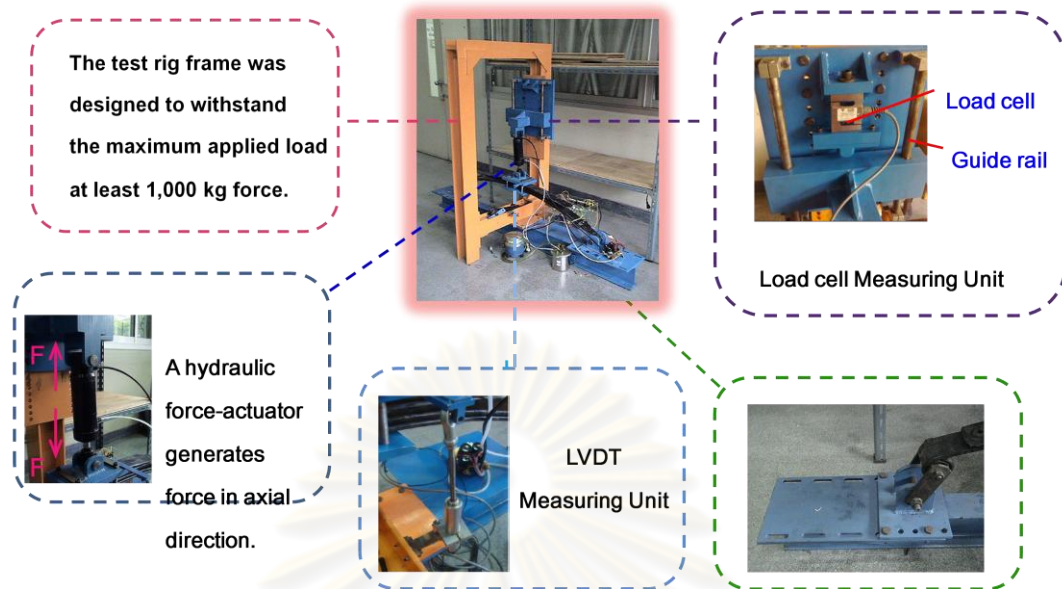


Fig.5-7 Configuration of the leaf spring test rig

5.2.1.2. Load Measuring Unit

In the experiment, the applied force was increased in step by a hydraulic actuator and was measured by a load cell. The load cell was placed on top of a guided slider to ensure that only axial load is applied to it.

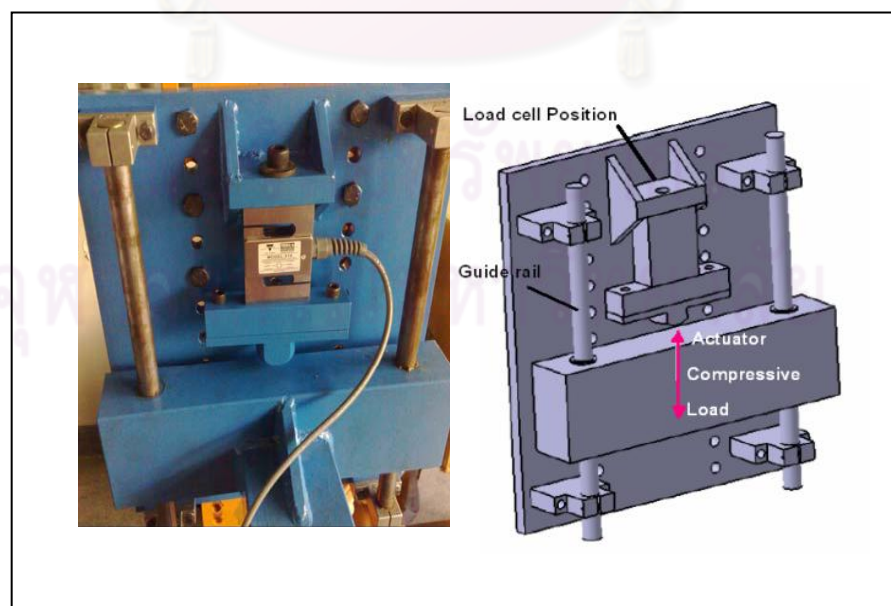


Fig.5-8 The guide base for load cell and force-actuator attachment

5.2.1.3. Deflection Measuring Unit

In the experiment, only leaf spring displacement in vertical direction was considered, hence an LVDT sensor was attached perpendicular to leaf spring with one side of LVDT connected to leaf spring's lock and the other side attached to the base of the test rig frame. For this design, the housing of LVDT can be fitted with different lengths of leaf spring and various types of sensor.

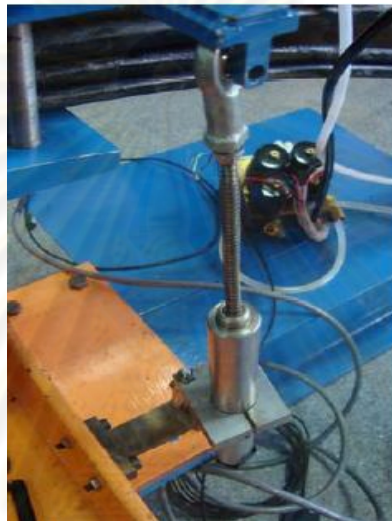


Fig.5-9 The LVDT measuring unit

5.2.2. Verification Testing

Fig.5-10 shows the two main components of the proposed leaf spring model which are the three link equivalent model that describes the mechanism in term of geometrical relation and the hysteresis Dahl's model.

When external force is applied in vertical direction, leaf spring starts to move from its original position. Each linkage moves in angle/ Θ (rad) with each other at the revolute joint so that the angular displacement is produced. At each joint, the input angular displacement generated the output restoring torque by hysteresis relationship as introduced in Eqs.(5-1) - (5-4). This restoring torque represents the resistance in spring which resists movement from the initial state. The vertical displacements of leaf spring at CG point in Y-axis at steady state position were recorded for every increasing

step of force. The relationship between the applied force (kg) and the corresponding displacement (cm) could be found.

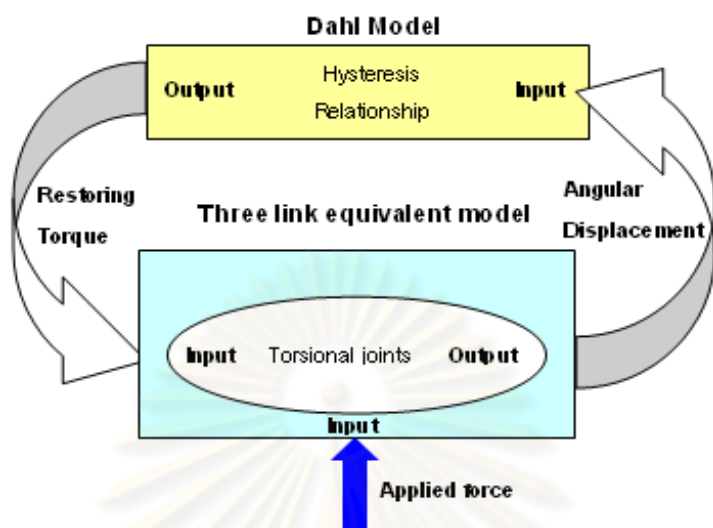


Fig.5-10 Five link mechanism of a leaf spring model

For solving the first order differential equations and the leaf spring movement, the model was implemented in SimMechanics, MATLAB software. The Force-displacement relation can be simulated and animation can be displayed graphically as shown in Fig.5-11. As the force was applied, the corresponding deflections started to form the hysteresis loop, according to different directions of loading.

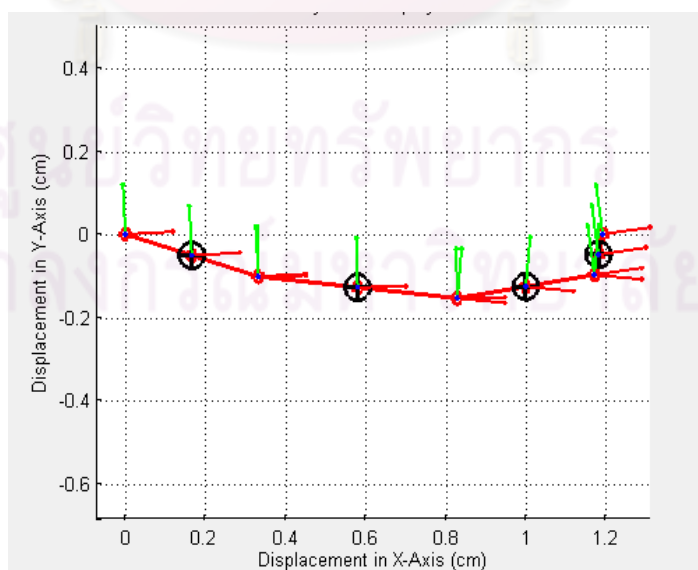


Fig.5-11 The animated results of simulated model

The experiment was carried out to measure the leaf spring vertical deflections when series of loads were applied. The spring was loaded with the load interval of 20 kg from zero to the prescribed maximum deflection and back to zero. The amount of force was initially generated from a hydraulic pump which was controlled via human-interfaced control panel by LabVIEW software. All values of the applied force were received via a load cell while the deflections of leaf spring were captured by an LVDT sensor. The results show a non-linear relationship between the applied loads and the leaf spring deflection for both directions of loading in form of a hysteresis loop shown in Fig.5-12.

	Load (kg)	Deflection (cm)
Load	29.9310	0.0034
	63.4771	0.5855
	86.7014	1.3098
	117.6670	2.1493
	149.9230	3.2116
	186.6950	4.8539
Unload	176.2410	4.7701
	115.3845	3.7293
	72.1125	2.6469
	54.6821	1.9905
	21.4910	0.7700
	-1.5429	0

Table 5-1 Experimental result of leaf spring deflection subjected to vertical applied load.

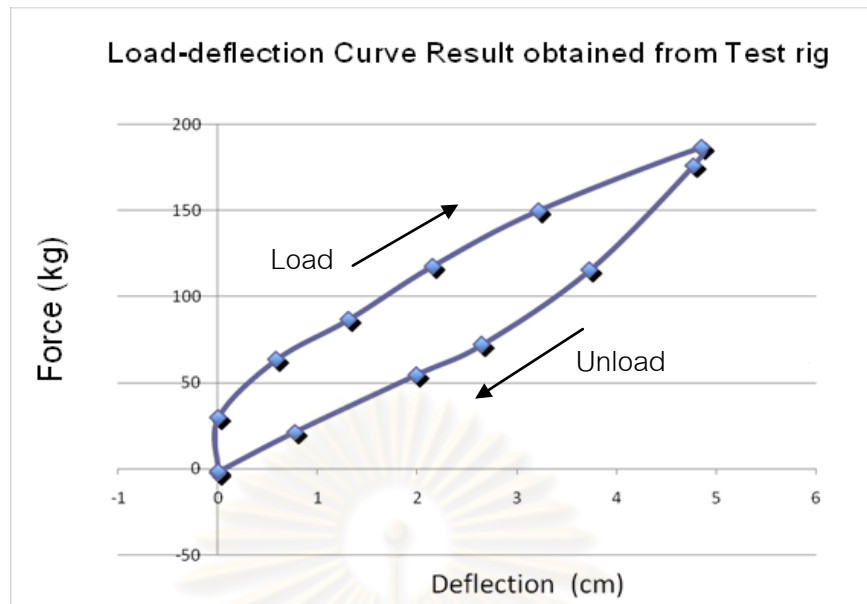


Fig.5-12 The load-deflection curve result obtained from test rig experiment.

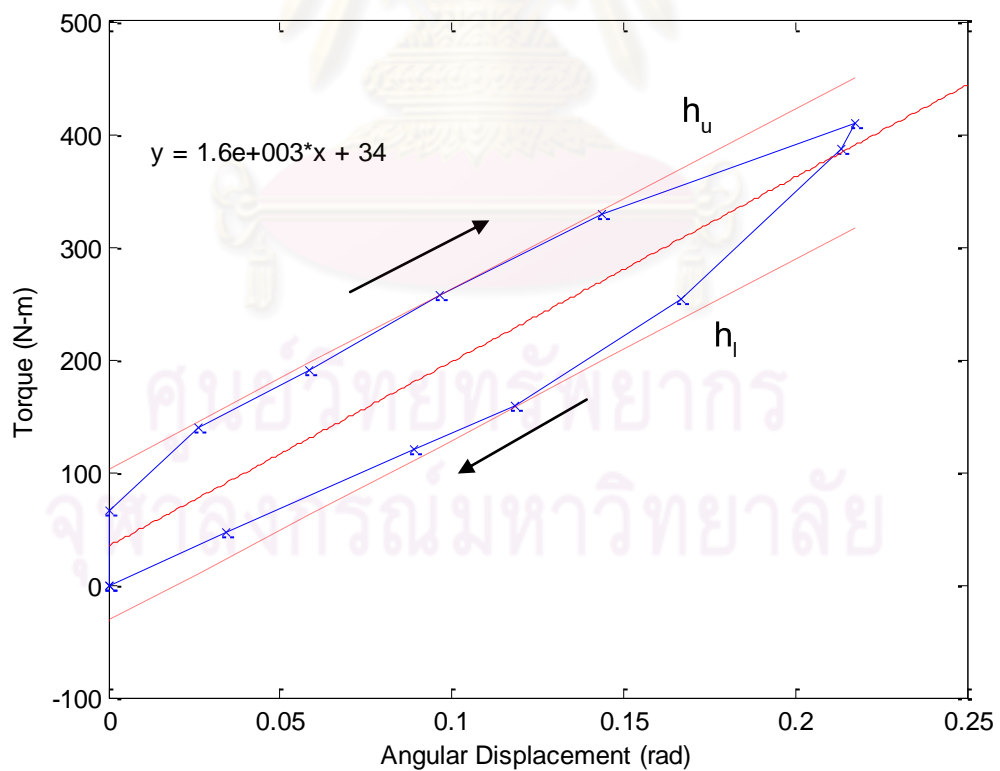


Fig.5-13 The load-deflection curve of torque and angular displacement

5.2.3. Parameters Identification

Parameters identification was made by comparison of the simulation and experimental result. The average regression line or nominal stiffness could be examined from the load-deflection curve obtained from the experiment. (a linear solid line in Fig.5-13). The slope of the line should reflect the average stiffness or value of a and d in Eqs.(5-3) and (5-4) which are the slope of the two linear curves, i.e., the upper boundary and the lower boundary, respectively.

A linear leaf spring model without friction/hysteresis component was use to calibrate a slope of a nominal stiffness (a linear solid line in Fig.5-13) which is located parallel to both upper and lower envelopes curves, h_u and h_l . Once the approximated nominal stiffness is known, the values of a and d are found which are the slope of the other two curves. These parameters were used in the hysteresis/Dahl's model. In this case, a and b are assumed to be equal so that the remaining unknown parameters are β , μ , b , and e . These parameters were adjusted until the best fit between the loop shapes was satisfied.

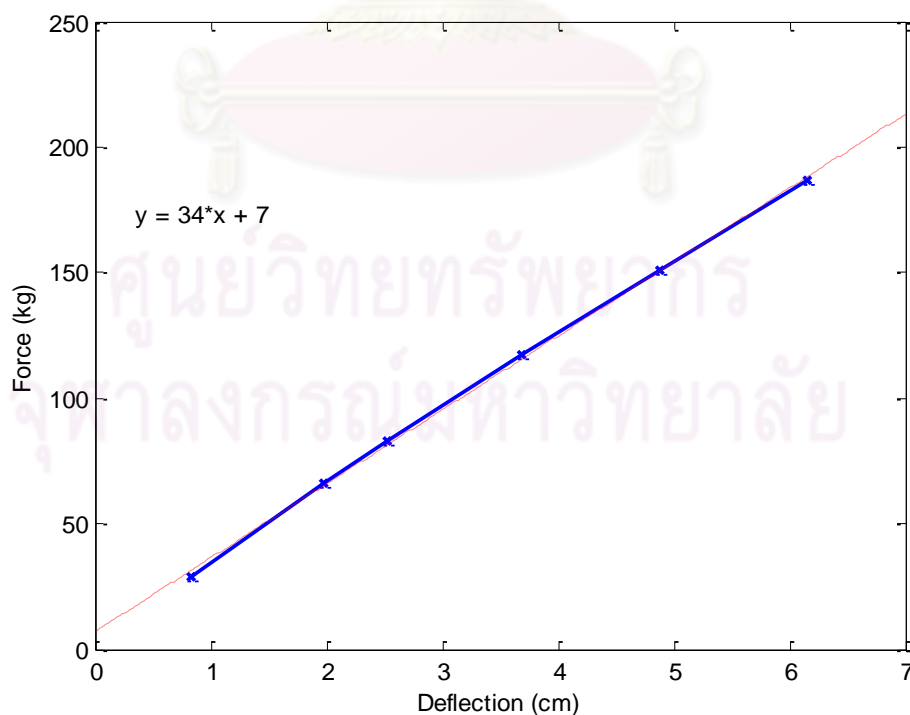


Fig.5-14 Load-deflection curve result of linear leaf spring model

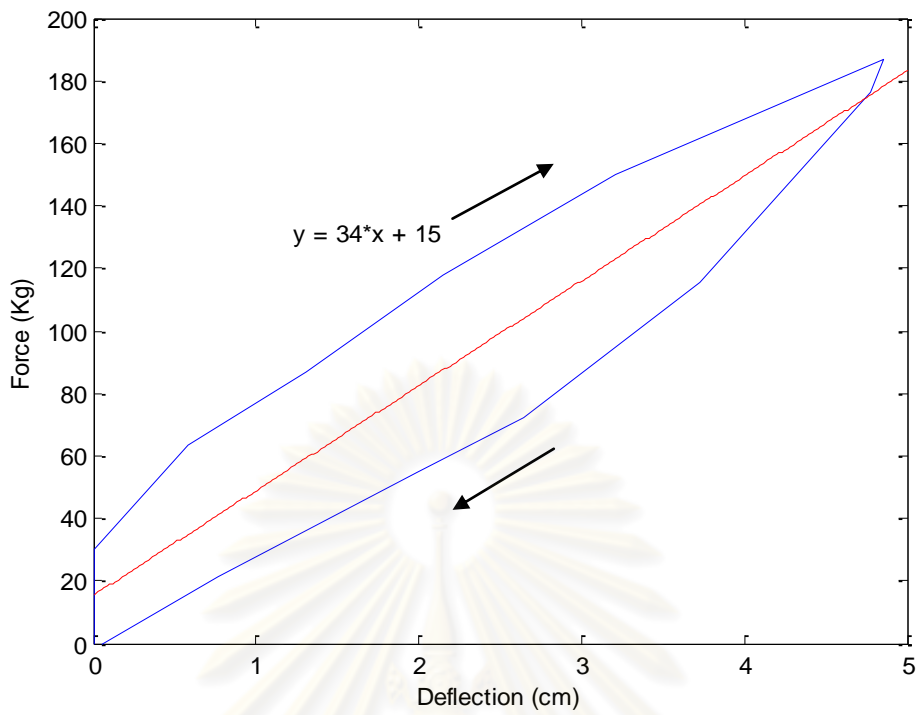


Fig.5-15 Load-deflection curve of force (kg) and displacement (cm)

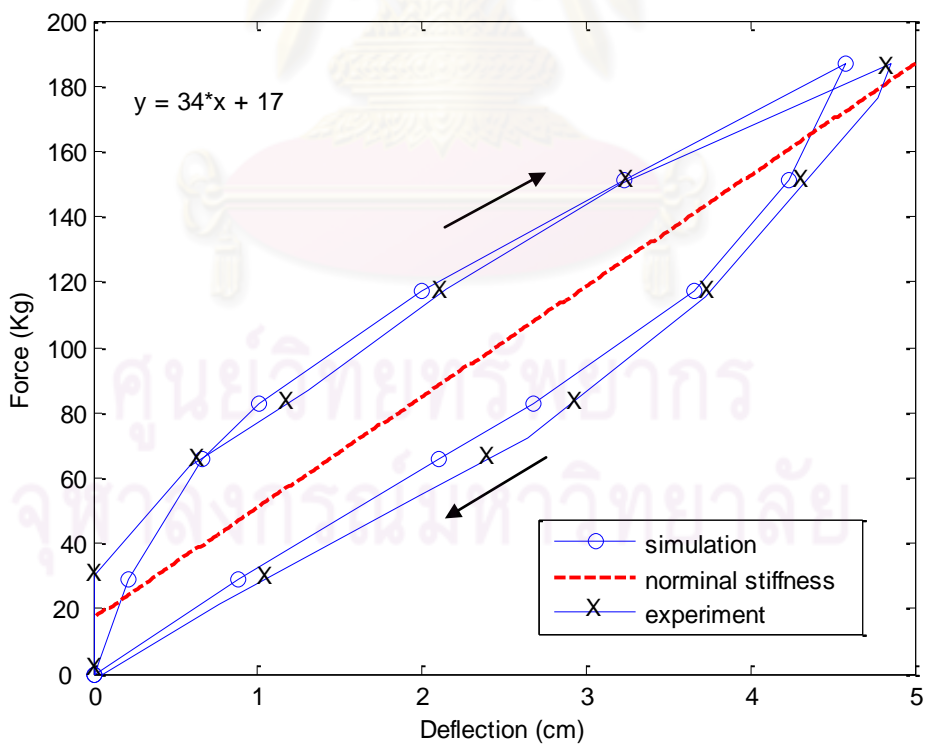


Fig.5-16 Comparison between load-deflection curve results from experiment and simulation

The final values obtained are below.

$$a = 3.3354 \times 10^4 \text{ N/m}, b = 4.9907 \times 10^2 \text{ N},$$

$$d = 3.3354 \times 10^4 \text{ N/m}, e = -2.0653 \times 10^2 \text{ N},$$

$$b = 100, \text{ and } \mu = 1$$

The shapes of curves are not exactly the same, but the model can establish most of the characteristics in steady state. Major difference appears at both ends of the loops as the model does not capture well in the transient state transition, however the result shows some agreements between the test rig experiment and the simulating model which is able to capture the overall characteristics of leaf spring. Further analysis should be carefully made again for these areas. However, the recent work was lack of sufficient data in the transition state which might be due to the limitation and ability of the leaf spring test rig that can allow for static testing only. Apart from this, some obstacles still exist to limit the performance of the test rig such as misalignment between the hydraulic actuator and the force sensor must be eliminated in order to provide better accuracy. The next step of this research is to identify parameters that can be used in leaf spring design and to find relationship between those parameters and vehicle ride comfort.

ศูนย์วิทยทรัพยากร
จุฬาลงกรณ์มหาวิทยาลัย

CHAPTER VI

SIMULATION OF SUSPENSION MODEL AND PARAMETRIC STUDY INTO THE EFFECTS ON RIDE COMFORT

In field test, operators are subjected to many influences in their environment. Therefore, with the help of modern computer tools/simulation to determine the influence of some suspension parameters on ride comfort of a light commercial vehicle, a simulation model was designed and used to investigate these parameters. In this thesis, the quarter-car model, with sub-system which represents the characteristics of suspension system was used to study the response of the vehicle to the road profile excitation, based on road surface roughness classification approved by ISO 8608 [14]. Power spectral density of the response to different road profiles with corresponding values of leaf spring parameters is analyzed and the average ride comfort/discomfort level (ride indices) as the evaluation of ride comfort in quantitative numbers are calculated through methods suggested by ISO 2631-1. The results obtained from preliminary study were developed with the simulating tools where interesting parameters were examined and properly adjusted.

6.1. Quarter-Car Model

The quarter car model is a well-known model that has been widely used in vehicle simulation to study the vehicle response to excitation inputs which can reflect characteristics of vehicle structures and performance. In this thesis, the quarter-car model with sub-system, representing the characteristics of suspension of a light commercial vehicle is used to investigate the effect of parameters settings for leaf spring and damper on ride comfort. The concept of model construction is to build up a simple model that represents suspension system with components. The parameters of leaf spring and damper are put into the investigation of this study. Fig.6-1 illustrates the conceptual design of the quarter-car model that was used in the simulation.

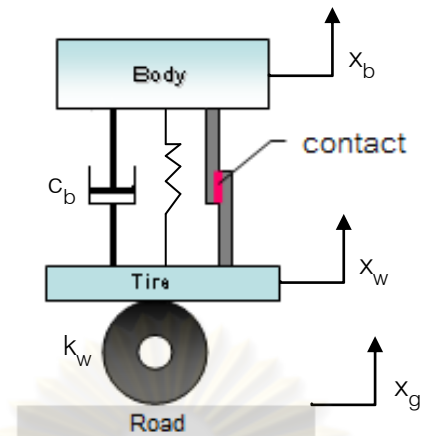


Fig.6-1 Conceptual design of the quarter-car model for suspension system

As shown in the picture, the suspension system between sprung mass (vehicle body) and unsprung mass (tire) is composed of a linear damper component, a spring, and two thin metal strips having a contact with each other which represents the hysteresis characteristics of a leaf spring. At this contact point, the relative motion occurs when the sprung and unsprung mass is moving in vertical direction, due to the road elevation that the vehicle is experienced. The relative movement at the contact point between the two thin strips also contributes to the dry friction force that lead to the appearance of nonlinear phenomena in suspension component.

6.1.1. Model Characteristics

The model was constructed based on following assumptions,

1. The vehicle bodies were considered to be rigid bodies.
2. The roll and pitch motions of the vehicle were small and neglected.
3. The tires were assumed to behave as a linear spring without damping.
4. The tires were not allowed to leave the road surface.
5. A nonlinear leaf spring model was developed used.
6. A suspension damper is linear function related to velocity.

6.1.2. Mathematical Equations of the Model

For the previous mentioned quarter-car model, the equations of motion can be obtained by summing the vertical forces acting on each of the two bodies in the system, and applying Newton's second law of motion, $F=ma$. The resulting two equations are second-order nonlinear, ordinary differential equations. The mathematical derivation, regarding the effect of nonlinearity property in leaf spring can be written as:

$$f_s + f_d = m_b \ddot{x}_b \quad 6-1$$

$$k_w(x_g - x_w) + c_w(\dot{x}_g - \dot{x}_w) - f_s - f_d = m_w \ddot{x}_w \quad 6-2$$

where f_s = nonlinear spring force (N)

f_d = damping force (N)

m_b = mass of the car body (kg)

m_w = mass x_w of the wheel/tire (kg)

k_w = wheel/tire stiffness (N/m)

c_w = tire damping coefficient (N-s/m)

x_b = vertical displacement of the car body (m)

x_w = vertical displacement of the wheel/tire (m)

x_g = vertical road elevation (m)

$x_g - x_w$ represents suspension displacement (m)

6.2. Road Input Profile

In real situation, vehicle system may be excited from multiple excitation sources such as the engine, rotating elements, etc. However, the road roughness is the primary concerned excitation source for simulation test performed in this thesis. In simulation test, the synthetic road profile was generated by the computational program and fed into a vehicle model as an input. The random road profile was constructed in MATLAB program according to the road surface roughness classification proposed by ISO 8608. The quality of road is classified based on the amplitudes of power spectral density as shown in Fig.6-2. The road type A is the classification of the "very good" quality road, type B for the "good" road, type C for the "average" road, type D for the "poor" road,

and type E for the “very poor” road. The result of simulated road inputs compared with the classification standard is shown in Fig.6-3 and the simple road model used for this research is shown in Fig.6-4.

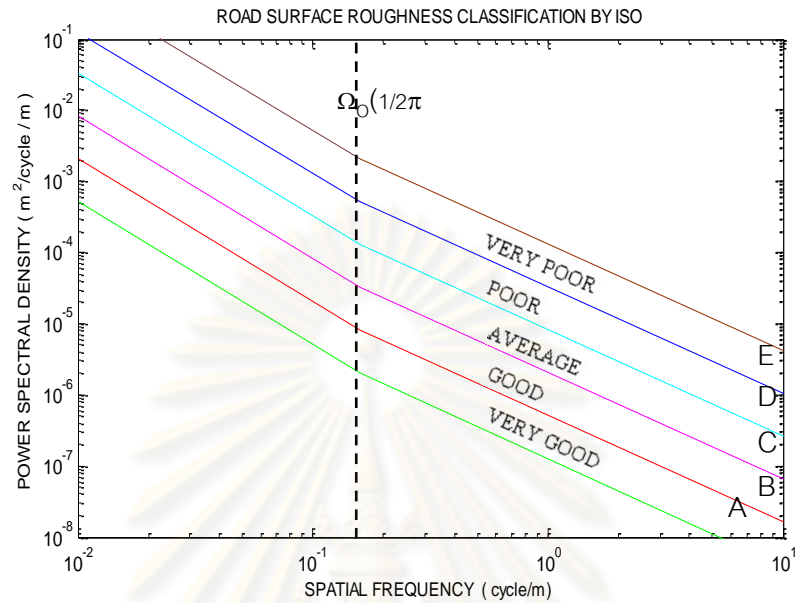


Fig.6-2 Road surface roughness classification by ISO

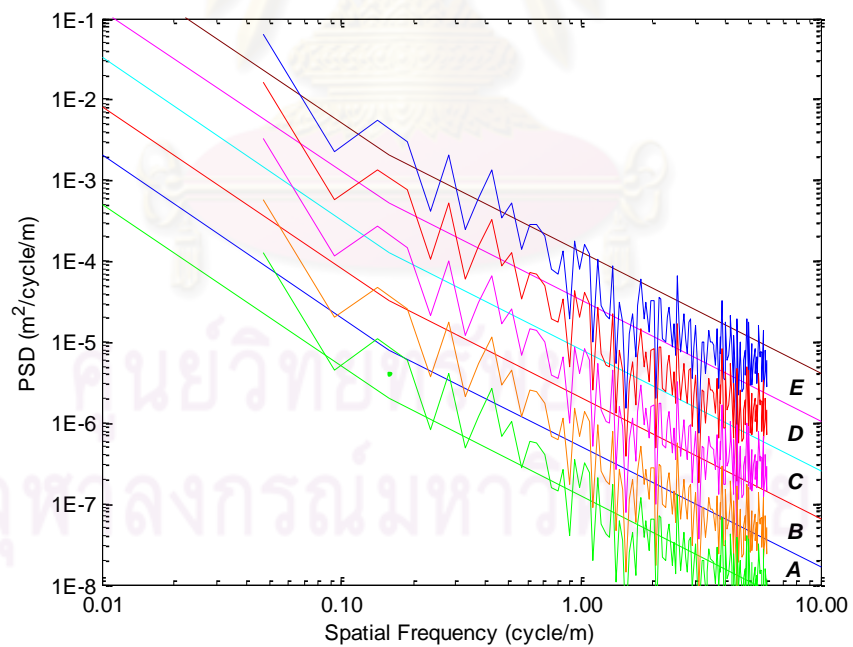


Fig.6-3 The result of simulated road inputs compared with the classification standard

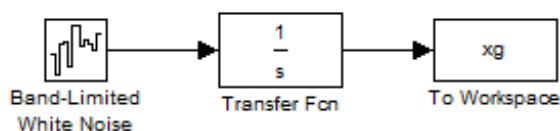


Fig.6-4 A simple road model used to simulate road inputs

6.3. Completed Vehicle Suspension Model

Full vehicle suspension model was completed by including the leaf spring model described in the previous chapter into a quarter-car model. This model represents a 1/4 vehicle system with a leaf spring type suspension that contains nonlinearities which were related to the parameters of hysteresis component.

6.4. Parametric Study by Simulation

The parametric study of the proposed leaf spring suspension model was performed by simulation. The synthetic road profile, representing road irregularities for five road classes were generated by the simple road model introduced in the previous section at the constant velocity 60 km/hr. The frequency weighting technique was employed in ride comfort evaluating process so that the value of weighted RMS acceleration for each type of road was calculated upon different values of shackle angle at initial installation of leaf spring.

Parameters	Symbols	Values	Units
Mass of vehicle body	m_b	467.5	kg
Mass of wheel/tire	m_w	30	kg
Damping coefficient of vehicle body	c_b	2369.3	N-s/m
Wheel/tire stiffness	k_w	118440	N/m

Table 6-1 Parameters of the simulated quarter-car model

Parameters used for simulating the quarter-car model is tabulated in Table 6-1. The damping coefficient of vehicle body was calculated based on value of damping ratio at 0.3 by equation 6-3.

$$\eta = \frac{c_b}{2k_l m_b} \quad 6-3(a)$$

$$c_b = 2\eta k_l m_b \quad 6-3(b)$$

where $\eta = \text{damping ratio} = 0.3$

$k_l = \text{linear elastic stiffness which was set to be equal to the value of nominal stiffness obtained from leaf spring experimental testing.}$

$m_b = \text{mass of vehicle body}$

The wheel/tire stiffness was calculated based on the assumption that its natural frequency is approximately at 10 Hz and was determined by the following equation,

$$f_n = \frac{1}{2\pi} \sqrt{\frac{k_w}{m_w}} \quad 6-4(a)$$

hence $k_w = m_w (2\pi f_n)^2 \quad 6-4(b)$

where $f_n = \text{natural frequency of wheel/tire} = 10 \text{ Hz}$

$m_w = \text{mass of wheel/tire}$

$k_w = \text{wheel/tire stiffness}$

ศูนย์วิทยทรัพยากร
จุฬาลงกรณ์มหาวิทยาลัย

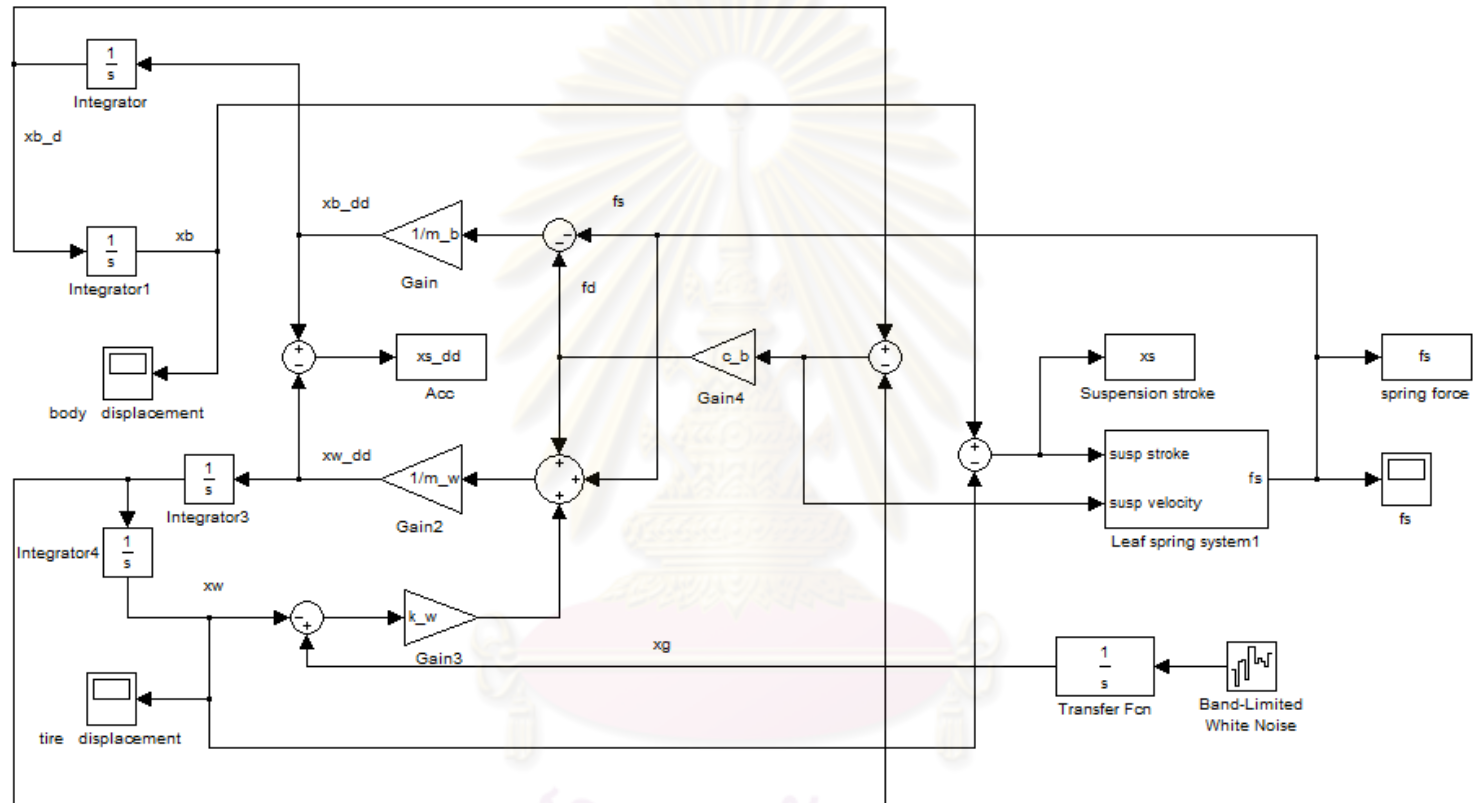


Fig.6-5 Completed vehicle suspension model

6.5. Ride Comfort Results from Simulating Model Subjected to Random White-Noise

Input

The completed vehicle suspension model was used for parametric study. For simulation subjected to different types of roads, the shackle angles were varied from 60 degree to 120 degree measured counterclockwise from the horizontal plane. The relationship between torque and angular displacement was also monitored and displayed as shown below,

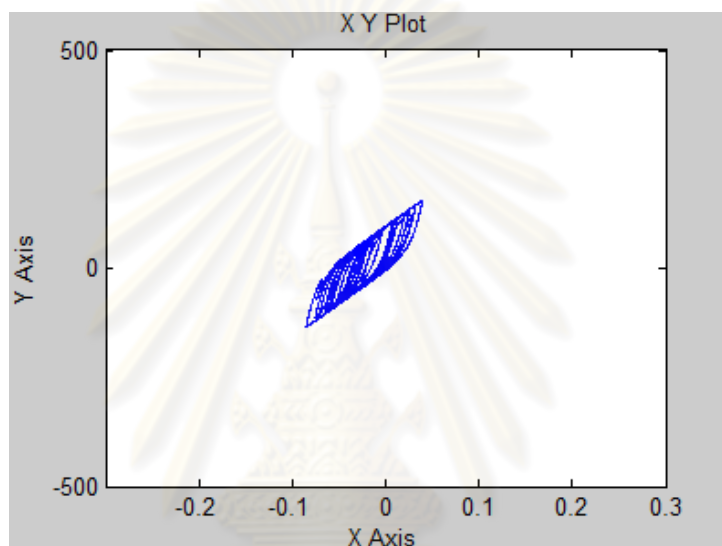


Fig.6-6 The relationship between torque and angular displacement at the rotational joints

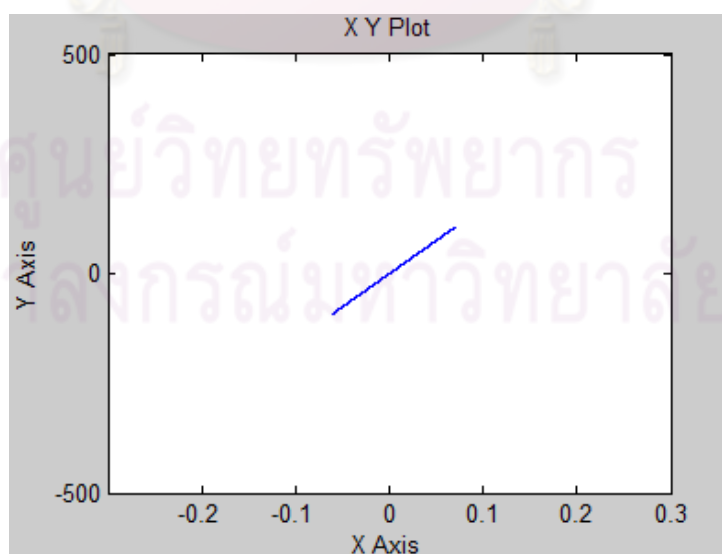


Fig.6-7 The relationship between torque and angular displacement obtained from linear-leaf spring suspension model

For simulation by linear leaf spring suspension model, the hysteresis component was excluded so that the relation between load and displacement was simple as linear function to each other as shown in Fig.6-7. The weighted RMS accelerations, representing the level of ride comfort/discomfort subjected to different classes of roads were tabulated in Table 6-1.

	Very good	Good	Average	Poor	Very Poor
60 degree	0.2211	0.6399	1.1315	2.6125	5.6427
70 degree	0.3870	0.6112	0.8351	2.1261	4.9186
80 degree	0.3067	1.2364	1.8286	5.0628	7.7244
90 degree	0.3109	0.9155	1.7317	3.7572	12.0981
110 degree	0.4877	0.8339	0.9617	3.2023	7.0052
120 degree	0.4950	1.0797	1.9207	2.8572	8.4904

Table 6-2 The weighted RMS accelerations, representing the level of ride comfort/discomfort subjected to different classes of roads (non-linear suspension)

From simulated results and calculation from the frequency-weighting method, the highest value was found at 90° of shackle angle by simulation of the “very poor” road while the lowest value was found at 60° of shackle angle by simulation of the “very good” road. The vertical acceleration of the suspension, vehicle body, and wheel/tire are also represented by the RMS of the 130 data/interval plots as shown in Figs 6-8(a), (b) and 6-9(a), (b). As seen from the graph, the magnitude of the RMS acceleration is highest at the tire, lower at the suspension and lowest at the vehicle’s body for both cases. This is reasonable as the suspension perceived the vibration transmitted from vehicle tire and tried to absorb and to dissipate the energy so that the amount of vibration transferred to the vehicle’s body was deteriorated.

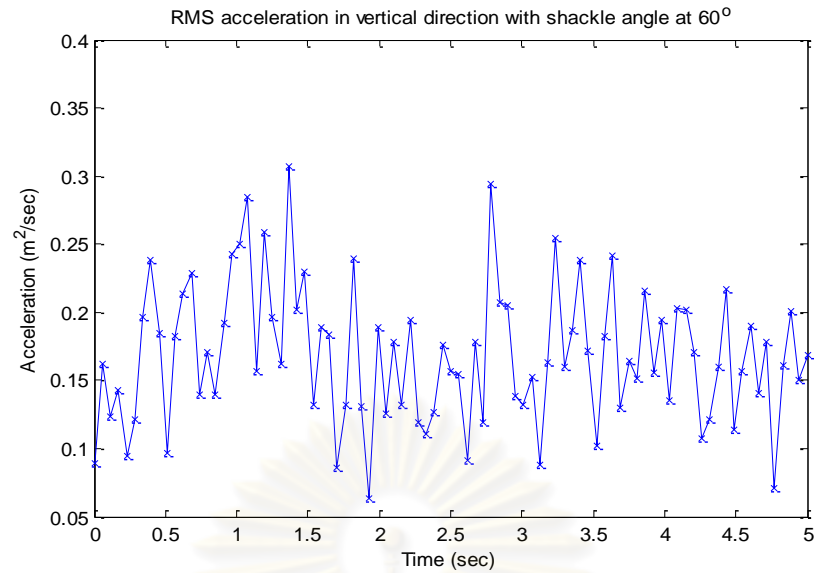


Fig.6-8(a) The plots of RMS vertical acceleration of vehicle suspension at 60° of shackle angle

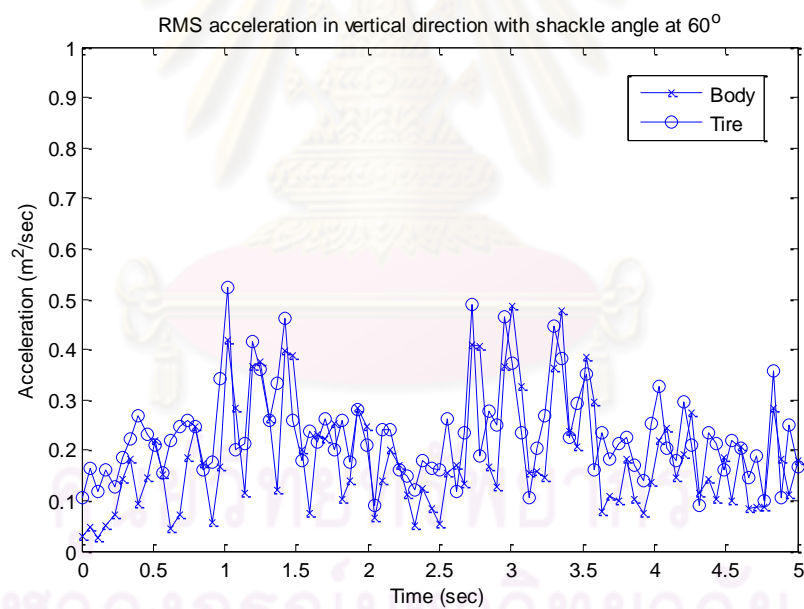


Fig.6-8(b) The plots of RMS vertical acceleration of vehicle body (cross line) and tire (circle line) at 60° of shackle angle

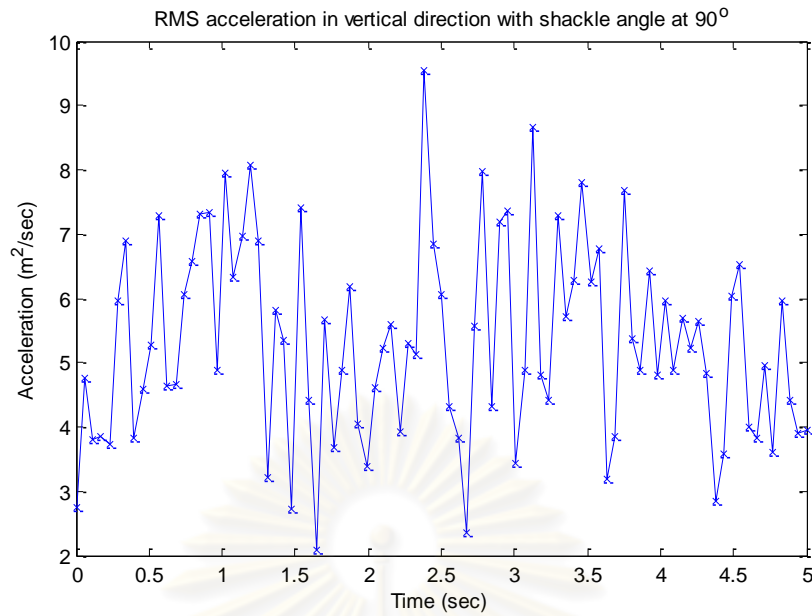


Fig.6-9(a) The plots of RMS vertical acceleration of vehicle suspension at 90° of shackle angle

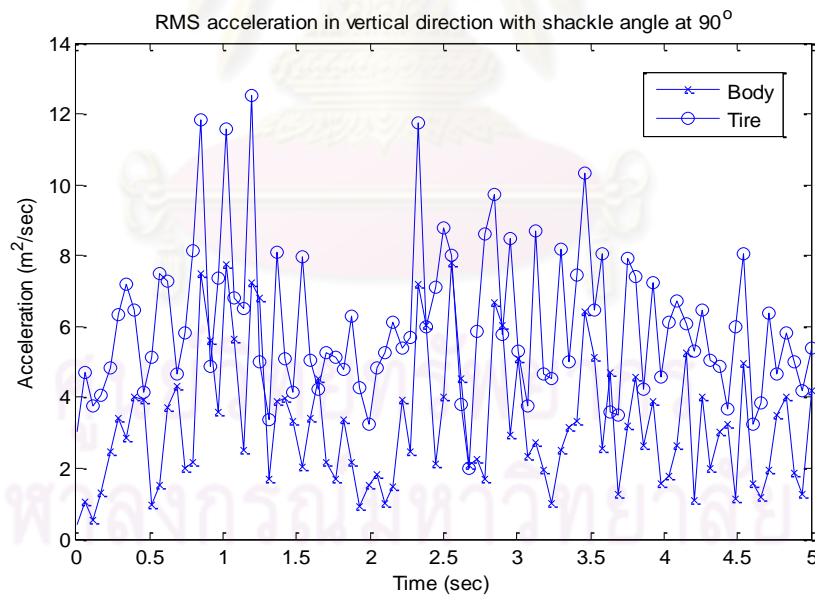


Fig.6-9(b) The plots of RMS vertical acceleration of vehicle body (cross line) and tire (circle line) at 90° of shackle angle

The results of weighted RMS acceleration obtained from nonlinear and linear model are also compared to each other as shown in Figs 6-10 – 6-15. The RMS acceleration values were plotted against different types of roads.

When the initial installation shackle angle is at 60 degree, the shape of curves are similar to each other which tends to increase when the road is rougher but when the road changes from “poor” to “very poor” the value obtained from nonlinear model seems to increase rapidly.

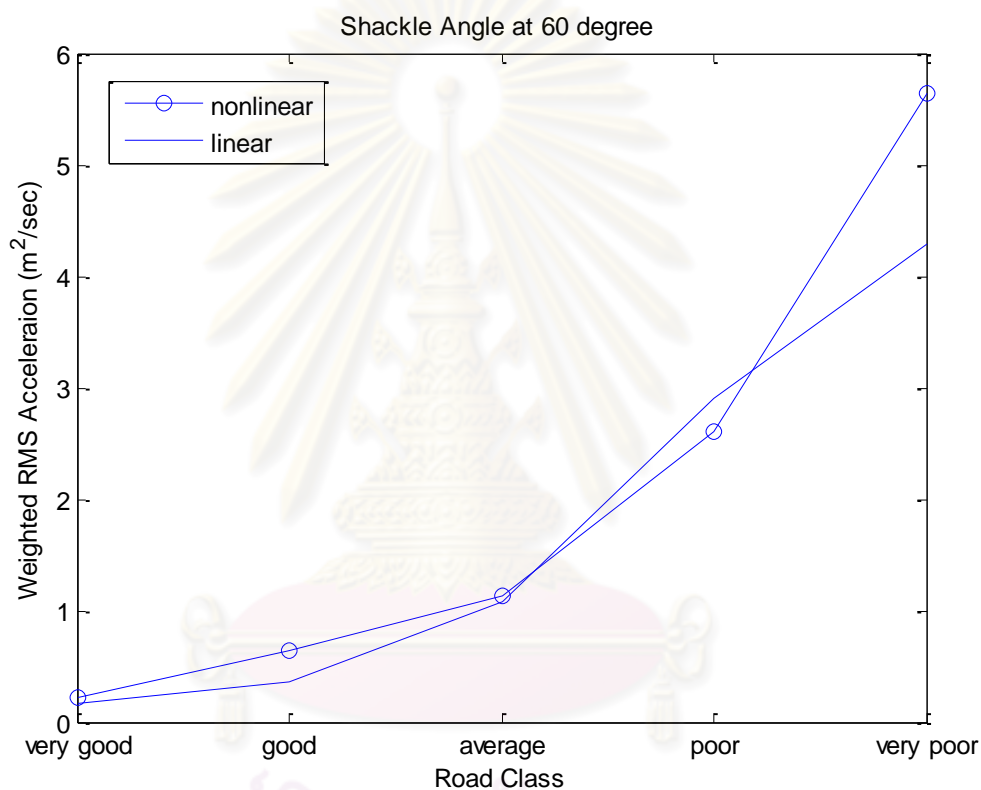


Fig.6-10 Ride comfort results of nonlinear and linear model at shackle angle 60°

At shackle angle of 70 degree, there's the significant difference between results of nonlinear and linear models as the values obtained from linear model changes faster than the nonlinear's, resulting in higher values of RMS weighted acceleration for almost every type of roads. When the shackle angle increased up to 80 degree, the results from both models are closer although the linear model seems to produce higher accelerations. At 90 degree, the curves are almost the same except for the very poor road as the value obtained from nonlinear model is higher.

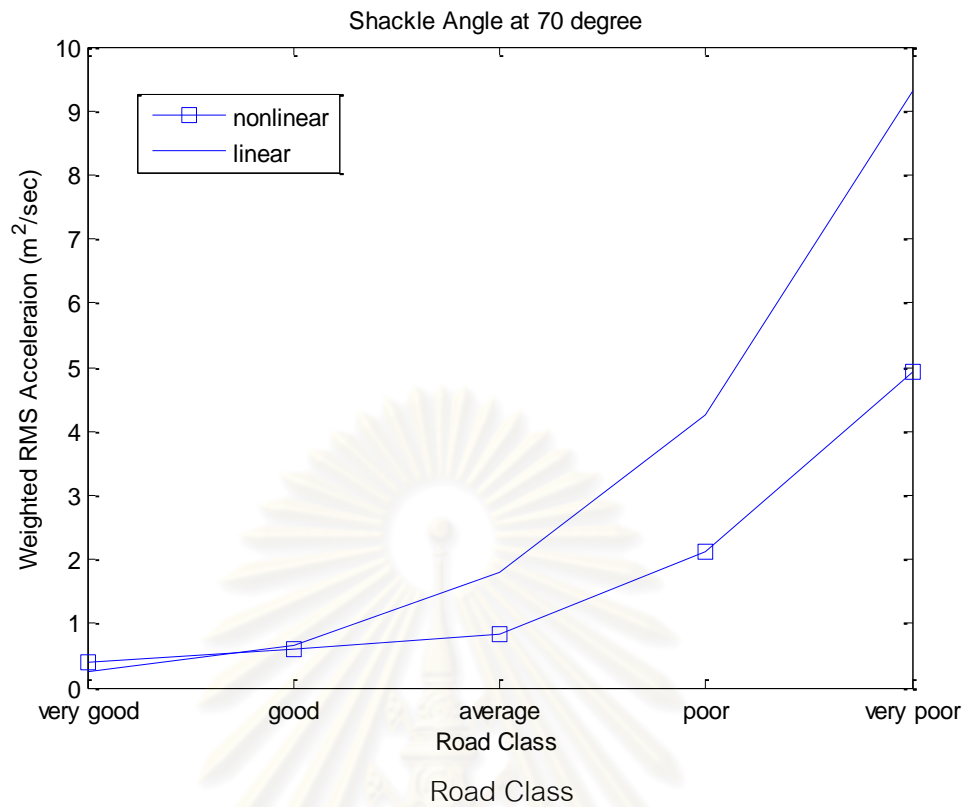


Fig.6-11 Ride comfort results of nonlinear and linear model at shackle angle 70°

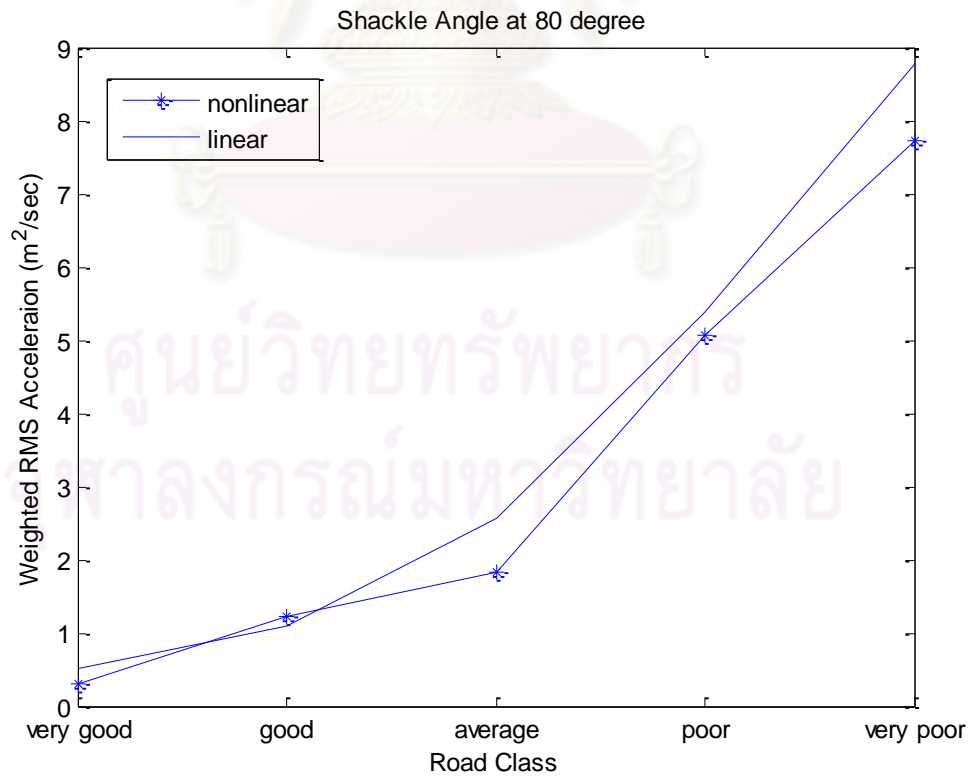


Fig.6-12 Ride comfort results of nonlinear and linear model at shackle angle 80°

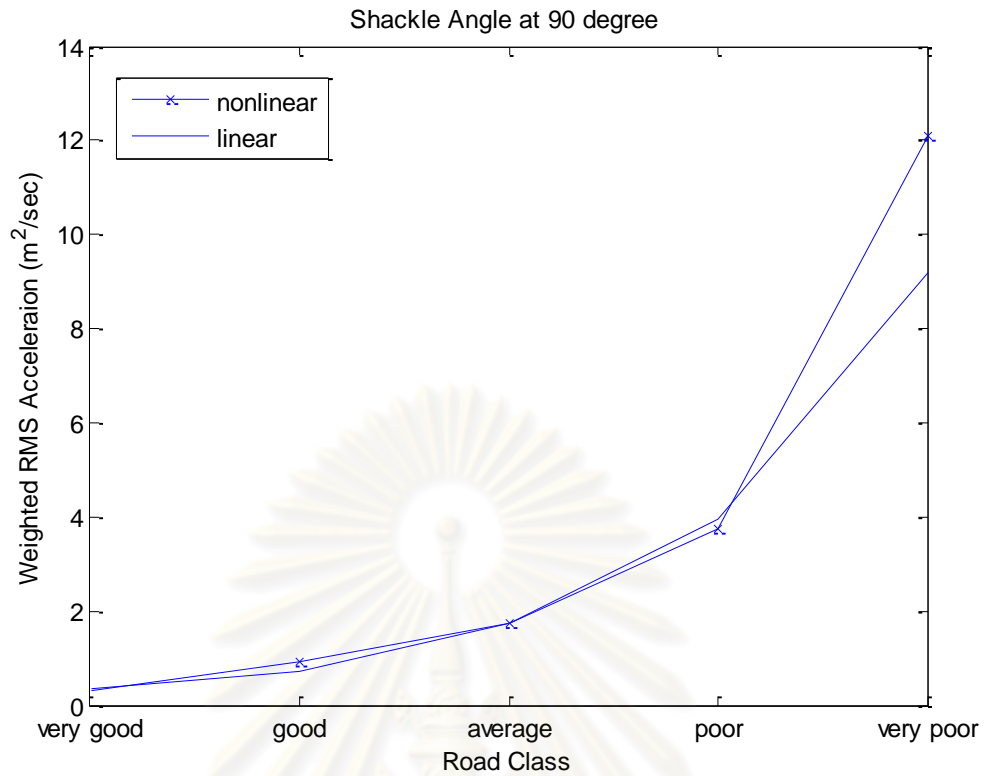


Fig.6-13 Ride comfort results of nonlinear and linear model at shackle angle 90°

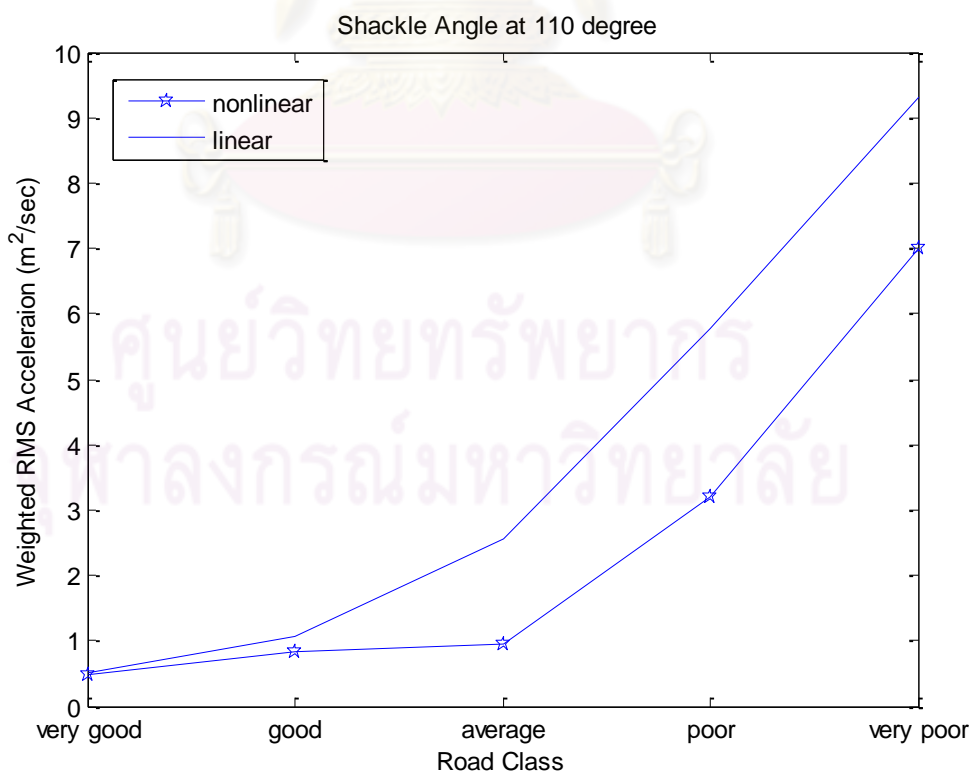


Fig.6-14 Ride comfort results of nonlinear and linear model at shackle angle 110°

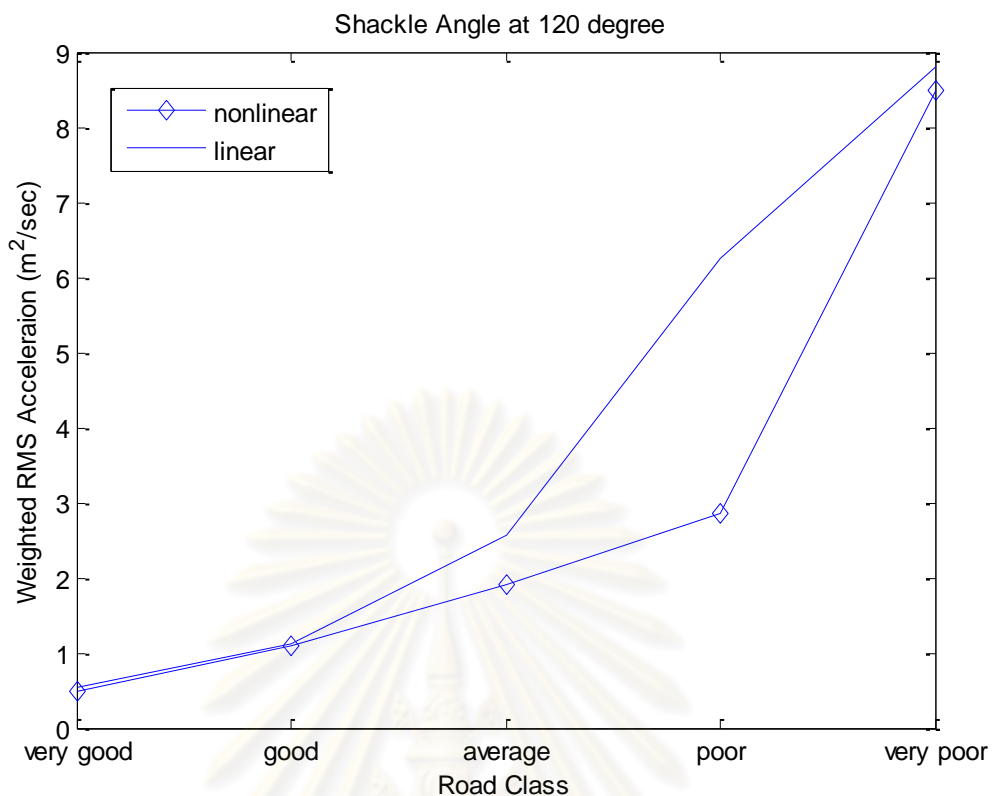


Fig.6-15 Ride comfort results of nonlinear and linear model at shackle angle 120°

The shapes of two curves are different again at 110° with the higher rate of change from the linear model's results and even faster when increasing to be at 120°. It can be said that for the overall results, ride comfort is better on smooth road with gradual changes from "very good" to "poor" road and sudden increase for the "very poor" road. When considering only for the results of nonlinear model, the RMS acceleration values were plotted against shackle angles for every type of road. It can be seen from the graph that for the "good", "average", and "poor" road, the RMS acceleration values are lowest when shackle angle is 70° while the lowest for the "very good road" appears at shackle angle of 60°. However, the obtained value of 70° is just slightly different from that of 60° and can be acceptable as it falls in to a "fairly uncomfortable" criteria. It is also found that at 80°, the weighted RMS acceleration value is highest for the "good" and "poor" road while the highest values for the "very good", "average", and "very poor" road are found at shackle angle of 110°/120°, 120°, and 90°, respectively.

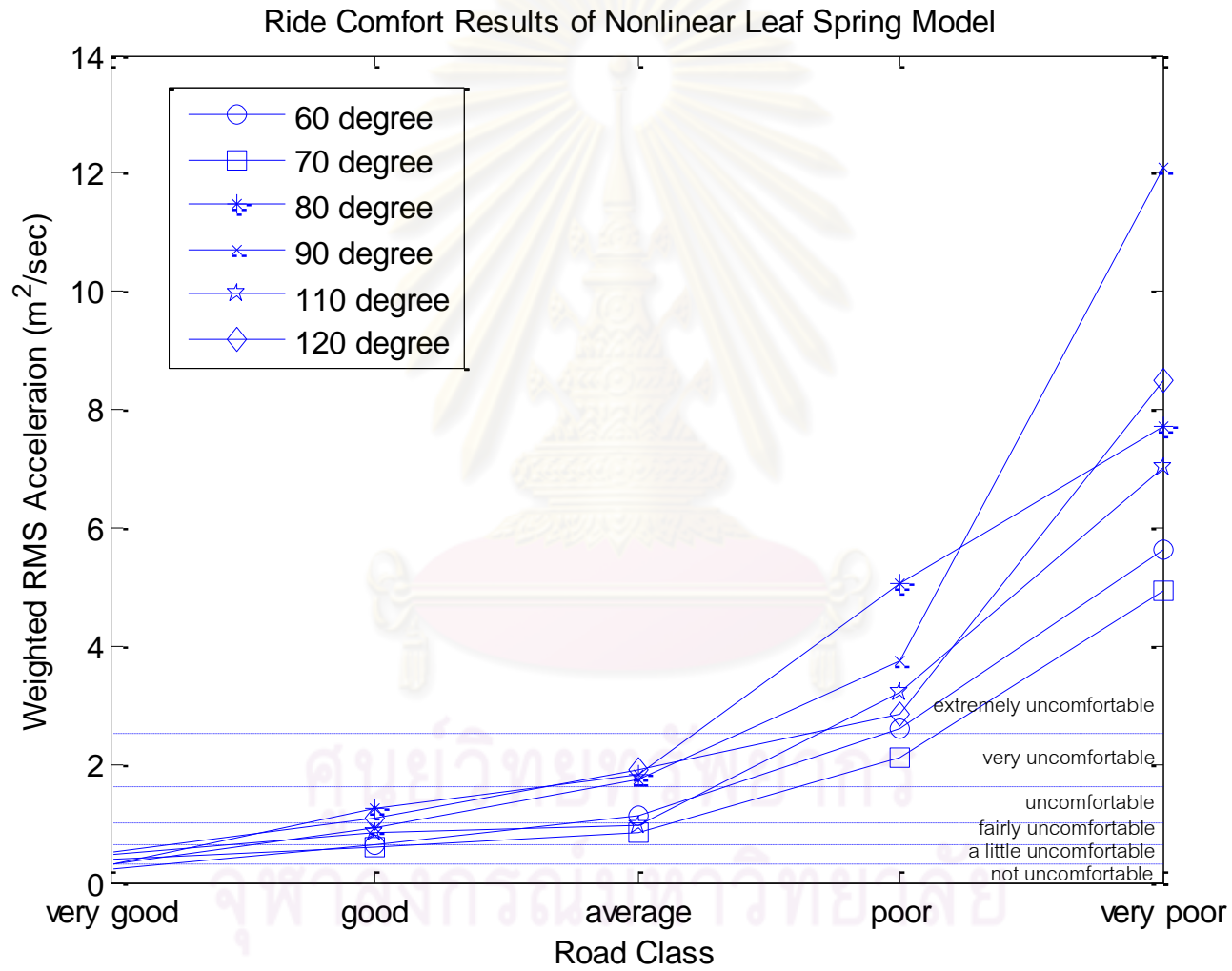


Fig.6-16(a) Ride comfort results of nonlinear leaf spring model at different shackle angles

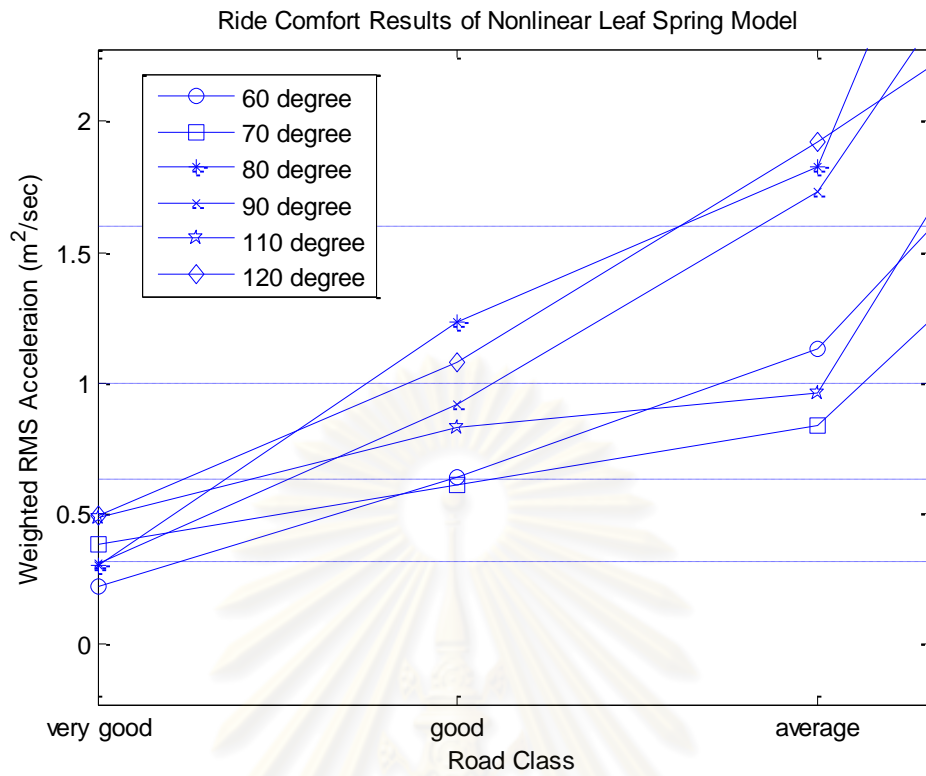


Fig.6-16(b) Ride comfort results of nonlinear leaf spring model for “very good” to “average” road

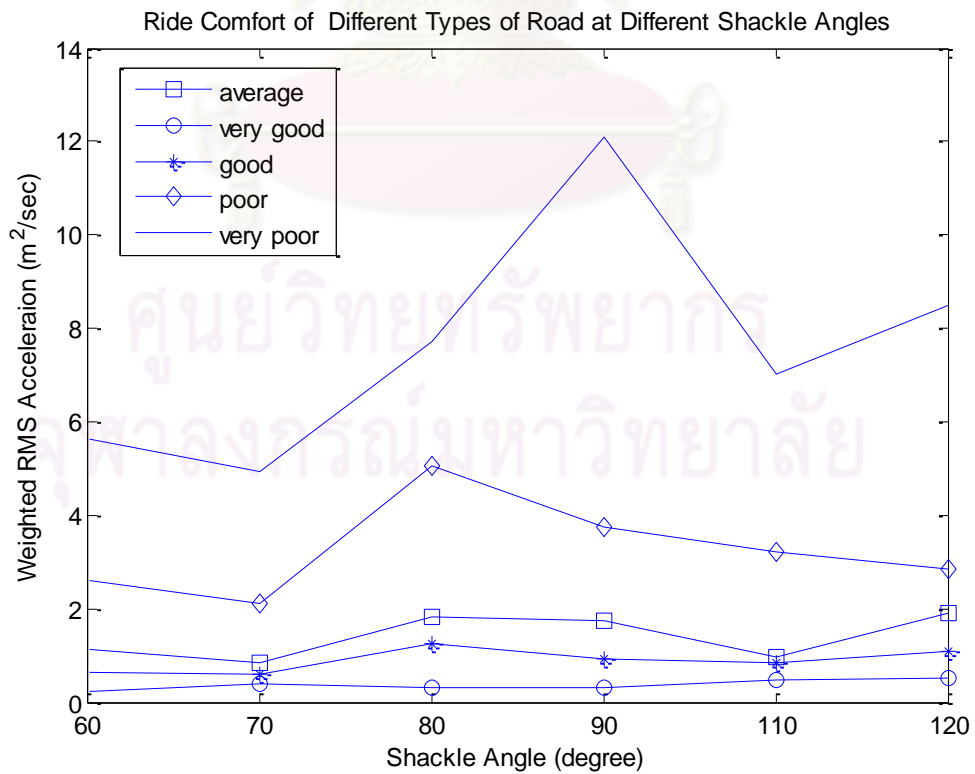


Fig.6-17 Ride comfort results of nonlinear leaf spring model at different classes of roads

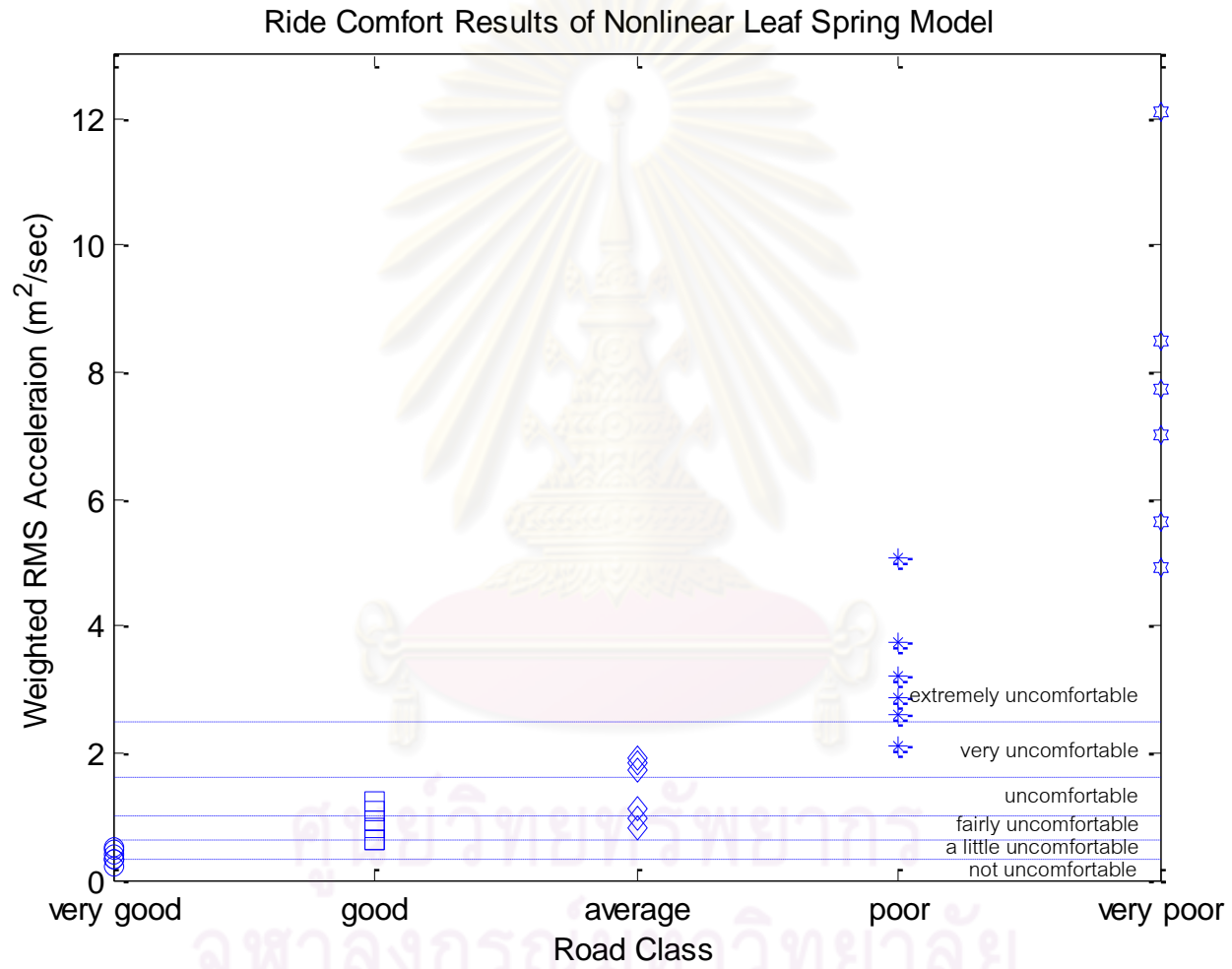


Fig.6-18 Ride comfort level of nonlinear leaf spring model at different classes of roads

6.6. Discussion of Results and Conclusion

From the results presented in the previous section, the overall results show that ride comfort is better on smooth road with gradual changes from “very good” to “poor” road and sudden increase for the “very poor” road. The values obtained from the nonlinear leaf spring suspension model mostly agrees with the suggested ride comfort/discomfort level proposed by ISO. The ride values lie within “not uncomfortable” and “a little uncomfortable” categories for simulation of “very good” road while those of the “good” road lie within “a little uncomfortable” to “uncomfortable” zone. For the “average” road, the values lie within two separate zones. The lower zone includes the results obtained from simulation of shackle angles at 60° , 70° , and 110° which lie within the “fairly uncomfortable” and “uncomfortable” categories while the higher zone includes the results obtained from simulation of shackle angles at 80° , 90° , and 120° which lie mostly in the “very uncomfortable” zone. For the “poor” road, the values lie in the “very uncomfortable” and mostly in the “extremely uncomfortable” zones. The worst case of ride comfort is in the “extremely uncomfortable” area for all values of shackle angles which is highest at 90° and lowest at 70° . From the comparison of the linear and nonlinear results, the linear model tends to produce higher value in degree of discomfort. This is because of the nonlinear leaf spring suspension model contains hysteresis and friction components that resist leaf spring movement and behave as a natural damper, resulting in less displacements. It is noticeable that at the position 90° of shackle angle at initial installation, the nonlinear leaf spring behaves similarly to the linear leaf spring. This may be explained by the knowledge of leaf spring installation effect from section 2.1.2.3.

When a leaf spring is not perpendicular to the datum line, the shackle load possesses its component in longitudinal axis (force P shown in Fig.6-19) which can be either compression or tension, depending on the direction of the swinging motion. If the shackle swings towards the fixed end of the leaf spring, it results in compressive load while it tends to produce tensile load as the shackle swings in the opposite direction. Under shackle tension, spring rate is increased while it is decreased when subjected to

shackle compression. At 90° , there's no effect from the longitudinal load so that the leaf spring's behavior of linear and nonlinear models are almost the same.

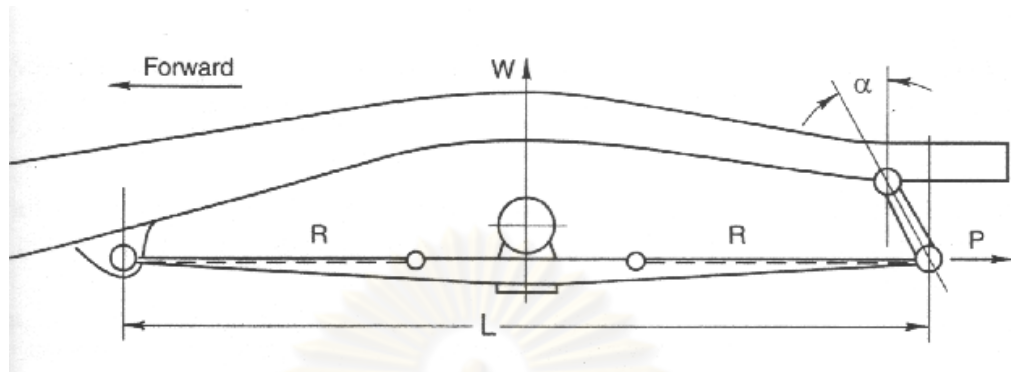


Fig.6-19 Symmetrical leaf spring with shackle [15]

ศูนย์วิทยทรัพยากร
จุฬาลงกรณ์มหาวิทยาลัย

CHAPTER VII

DISCUSSION OF RESULTS AND CONCLUSION

7.1. Summary of the Research

In this thesis, a simulation-based leaf spring model was created to study the effect of leaf spring suspension parameters on vehicle ride comfort. The main objective is to build a simulation model for ride comfort prediction from leaf spring parameters which can be used in design process, in an attempt to save time, cost, and eliminate uncertainties that may exist in field experiments. The basic idea for the model was using five massless links connected with rotational stiffnesses with the axle mounted at the center of the middle link. For a leaf spring modeling, a massless approximation is reasonable since the masses involved in rigid axles, wheels and the body of the vehicle are considerably higher than the mass of the leaf spring. The model was then verified by using a leaf spring test rig that can measure vertical static deflection of leaf spring under static loading condition. Some experiments were carried out to compare the results with those of the simulation's and finally obtained the values of the unknown parameters. The quarter-car model, with sub-system which represents the characteristics of suspension system was used to study the response of the vehicle to the road profile excitation, based on road surface roughness classification approved by ISO 8608 and the completed vehicle suspension model was constructed by including the leaf spring model into a quarter-car model. The synthetic road profile, representing road irregularities for five road classes were generated by the simple road model as the input of the system at constant velocity of 60 km/hr. For simulation subjected to different types of roads, the shackle angles were varied from 60 degree to 120 degree measured counterclockwise from the horizontal plane. The vertical acceleration of the suspension was captured and used to calculate ride comfort value in the form of weighted RMS acceleration by using the frequency weighting technique recommended by ISO 2631-1.

The overall results show that ride comfort is better on smooth road with gradual changes from "very good" to "poor" road and sudden increase for the "very poor" road. The values obtained from the non-linear and linear leaf spring suspension model are

slightly different from each other. The worst case of ride comfort is in the “extremely uncomfortable” area for all values of shackle angles which is highest at 90° and lowest at 70° while the best one was found at 60° of shackle angle by simulation of the “very good” road. the linear model tends to produce higher value in degree of discomfort. At the position 90° of shackle angle at initial installation, the nonlinear leaf spring behaves similarly to the linear leaf spring because there' no effect from the longitudinal load when a leaf spring is perpendicular to the datum line.

7.2. Conclusion

The non-linear leaf spring has significant effects on the leaf spring's kinematics as the results show that ride comfort values depend on suspension' s characteristics. The results obtained from both non-linear and linear leaf spring suspension are different and the linear model tends to produce higher degree of discomfort. This is reasonable as in nature, friction always resists movement in mechanical system so that the proposed leaf spring model is reliable. For standard tool used in the research, the use of ISO 2631-1 for ride comfort evaluation results in the acceptable values compared to the level of the suggested comfort/discomfort. Indices of comfort are calculated taking into account the human sensitivity. The examples show that the proposed comfort indices depend on leaf spring suspension's parameters and, hence, are useful design tools.

7.3. Further Recommendations

Firstly, the recommendations shall be commented on the process of the leaf spring modeling. In the research, the completed leaf spring model includes the geometrical property and hysteresis/friction effects which cannot be neglected. The verification of the leaf spring was made by identifying the leaf spring's parameters based on the comparison of the experimental results with those of the simulation's which is just the trial and error approximation. The recent work was lack of sufficient data in the transition state which might be due to the limitation and ability of the leaf spring test rig that can allow for static testing only so that the model does not capture well in the

transient state transition. In the identifying procedure of model's parameters, the method of optimization and numerical calculations can be employed to provide better results and more accurate values. Apart from this, some obstacles still exist to limit the performance of the test rig such as misalignment between the hydraulic actuator and the force sensor must be eliminated in order to provide better accuracy. For comfort study, the focused parameter taken into consideration was only the shackle angle which is just one example of many factors that can contribute to nonlinearities of the system. The other component such as bushing which has not yet been included into the present proposed model can be added to represent more about the leaf spring's characteristics such as the work of Hoyle [17]. For the hysteresis modeling, there are different models of friction available at present, apart from Dahl's model which can be used and compared among one another to prove the reliability of the proposed model. The detailed description and comparison can be found in ref. [18].

In the ride simulation, road input profiles were generated randomly by a stochastic process which was illustrated by a power spectral density (PSD) function. The other road model in time domain such as white noise filtration method proposed by Zhang Yonglin et al. [19] can be applied with the proposed leaf spring model in order to see different results. Furthermore, the validation of the leaf spring model by field experiment has not yet been performed. The real road irregularities can be collected and used with the model in order to compare the results with those obtained from real situation. The various standard methods for ride comfort evaluation [8] can be employed with the experiment and simulation data to prove the reliabilities of the results. Finally, the fulfillment of the research can be made through the other ride comfort measuring scheme that is the subjective measurement in order to relate the design parameters of vehicle with the human sensitivity on ride comfort.

REFERENCES

- [1] Society of Automotive Engineers. Spring Design Manual. SAE J1123. Warrendale: Society of Automotive Engineers, 1985.
- [2] International Organization for Standardization. Mechanical Vibration and Shock Human Exposure –Vocabulary. ISO 5805. Geneva: International Organization for Standardization, 1997.
- [3] Wong, J.Y. Theory of Ground Vehicles. 3rd ed. Wiley-Interscience, 2001.
- [4] Frendo, F., Sgueglia, M., Vitale, E., and Hippoliti, R. Analysis of Motorscooter Ride Comfort. SAE Number: 2002-01-2177. Warrendale: Society of Automotive Engineers, 2002.
- [5] David, P., et al. Analysis of vibrations induced during wheelchair propulsion. Journal of Rehabilitation Research and Development 38, 4 (July/August 2001): 409–421.
- [6] Johan Lindén. Test methods for ride comfort evaluation of truck seats. Master's Thesis, Department of Signals, Sensors & Systems Automatic Control, Royal Institute of Technology, Stockholm, 2003.
- [7] Gillespie, Thomas D. Fundamentals of Vehicle Dynamics. Warrendale: Society of Automotive Engineers, 1992.
- [8] Society of Automotive Engineers. Subjective Rating Scale for Evaluation of Noise and Ride Comfort Characteristics Related to Motor Vehicle Tires. SAE J1060, Issued 1973-11. Warrendale: Society of Automotive Engineers, 1973.
- [9] Griffin, M.J. Handbook of Human Vibration. London: Academic Press, 1990.
- [10] Griffin, M.J. A comparison of standardized methods for predicting the hazards of whole-body vibration and repeated shocks. Journal of Sound and Vibration 215, 4 (27 August 1998): 883-914.
- [11] International Organization for Standardization. Mechanical Vibration and Shock-Evaluation of Human Exposure to Whole-Body-Vibration - Part 1: General Requirements. 2nd ed. ISO 2631-1. Geneva: International Organization for Standardization, 1997.

- [12] British Standards Institution. Measurement and Evaluation of Human Exposure to Whole-Body Mechanical Vibration and Repeated Shock. BS 6841. London: British Standards Institution, 1987.
- [13] Heisler, H. Vehicle and Engine Technology. 2nd ed. Warrendale: Society of Automotive Engineers, 1985.
- [14] International Organization for Standardization. Mechanical vibration – Road surface profiles – Reporting of measured data. ISO 8608. International Organization for Standardization, 1995.
- [15] Milliken, W.F. and Milliken, D.L. Chassis Design Principles and Analysis. 1st ed. Warrendale: Society of Automotive Engineers, 1988.
- [16] Ekici, B. Multi-response optimisation in a three-link leaf-spring model. International Journal of Vehicle Design 38, 4 (2005): 326-346.
- [17] Al Majid, A. and Dufour, R. Formulation of a hysteresis restoring force model: application to vibration isolation. Journal of Nonlinear Dynamics 27 (2002): 69-85.
- [18] Chatelet, E., Michon, G., Manin, L., and Jacquet, G. Stick/slip phenomena in dynamics: choice of contact model, numerical predictions and experiments. Mechanism and Machine Theory 43 (2008): 1211–1224.
- [19] Hoyle, J.B. Modelling the static stiffness and dynamic frequency response characteristics of a leaf spring truck suspension. Proceedings of the Institution of Mechanical Engineers. Part D. Journal of Automobile engineering. ISSN 0954-4070. London: Professional Engineering, 1989
- [20] Claudio Garcia. Comparison of friction models applied to a control valve. Control Engineering Practice 16, 10 (October 2008): 1231-1243.
- [21] Zhang Yonglin and Zhang Jiafan. Numerical simulation of stochastic road process using white noise filtration. Mechanical Systems and Signal Processing 20, 2 (February 2006): 363-372.



APPENDICES

ศูนย์วิทยทรัพยากร
จุฬาลงกรณ์มหาวิทยาลัย



APPENDIX A

ศูนย์วิทยทรัพยากร
จุฬาลงกรณ์มหาวิทยาลัย

PRINCIPAL FREQUENCY WEIGHTINGS IN ONE-THIRD OCTAVES

Frequency band number x	Frequency f Hz	W_k		W_d		W_f	
		factor		factor		factor	
		X 1000	dB	X 1000	dB	X 1000	dB
-17	0.02					24.2	-32.33
-16	0.025					37.7	-28.48
-15	0.0315					59.7	-24.47
-14	0.04					97.1	-20.25
-13	0.05					157	-16.10
-12	0.063					267	-11.49
-11	0.08					461	-6.73
-10	0.1	31.2	-30.11	62.4	-24.09	695	-3.16
-9	0.125	48.6	-26.26	97.3	-20.24	895	-0.96
-8	0.16	79.0	-22.05	158	-16.01	1006	0.05
-7	0.2	121	-18.33	243	-12.28	992	-0.07
-6	0.25	182	-14.81	365	-8.75	854	-1.37
-5	0.315	263	-11.60	530	-5.52	619	-4.17
-4	0.4	352	-9.07	713	-2.94	384	-8.31
-3	0.5	418	-7.57	853	-1.38	224	-13.00
-2	0.63	459	-6.77	944	-0.50	116	-18.69
-1	0.8	477	-6.43	992	-0.07	53.0	-25.51
0	1	482	-6.33	1011	0.10	23.5	-32.57
1	1.25	484	-6.29	1008	0.07	9.98	-40.02
2	1.6	494	-6.12	968	-0.28	3.77	-48.47
3	2	531	-5.49	890	-1.01	1.55	-56.19
4	2.5	631	-4.01	776	-2.20	0.64	-63.93
5	3.15	804	-1.90	642	-3.85	0.25	-71.96
6	4	967	-0.29	512		0.097	-80.26

Frequency band number x	Frequency f Hz	W_k		W_d		W_f	
		factor		factor		factor	
		X 1000	dB	X 1000	dB	X 1000	dB
7	5	1039	0.33	409	-7.76		
8	6.3	1054	0.46	323	-9.81		
9	8	1036	0.31	253	-11.93		
10	10	988	-0.10	212	-13.91		
11	12.5	902	-0.89	161	-15.87		
12	16	768	-2.28	125	-18.03		
13	20	636	-3.93	100	-19.99		
14	25	513	-5.80	80.0	-21.94		
15	31.5	405	-7.86	63.2	-23.98		
16	40	314	-10.05	49.4	-26.13		
17	50	246	-12.19	38.8	-28.22		
18	63	186	-14.61	29.5	-30.60		
19	80	132	-17.56	21.1	-33.53		
20	100	88.7	-21.04	14.1	-36.99		
21	125	54.0	-25.35	8.63	-41.28		
22	160	28.5	-30.91	4.55	-46.84		
23	200	15.2	-36.38	2.43	-52.30		
24	250	7.90	-42.04	1.26	-57.97		
25	315	3.98	-48.00	0.64	-63.92		
26	400	1.95	-54.20	0.31	-70.12		

Table A-1 Principal frequency weightings in one-third octaves [11]



APPENDIX B

ศูนย์วิทยทรัพยากร
จุฬาลงกรณ์มหาวิทยาลัย

DEFINITION OF VEHICLE'S COORDINATE SYSTEM

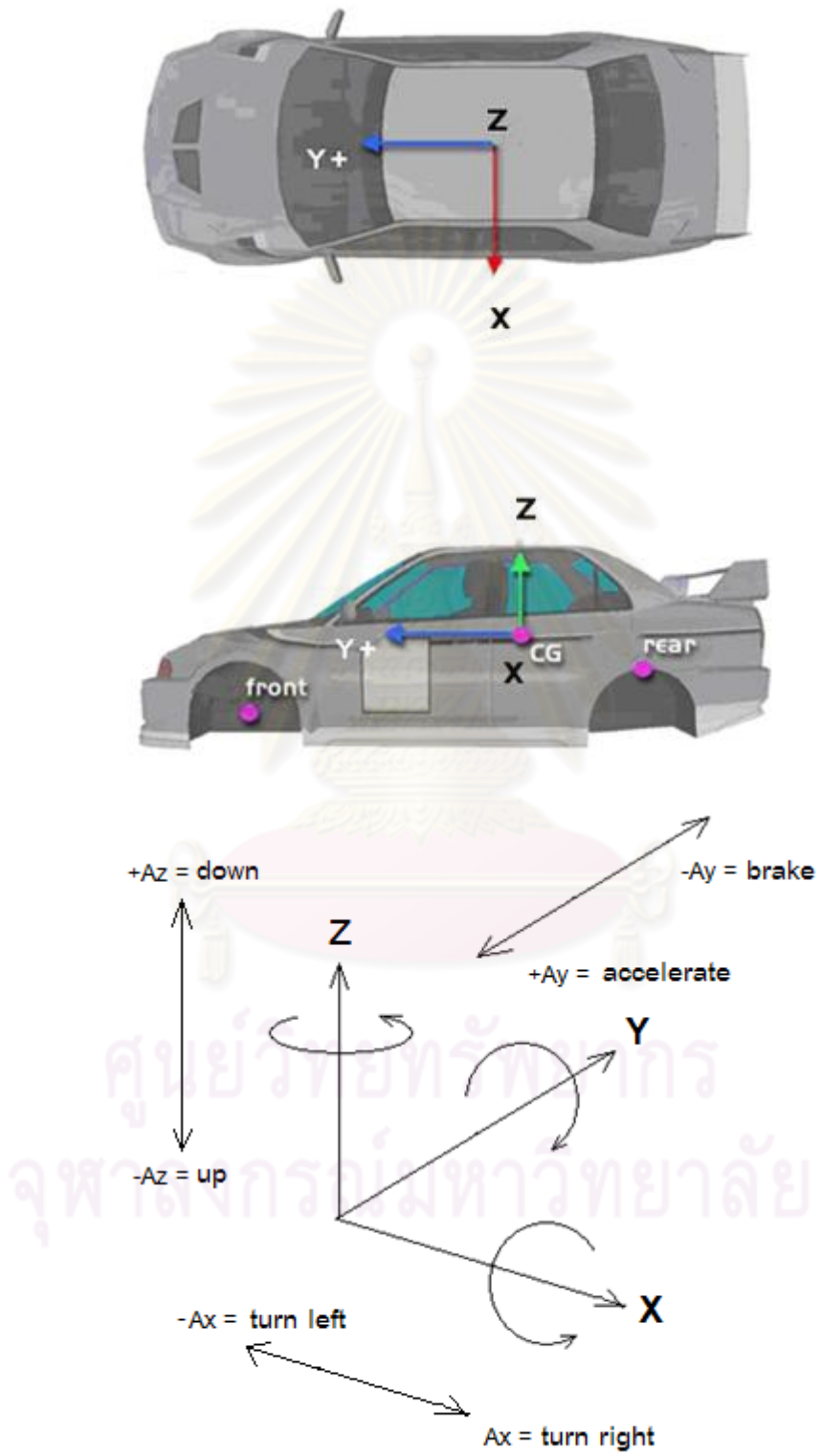


Fig.B-1 Definition of vehicle coordinate system



APPENDIX C

ศูนย์วิทยทรัพยากร
จุฬาลงกรณ์มหาวิทยาลัย

MATLAB M-FILE CODE

C1 Leaf Spring Suspension Property

```

1     s=-0.15 %%camber height
2     H=2*s
3     AE=1.19;AB=0.37125;
4     CD=0.37125;
5     DE=0.1;
6     r=pi/180;
7     z10=340*r;
8     z40=110*r; %%Shackle angle
9     z50=180*r;
10    y1=AB*sin(z10);x1=AB*cos(z10);y2=H-y1;
11    x3=AE-DE*cos(z40);y3=-DE*sin(z40);z30=asin((y3-y2)/CD);
12    x2=x3-CD*cos(z30);
13    z20=atan2((y2-y1),(x2-x1));
14    BC=(x2-x1)/cos(z20);
15    a=1511;b=111.4418;d=a;e=-21.0535;beta=100;nu=1; %%Dahl
    parameters
16    m_b=1870/4;m_w=30;k_w=118440;c_b=2369.3; %% Quarter Car
    parameters

```

C2 Ride Comfort Calculation

```

1     Fs=200;
2     ax=0;ay=0;az=xs_dd;
3     h = spectrum.periodogram('rectangular');
4     hopts3 = psdopts(h);
5     set(hopts3,'NFFT',2^8,'Fs',Fs,'SpectrumType','onesided');
6     hpsdz = psd(h,az,hopts3);

7     fb=[0.5;0.63;0.8;1;1.25;1.6;2;2.5;3.15;4;5;6.3;8;10;12.5;16;
    20;25;31.5;40;50;63;80;100];

8     Wk=[-7.57;-6.77;-6.43;-6.33;-6.29;-6.12;-5.49;-4.01;-1.90;
    -0.29;0.33;0.46;0.31;-0.10;-0.89;-2.28;-3.93;-5.80;-7.86;
    -10.05;-12.19;-14.61;-17.56;-10.05];
9     wk=10.^(Wk/20);
10    Wd=[-1.38;-0.50;-0.07;0.10;0.07;-0.28;-1.01;-2.20;-3.85;-5.82;
    -7.76;-9.81;-11.93;-13.91;-15.87;-18.03;-19.99;-21.94;-23.98;
    -26.13;-28.22;-30.60;-33.53;-36.99];
11    wd=10.^(Wd/20);
12    for i=1:24;
13        fmin(i)=fb(i)/sqrt(2^(1/3));
14    end
15    for i=1:23;
16        fmax(i) =(2^(1/3))*fmin(i);
17    end
18    fmax(24)= 100;
19    for i=1:24;
20        pwrz(i)=avgpower(hpsdz,[fmin(i) fmax(i)]);
21        Pz(i)= pwrz(i)*wk(i);
22    end
23    P1=sum(Pz);

```



```
24 awz=sqrt(P1);
25 awx=0;
26 awy=0;
27 ride=sqrt((awz^2)+(awx^2)+(awy^2))
```

C3 RMS Acceleration

```
1 for i=0:88;
2 n(i+1)= norm(xs_dd((i*130)+1:(i*130)+130));
3 r(i+1)=n(i+1)/sqrt(150);
4 end
5 plot((0:5/88:5),r,'-x')
6 for i=0:88;
7 n(i+1)= norm(xw_dd((i*130)+1:(i*130)+130));
8 r(i+1)=n(i+1)/sqrt(150);
9 end
10 figure,plot((0:5/88:5),r,'-x')
11 hold on;
12 for i=0:88;
13 n(i+1)= norm(xb_dd((i*130)+1:(i*130)+130));
14 r(i+1)=n(i+1)/sqrt(150);
15 end
16 plot((0:5/88:5),r,'-x')
```



ศูนย์วิทยทรัพยากร
จุฬาลงกรณ์มหาวิทยาลัย

BIOGRAPHY

Mrs. Saelem, Sirithon was born on 26 August 1978 at Ramathibodi hospital, Bangkok. She is a daughter of Mr. Anake and Mrs. Chanthana Meethip. She got married with Mr. Saelem, Sittichai in 2002 and has got two children. For her education, she obtained a Bachelor of Engineering degree in Mechanical Engineering from Thammasat University and the University of Nottingham in the year 2001 and attended the Master of Engineering Program in the year 2006 at the Department of Mechanical Engineering, Chulalongkorn University. During her study, she attended the 23th Mechanical Engineering Network conference held at The Imperial Mae Ping Hotel, Chiang Mai, Thailand during 4 to 7 November 2009 with the article under the topic of "Experimental Verification of Leaf Spring Model by Using a Leaf Spring Test Rig".



ศูนย์วิทยทรัพยากร
จุฬาลงกรณ์มหาวิทยาลัย